Electronic Supplementary Material (ESI) for Organic Chemistry Frontiers.
This journal is © the Partner Organisations 2021

Supporting Information

Generation of powerful organic electron donors by water-assisted decarboxylation of benzimidazolium carboxylate.

Guillaume Tintori,[a] Arona Fall, [a] Nadhrata Assani, [a] Yuxi Zhao, [a] David Bergé-Lefranc, [b] Sébastien Redon, [a] Patrice Vanelle [a]* and Julie Broggi [a]*

a) Aix Marseille Univ, CNRS, Institut de Chimie Radicalaire ICR, Faculté de Pharmacie, 13005 Marseille, France.
b) Aix Marseille Univ, CNRS, IRD, Laboratoire IMBE UMR 7263, Faculté de Pharmacie, 13005 Marseille, France.

[julie.broggi@univ-amu.fr and patrice.vanelle@univ-amu.fr]

1. General considerations

All reagents and extra dry solvents were purchased from commercial suppliers and used as received. The reactions were performed in an MBraun glovebox containing dry argon and less than 1 ppm of oxygen and water. Reactions under UV-irradiations were performed with the LED Light Source LIGHTNINGCURE™ LC-L1 V5 of Hamamatsu (Wavelength 365 ± 5 nm, UV light intensity: 14000 mW/cm^2). The following adsorbent was used for column chromatography: silica gel 60 (Merck, particle size 0.063-0.200 mm, 70-230 mesh ASTM). TLC was performed on 5 cm × 10 cm aluminium plates coated with silica gel 60F-254 (Merck) using an appropriate eluent. ^{1}H NMR (250 or 400 MHz) and ^{13}C NMR (62 or 100 MHz) spectra were recorded at ambient temperature in solutions of $CDCl_3$ (δ_H = 7.26 ppm and δ_C = 77.16 ppm), DMSO-d_6 (δ_H = 2.50 ppm and δ_C = 39.52 ppm), D_2O (δ_H = 4.79 ppm) or C_6D_6 (δ_H = 7.16 ppm and δ_C = 128.06 ppm), unless otherwise noted. Chemical shifts are given in ppm, coupling constants "*J*" are expressed in Hertz (multiplicity: s = singlet, br s = broad singlet, d = doublet, dd = double doublet, t = triplet, q = quadruplet, qi = quintuplet, sext = sextuplet, m = multiplet). HRMS and elemental analyses were carried out at the Spectropole, Faculté des Sciences et Techniques de Saint-Jérôme, Marseille. Cyclic iminium salts, 1,3-dimethylimidazolium iodide **IMe.HI** [CAS 4333-62-4],[1] 3-butyl-1-methyl-1*H*-imidazol-3-ium bromide **IMe-^{n}Bu.HBr** [CAS 85100-77-2],[2] 3-ethyl-1-methyl-1*H*-imidazol-3-ium bromide **IMe-Et.HBr** [CAS 65039-08-9],[3] 3-di-*tert*-butylimidazolium chloride **I^{t}Bu.HCl** [CAS 157197-54-1],[4] 4-(dimethylamino)-1-methylpyridinium iodide **DMAP-Me.HI** [CAS 7538-79-6],[5] 1,3-dimethyl-1*H*-benzo[*d*]imidazol-3-ium iodide **BzIMe.HI** [CAS 7181-87-5],[6] 3,3'-(propane-1,3-diyl)bis(1-methyl-1*H*-benzo[*d*]imidazol-3-ium) iodide **Bis-BzIMe.HI** [CAS 174841-32-8][7] were prepared following reported procedures. Methyl 2-iodobenzoate **1d** [CAS 610-97-9], 2-iodoacetophenone **1e** [CAS 2142-70-3], 4-bromo-3-methylbenzonitrile **1f** [CAS 41963-20-6], 1-iodonaphthalene **1i** [CAS 90-14-2], 1-iodo-2-naphthol **1j** [CAS 2033-42-3], 1-chloro-4-iodobenzne **12** [CAS 637-87-6], 1,1-diphenylethylene **13** [CAS 530-48-3] and *N*-methylpyrrole **16** [CAS 96-54-8] were purchased from

commercial suppliers and used as received. 1-Iodo-2-(3-phenoxypropyl)benzene **1a** [CAS 939990-21-3],[8] ethyl 2-(2-iodophenoxy)-2-methylpropanoate **1b** [CAS 59477-79-1],[9] ethyl 2-(2-iodobenzyl)-2-methylpropanoate **1c,**[9] 1-Bromo-2-(3-phenoxypropyl)benzene [CAS 1011717-62-6],[8] 1-iodo-4-(3-phenoxypropyl)benzene **1h** [CAS 854764-32-2],[10] 1-*p*-toluenesulfonyl-1*H*-indole **1g** [CAS 31271-90-6], [11] 1-iodo-2-((3-methylbut-2-en-1-yl)oxy)benzene **6** [CAS 120568-94-7],[12] 1-iodo-2-(2-propen-1-yloxy)-benzene **9** [CAS 24892-63-5][13] were prepared following previously reported procedures. Spectroscopic data for the title compounds were consistent with those reported in the literature.

2. Synthesis and characterization of OED-precursors and related derivatives

1,3-Dimethylimidazolium-2-carboxylate, IMe-CO_2 [CAS 536755-29-0]

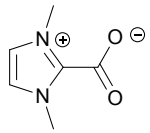

In the glovebox, a solution of 1-methylimidazole (2.5×10^{-2} mol, 2 mL, 1 equiv.) and anhydrous dimethyl carbonate (3.6×10^{-2} mol, 3 mL, 1.4 equiv.) was added to a sealed flask. Out of the glovebox, the mixture was vigorously stirred at 100°C for two days. A white solid gradually appeared. The suspension was then cooled down at -10 °C and filtered. The white precipitate was washed with cold acetone and diethyl ether to give **IMe-CO_2** as a white solid (1.78 g, 51%). Procedure reported in Ref. 14.

^{1}H NMR (250 MHz, DMSO-d_6): δ = 3.95 (s, 6H, N-CH_3); 7.53 (s, 2H, H^{Ar}).

IR (cm^{-1}) = 1245 (s, C-O); 1513 (m, C=C); 1645 (s, C=O); 1662 (m, C=N); 3105 (m, CH).

^{1}H NMR was consistent with the literature.[15]

1,3-Di-*tert*-butylimidazolium-2-carboxylate, I^{t}Bu-CO_2 [CAS 479641-76-4]

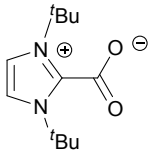

In the glovebox, a solution of 1,3-di-*tert*-butyl-1*H*-imidazol-3-ium chloride **I^{t}Bu.HCl** (5.5×10^{-3} mol, 1.2 g, 1 equiv.) in tetrahydrofuran (50 mL) was treated with potassium bis(trimethylsilyl)amide (KHMDS 95%) (6.6×10^{-3} mol, 1.3 g, 1.2 equiv.). The mixture was stirred for two hours at room temperature, and subsequently filtered on a celite pad. The solution was placed into a Schlenk and connected to a CO_2-filled Schlenk line (3 mbar). The solution was stirred 30 min under CO_2 atmosphere. After filtration and washing with THF (2 x 5 mL) and Et_2O (2 x 10 mL), **I^{t}Bu-CO_2** was obtained as a white solid (0.85 g, 70%).
Procedure reported in Ref. 14

^{1}H NMR (400 MHz, $CDCl_3$): δ = 1.76 (s, 18H, CH_3); 7.39 (s, 2H, H^{Ar}).

IR (cm^{-1}) = 1207 (s, C-$(CH_3)_3$)); 1320 (s, C-O); 1377 (s, CH_3); 1609 (m, C=O); 1659 (m, C=N); 2984 (w, CH); 3101 (w, CH).

^{1}H NMR was consistent with the literature.[16]

3-Butyl-1-methyl-1*H*-imidazol-3-ium-2-carboxylate IMe-^{n}Bu-CO_2 [671779-18-3]

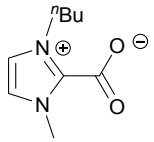

In the glovebox, a solution of 1-butyl-3-methyl-1*H*-imidazol-3-ium bromide **IMe-^{n}Bu.HBr** (9.1×10^{-3} mol, 2 g, 1 equiv.) in tetrahydrofuran (30 mL) was treated with potassium bis(trimethylsilyl)amide (KHMDS 95%) (1.1×10^{-2} mol, 2.2 g, 1.2 equiv.). The mixture was stirred for 16 h at room temperature, and subsequently filtered on a celite pad. The solution was placed into a Schlenk and connected to a CO_2-filled Schlenk line (3 mbar). The solution was stirred 16 h under CO_2 atmosphere. After filtration and washing with Et_2O (2 x 15 mL), **IMe-^{n}Bu-CO_2** was obtained as a white solid (1.48 g, 89%).

^{1}H NMR (400 MHz, DMSO-d_6) δ = 0.87 (t, *J* = 7.2 Hz, 3H, *C*H_3-CH_2); 1.25 (sext, *J* = 7.2 Hz, 2H, CH_3-*C*H_2); 1.71 (qi, *J* = 7.2 Hz, 2H, CH_2-*C*H_2-CH_2); 3.94 (s, 3H, N-CH_3); 4.45 (t, *J* = 7.2 Hz, 2H, N^+CH_2); 7.53 (d, *J* = 2.0 Hz, 1H, H^{Ar}); 7.59 (d, *J* = 2.0 Hz, 1H, H^{Ar}).

^{13}C NMR (100 MHz, DMSO-d_6) δ = 13.4 (*C*H_3-CH_2); 18.9 (CH_3-*C*H_2); 32.1 (CH_2-*C*H_2-CH_2); 36.5 (N-CH_3); 48.2 (N^+CH_2); 120.8 (CH^{Ar}); 122.2 (CH^{Ar}); 142.1 (N^+CN); 154.1 (CO_2^-).

IR (cm^{-1}) = 1215 (w, C-C); 1244 (m; C-C); 1264 (m, C-C); 1317 (m, C-O); 1381 (m, C-C); 1432 (m, C=C); 1501 (s, C=C); 1657 (s, C=O); 2874 (w, CH); 2933 (w, CH); 2958 (w, CH); 3116 (w, CH).

^{1}H and ^{13}C NMR were consistent with the literature.[17]

3-Butyl-1-methyl-1*H*-imidazol-3-ium-2-sulfinate IMe-^{n}Bu-SO_2

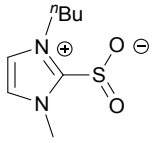

In the glovebox, a solution of 1-butyl-3-methyl-1*H*-imidazol-3-ium bromide of **IMe-^{n}Bu.HBr** (6.0×10^{-3} mol, 1.3 g, 1 equiv.) in tetrahydrofuran (30 mL) was treated with sodium hydride NaH (7.3×10^{-3} mol, 0.17 g 1.22 equiv.) and a catalytic amount of potassium *tert*-butoxide KO^{t}Bu (3.6×10^{-4} mol, 0.04 g, 0.06 equiv.). The mixture was stirred for 16 h at room temperature, and subsequently filtered on a celite pad. The solution was placed into a Schlenk at 0°C and connected to a SO_2-filled Schlenk line (1 mbar). The solution was stirred 30 min under SO_2 atmosphere. After evaporation, **IMe-^{n}Bu-SO_2** was obtained as a yellow solid (NMR yield = 98 %) in an inseparable 92/8 mixture (1.3 g) with the corresponding salt **IMe-^{n}Bu.HX** (NMR yield = 8 %).

^{1}H NMR (400 MHz, D_2O) δ = 0.92 (t, *J* = 7.2 Hz, 3H, *C*H_3-CH_2); 1.31 (sext, *J* = 7.2 Hz, 2H, CH_3-*C*H_2); 1.84 (qi, *J* = 7.2 Hz, 2H, CH_2-*C*H_2-CH_2); 3.89 (s, 3H, N-CH_3); 4.19 (t, *J* = 7.2 Hz , 2H, N^+CH_2); 7.42 (d, *J* = 1.6 Hz, 1H, H^{Ar}); 7.47 (d, *J* = 1.6 Hz, 1H, H^{Ar}).

^{13}C NMR (100 MHz, D_2O + dioxane) δ = 13.2 (*C*H_3-CH_2); 19.3 (CH_3-*C*H_2); 31.9 (CH_2-*C*H_2-CH_2); 36.2 (N-CH_3) ; 49.8 (N^+CH_2) ; 122.8 (CH^{Ar}); 124.0 (CH^{Ar}); 136.2 (N^+CN).

IR (cm^{-1}) = 961 (m, C-C); 1019 (s, C-C); 1113 (s, S=O); 1171 (w, C-C); 1467 (m, C-C); 1495 (m, C=C^{Ar}); 1568 (m, C=C^{Ar}); 2875 (w, CH); 2935 (m, CH); 2960 (m, CH); 3095 (m, CH).

HRMS (ESI) *m/z* calcd for $C_8H_{14}N_2O_2S$ 202.0776.

Under HRMS conditions, the sulfinate adduct **IMe-^{n}Bu-SO$_2$** decomposed into the 1-butyl-3-methyl-1*H*-imidazol-3-ium hydrogen sulfite **IMe-^{n}Bu.HHSO$_3$**. The cation of **IMe-^{n}Bu.HHSO$_3$** was observed by mass spectroscopy (*m/z* 139.1231 $[M]^+$).

Exposed to air moisture, **IMe-^{n}Bu-SO$_2$** also quickly decomposed into the corresponding hydrogen sulfite salt **IMe-^{n}Bu.HHSO$_3$**.

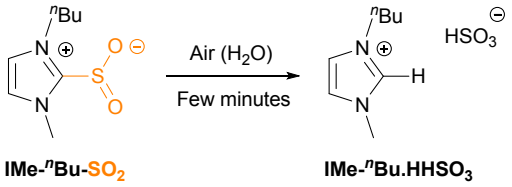

Scheme S1. Decomposition of sulfinate adduct at air.

^{1}H NMR (400 MHz, D_2O) δ = 0.92 (t, *J* = 7.2 Hz, 3H, *C*H_3-CH_2); 1.31 (sext, *J* = 7.2 Hz, 2H, CH_3-*C*H_2); 1.85 (qi, *J* = 7.2 Hz, 2H, CH_2-*C*H_2-CH_2); 3.89 (s, 3H, N-CH_3); 4.19 (t, *J* = 7.2 Hz, 2H, N^+CH_2); 7.42 (m, 1H, H^{Ar}); 7.47 (m, 1H, H^{Ar}); 8.70 (s, 1H, N^+CHN).

^{13}C NMR (100 MHz, D_2O + dioxane) δ = 13.2 (*C*H_3-CH_2); 19.3 (CH_3-*C*H_2); 31.9 (CH_2-*C*H_2-CH_2); 36.2 (N-CH_3); 49.9 (N^+CH_2); 122.8 (CH^{Ar}); 124.1 (CH^{Ar}); 136.4 (N^+CHN).

HRMS (ESI) *m/z* 139.1231 $[M]^+$, calcd for $C_8H_{15}N_2^+$ 139.1230.

IR (cm^{-1}) = 1047 (w, C-C); 1081 (w, C-C); 1166 (s, S=O); 1384 (w, C-C); 1466 (m, C-C); 1571 (m, C=C); 1653 (w, C=N); 2876 (w, CH); 2964 (w, CH); 3100 (w, CH); 3151 (w, CH); 3419 (m, OH).

^{1}H and ^{13}C NMR of **IMe-^{n}Bu.HHSO$_3$** were consistent with the reported spectra of **IMe-^{n}Bu.HHSO$_4$**.[18] Due to the difference of anion, a slight shift of the peaks was observed, notably for the acid hydrogen (N^+CHN).

3-Ethyl-1-methyl-1*H*-imidazol-3-ium-2-sulfinate IMe-Et-SO$_2$ [CAS 2055505-72-9]

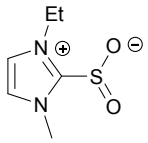

In the glovebox, a solution of 1-ethyl-3-methyl-1*H*-imidazol-3-ium bromide **IMe-Et.HBr** (1.6×10^{-2} mol, 3 g, 1 equiv.) in tetrahydrofuran (50 mL) was treated with sodium hydride NaH (1.9×10^{-2} mol, 0.46 g, 1.22 equiv.) and a catalytic amount of potassium *tert*-butoxide KO^{t}Bu (9.6×10^{-4}, 0.11 g, 0.06 equiv.). The mixture was stirred for 16 h at room temperature, and subsequently filtered on a celite pad. The solution was placed into a Schlenk at 0°C and connected to a SO_2-filled Schlenk line (1 mbar). The solution was stirred 30 min under SO_2 atmosphere. After evaporation, **IMe-Et-SO$_2$** was obtained as a white solid (NMR yield = 90 %) in an inseparable 97/3 mixture (2.6 g) with the corresponding salt **IMe-Et.HX** (NMR yield = 3 %).

^{1}H NMR (400 MHz, D_2O) δ = 1.49 (t, *J* = 7.2 Hz, 3H, *C*H_3-CH_2); 3.89 (s, 3H, N-CH_3); 4.22 (q, *J* = 7.2 Hz, 2H, N^+CH_2); 7.41 (d, *J* = 3.0 Hz, 1H, H^{Ar}); 7.48 (d, *J* = 3.0 Hz, 1H, H^{Ar}).

^{13}C NMR (100 MHz, D_2O + dioxane) δ = 15.1 (*C*H_3-CH_2); 36.2 (N-CH_3); 45.3 (N^+CH_2); 122.4 (CH^{Ar}); 124.0 (CH^{Ar}); 135.9 (N^+CN).

IR (cm^{-1}) = 1092 (s, S=O); 1155 (m, C-C); 1177 (m, C-C); 1502 (w, C=C); 1578 (m, C=C); 1673 (w, C=N); 2982 (w, CH); 3088 (m, CH); 3146 (w, CH).

^{1}H NMR was consistent with the literature.[19]

Exposed to air moisture, **IMe-Et-SO$_2$** quickly decomposed into the corresponding 1-ethyl-3-methyl-1*H*-imidazol-3-ium hydrogen sulfite **IMe-Et.HHSO$_3$**.

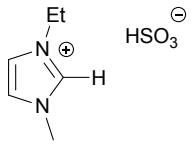

IMe-Et.HHSO$_3$

^{1}H NMR (400 MHz, D_2O) δ = 1.50 (t, *J* = 7.2 Hz, 3H, *C*H_3-CH_2); 3.89 (s, 3H, N-CH_3); 4.22 (q, *J* = 7.2 Hz, 2H, N^+CH_2); 7.41 (m, 1H, H^{Ar}); 7.48 (m, 1H, H^{Ar}); 8.70 (s, 1H, N^+CHN).

^{13}C NMR (100 MHz, D_2O + dioxane) δ = 15.3 (*C*H_3-CH_2); 36.4 (N-CH_3); 45.6 (N^+CH_2); 122.7 (CH^{Ar}); 124.2 (CH^{Ar}); 136.4 (N^+CHN).

IR (cm^{-1}) = 1047 (w, C-C); 1080 (m, C-C); 1166 (s, S=O); 1571 (m, $C=C^{Ar}$); 1641 (m, C=N); 3100 (w, CH); 3149 (w, CH); 3402 (m, OH).

HRMS (ESI) *m/z* 111.0918 $[M]^+$, calcd for $C_6H_{11}N_2^+$ 111.0917.

^{1}H and ^{13}C NMR of **IMe-Et.HHSO$_3$** were consistent with the reported spectra of **IMe-Et.HHSO$_4$**.[18] Due to the difference of anion, a slight shift of the peaks was observed, notably for the acid hydrogen (N^+CHN).

4-(Dimethylamino)-1-methylpyridinium-2-carboxylate, DMAP-Me-CO$_2$

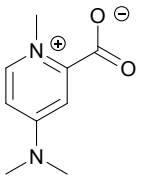

In the glovebox, a solution of 4-(dimethylamino)-1-methylpyridin-1-ium iodide **DMAP-Me.HI** (5.7 x 10^{-3} mol, 1.5 g, 1 equiv.) in tetrahydrofuran (30 mL) was treated with potassium bis(trimethylsilyl)amide (KHMDS 95%) (6.8 x 10^{-3} mol, 1.36 g, 1.2 equiv.). The mixture was stirred for 1 h at room temperature, and subsequently filtered on a celite pad. The solution was placed into a Schlenk and connected to a CO_2-filled Schlenk line (3 mbar). The solution was stirred 16 h under CO_2 atmosphere. The beige solid **DMAP-Me-CO$_2$** (0.71 g, 70%) was obtained after filtration and washing with CH_3CN (2 x 5 mL) and Et_2O (2 x 10 mL).
Procedure reported in Ref.14.

^{1}H NMR (250 MHz, DMSO-d_6): δ = 3.14 (s, 6H, $N(CH_3)_2$); 3.88 (s, 3H, N^+CH_3); 6.76 (d, *J* = 3 Hz, 1H, H^{Ar}); 6.86 (dd, *J* = 3 and 7.5 Hz, 1H, H^{Ar}); 8.05 (d, *J* = 7.5 Hz, 1H, H^{Ar}).

^{13}C NMR (100 MHz, D_2O + dioxane): δ = 40.0 ($N(CH_3)_2$); 43.1 (N^+CH_3); 105.5 (CH); 107.5 (CH); 143.5 (N^+-HC^{Ar}=); 150.9 (C^{Ar}=N^+), 157.2 (C^{Ar}-NMe_2); 168.2 (CO_2^-).

IR (cm^{-1}) = 1297 (s, C-O); 1350 (s, C-N); 1429 (m, C=C); 1564 (s, C=C); 1624 (s, C=O); 3050 (w, CH); 3339 (m, OH).

^{1}H and ^{13}C NMR were consistent with the litterature.[14]

1,3-Dimethyl-1*H*-benzo[*d*]imidazol-3-ium-2-carboxylate, BzIMe-CO_2 [CAS 1449571-31-6]

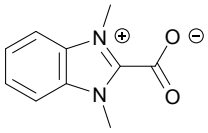

In the glovebox, a solution of 1,3-dimethyl-1*H*-benzo[*d*]imidazol-3-ium iodide **BzIMe.HI** (1.1 x 10^{-2} mol, 3 g, 1 equiv.) in tetrahydrofuran (50 mL) was treated with potassium bis(trimethylsilyl)amide (KHMDS 95%) (1.3 x 10^{-2} mol, 2.62 g, 1.2 equiv.). The mixture was stirred for 16 h at room temperature, and subsequently filtered on a celite pad. The solution was placed into a Schlenk and connected to a CO_2-filled Schlenk line (3 mbar). The solution was stirred 16 h under CO_2 atmosphere. After filtration and washing with THF (2 x 10 mL), **BzIMe-CO_2** was obtained as a white solid (1.90 g, 90%).

^{1}H NMR (400 MHz, DMSO-d_6) δ = 4.14 (s, 6H, N-CH_3); 7.63-7.65 (m, 2H, H^{Ar}); 7.93-7.95 (m, *2*H, H^{Ar}).

^{13}C NMR (100 MHz, DMSO-d_6) δ = 32.6 (2 x N-CH_3); 113.3 (2 x CH^{Ar}); 126.3 (2 x CH^{Ar}); 130.9 (2 x C^{Ar}); 147.6 (N^+CN); 153.9 (CO_2^-).

IR (cm^{-1}) = 1207 (s, C-O); 1485 (w, C=C); 1520 (w, C=C); 1632 (s, C=O).

^{1}H and ^{13}C NMR were consistent with the literature.[20]

3,3'-(Propane-1,3-diyl)bis(1-methyl-1*H*-benzo[*d*]imidazol-3-ium-2-carboxylate), Bis-BzIMe-CO_2

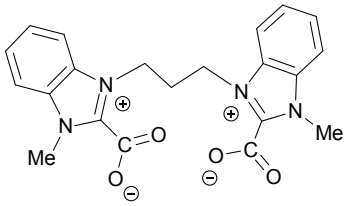

In the glovebox, a solution of 1-methyl-3-(3-(3-methyl-1*H*-benzo[*d*]imidazol-3-ium-1-yl)propyl)-1*H*-benzo[*d*]imidazol-3-ium **Bis-BzIMe.HI** (1.25 x 10^{-3} mol, 0.7 g, 1 equiv.) in tetrahydrofuran (20 mL) was treated with potassium bis(trimethylsilyl)amide (KHMDS 95%) (3.0 x 10^{-3} mol, 0.59 g, 2.4 equiv.). The mixture was stirred for 16 h at room temperature, and subsequently filtered on a celite pad. The solution was placed into a Schlenk and connected to a CO_2-filled Schlenk line (3 mbar). The solution was stirred 16 h under CO_2 atmosphere. After filtration and washing with THF (2 x 10 mL), **Bis-BzIMe-CO_2** was obtained as a white solid (0.45 g, 90%).

^{1}H NMR (400 MHz, DMSO-d_6) δ = 2.46 (m, 2H, CH_2-*C*H_2-CH_2); 4.13 (s, 6H, 2 x N-CH_3); 4.84 (t, *J* = 7.2 Hz, 4H, 2 x N^+CH_2); 7.61-7.64 (m, 4H, H^{Ar}); 7.92-7.99 (m, 4H, H^{Ar}).

^{13}C NMR (100 MHz, DMSO-d_6) δ = 29.0 (CH_2); 32.6 (2 x N-CH_3); 43.4 (2 x N^+CH_2) 113.2 (2 x CH^{Ar}); 113.4 (2 x CH^{Ar}); 126.2 (2 x CH^{Ar}); 126.3 (2 x CH^{Ar}); 129.9 (2 x C^{Ar}); 131.1 (2 x C^{Ar}); 147.5 (2 x N^+CN); 153.6 (2 x CO_2^-).

IR (cm^{-1}) = 1304 (s, C-O); 1361 (w, C-C); 1480 (m, C-C); 1513 (w, C=C); 1669 (s, C=O); 2963 (w, CH); 3030 (w, CH).

HRMS (ESI) *m/z* calcd for $C_{21}H_{20}N_4O_4$ 392.1485.

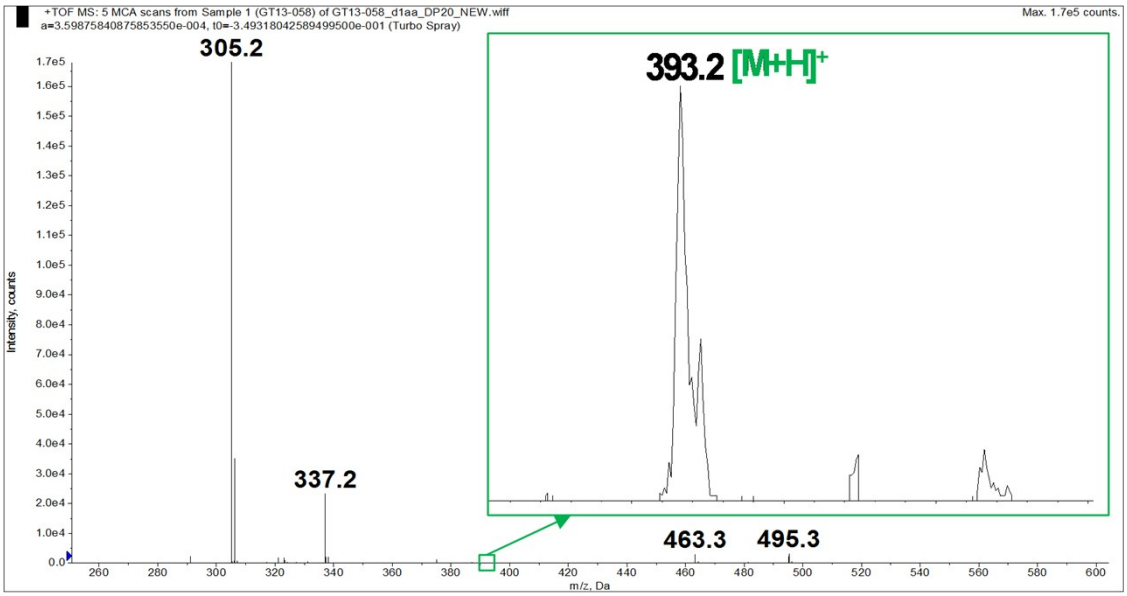

Figure S1. HRMS analysis of **Bis-BzIMe-CO_2**.

Under HRMS conditions, **Bis-BzIMe-CO_2** was not stable. Traces of **BisBzIMe-CO_2** was observed along with various decomposition derivatives formed upon decarboxylation and reaction with oxygen. The following mass was observed by mass spectroscopy and assigned to the most likely structures:

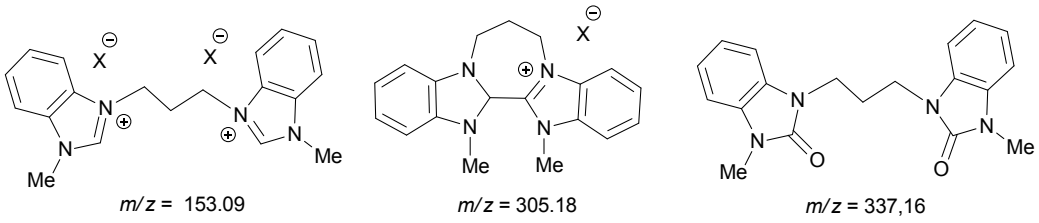

m/z = 153.09 *m/z* = 305.18 *m/z* = 337,16

1,1',3,3'-Tetramethyl-1,1',3,3'-tetrahydro-2,2'-bibenzo[*d*]imidazolinylidene, DiBzIMe [CAS 24648-10-0]

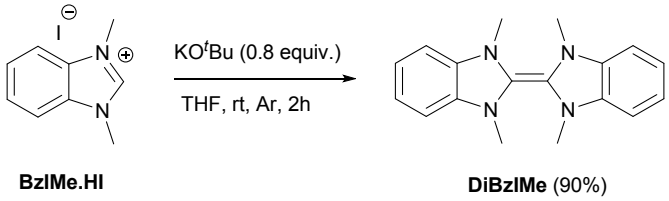

BzIMe.HI **DiBzIMe** (90%)

Scheme S2. Formation of the di-1,3-dimethylbenzimidazolin-2-ylidene **DiBzIMe**.

In the glovebox, potassium *tert*-butoxide KO^{t}Bu (3.0 x 10^{-3} mol, 0.33 g, 0.8 equiv.) was added to a solution of 1,3-dimethyl-1*H*-benzo[*d*]imidazol-3-ium iodide **BzIMe.HI** (3.7 x 10^{-3} mol, 1 g, 1 equiv.) in dry tetrahydrofuran (30 mL). After 2h stirring at room temperature, the reaction mixture was filtered on celite pad. The solvent was removed under vacuum. Pentane was then added in several fractions. After filtration, the di-1,3-dimethylbenzimidazolin-2-ylidene **DiBzIMe** was obtained as a yellow solid (0.49 g, 90%). **DiBzIMe** was stable under inert atmosphere in solid form or in solution in C_6D_6 during several months.

^{1}H NMR (400 MHz, C_6D_6) δ = 2.70 (s, 12H, N-CH_3); 6.44-6.46 (m, 4H, H^{Ar}); 6.79-6.82 (m, 4H, H^{Ar}).

^{13}C NMR (100 MHz, C_6D_6) δ = 36.1 (4 x N-CH_3); 108.6 (4 x CH^{Ar}); 121.1 (4 x CH^{Ar}); 124.5 (2 x C^{Et}); 143.6 (4 x C^{Ar}).

^{1}H and ^{13}C NMR were consistent with the literature.[21]

1,3-Dimethyl-1,3-dihydro-2*H*-benzo[*d*]imidazol-2-one, BzIMeO (4) [CAS 3097-21-0]

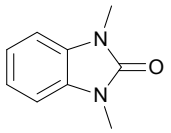

A solution of di-1,3-dimethylbenzimidazolin-2-ylidene **DiBzIMe** (6.8 x 10^{-4} mol, 0.2 g, 1 equiv.) in dry tetrahydrofuran (30 mL) was submitted to an oxygen atmosphere (1 atm). After 1h stirring at room temperature, water was added, and the reaction mixture was extracted with Et_2O (3 x 10 mL). The combined organic layers were washed with water (3 x 20 mL) and dried with Na_2SO_4. After evaporation of the solvent, **BzIMeO** (**4**) was obtained as a brown solid (0.19 g, 84%).

^{1}H NMR (400 MHz, $CDCl_3$) δ = 3.43 (s, 6H, N-CH_3); 6.96-6.99 (m, 2H, H^{Ar}); 7.09-7.12 (m, 2H, H^{Ar}).

^{13}C NMR (100 MHz, $CDCl_3$) δ = 27.3 (2 x N-CH_3); 107.4 (2 x CH^{Ar}); 121.3 (2 x CH^{Ar}); 130.2 (2 x C^{Ar}); 154.8 (C=O).

^{1}H and ^{13}C NMR were consistent with the literature.[22]

1,1',3,3'-Tetramethyl-1*H*,1'*H*-[2,2'-bibenzo[*d*]imidazole]-3,3'-diium salt, DiBzIMe^{2+} (5)

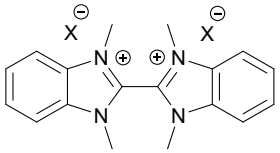

X = I, Cl

In the glovebox, potassium bis(trimethylsilyl)amide (KHMDS 95%) (1.47 x 10^{-2} mol, 2.9 g, 2 equiv.) was added to a solution of 1,3-dimethyl-1*H*-benzo[*d*]imidazol-3-ium iodide **BzIMe.HI** (7.30 x 10^{-3} mol, 2 g, 1 equiv.) in dry tetrahydrofuran (30 mL). After 2h stirring at room temperature, the reaction mixture was filtered on celite pad. A solution of hexachloroethane C_2Cl_6 (1.47 x 10^{-2} mol, 3.48 g, 2 equiv.) in tetrahydrofuran (5 mL) was added to the filtrate and the resulting suspension was stirred for 30 min. After filtration and washing with Et_2O, **DiBzIMe^{2+}** (**5**) was obtained as a brown solid (1.12 g, 85%).

The same oxidation reaction and yields were obtained with iodine I_2 (1.47 x 10^{-2} mol, 3.8 g, 2 equiv.) as oxidant. **DiBzIMe^{2+}** displays the same NMR spectrum with I or Cl as counter ion.

^{1}H NMR (400 MHz, DMSO-d_6) δ = 4.26 (s, 12H, N-CH_3) ; 7.96-7.99 (m, 4H, H^{Ar}); 8.33-8.36 (m, 4H, H^{Ar}).

^{13}C NMR (100 MHz, DMSO-d_6) δ = 34.2 (4 x N-CH_3); 114.7 (4 x CH^{Ar}); 128.8 (4 x CH^{Ar}); 130.6 (4 x C^{Ar}); 133.5 (2 x N^+CN).

HRMS (ESI) *m/z* 146.0841 $[M]^+$, calcd for $C_{18}H_{20}N_4^{2+}$146.0838.

3. Physicochemical analysis of OED-precursors and related derivatives

OED-precursors and related derivatives	T-CO_2 or -SO_2 [°C][a]	υ_{COasym} [cm^{-1}][a]	Wavelength range of the absorption band [nm]	λ_{max} [nm]
IMe-^{n}Bu-SO_2	190	-	235-330	274
DMAP-Me-CO_2	181	1624	230-330	288
IMe-Et-SO_2	160	-	235-330	274
IMe-^{n}Bu-CO_2	141	1657	250-330	274
IMe-CO_2	140	1645	252-330 (weak)	273
BzIMe-CO_2	52, 70, 119	1632	224-330	270, 277
Bis-BzIMe-CO_2	50, 219	1669	231-330	272, 277
I^{t}Bu-CO_2	63, 115	1609	247-330 (weak)	269
DiBzIMe	-	-	264-350	285, 314
DiBzIMe^{2+} (5)	-	-	246-350	300

Table S1. Physicochemical analysis of OED precursors and related derivatives.

[a] Data excerpted from Ref. 14 for **DMAP-Me-CO_2**, **IMe-CO_2** and **I^{t}Bu-CO_2**.

A- Thermogravimetric analysis (TGA) - T-CO_2 or -SO_2 [°C]

TGA analyses were carried out on a Setaram TGA 92-16.18 with argon at 40 mL.h^{-1} as furnace gas and carrier gas. In the glove box, the samples (3-4 mg) were disposed in a Al_2O_3 crucible of 100 µL. Data acquisition was performed using Calisto version 1.4.1. TGA instrument was previously calibrated with copper sulfated penta-hydrated. The temperature scanning rate of 1 K.min^{-1} was applied from 22°C to 300°C. The data were reported in Figure S2 and Table S1. Data excerpted from Ref. 14 for **DMAP-Me-CO_2**, **IMe-CO_2** and **I^{t}Bu-CO_2**.

The degradation of the imidazolium carboxylate **IMe-CO_2** (140°C) and **I^{t}Bu-CO_2** (63°C) followed the same trend than in the literature.[23] The steric hindrance around the carboxylate moiety of **I^{t}Bu-CO_2** decreased the temperature of decomposition. At the solid state, introduction of a longer *N*-butyl chain did not affect the temperature of decomposition (**IMe-^{n}Bu-CO_2** (141°C)). As reported in our previous study, the well-organized arrangement of the solid state of **DMAP-Me-CO_2** induces an overestimated thermal stability with a decomposition at 181°C.[14] In solution, its thermal decarboxylation was estimated at 120°C.

Three events were observed during the decomposition of **BzIMe-CO_2**. Interestingly, the first two decompositions (52°C and 70°C) represented a total loss of mass of 17%, close to the theoretical 23% representing the loss of mass of the carboxylate moiety CO_2. After decarboxylation of **BzIMe-CO_2**, the generated species (supposedly the reducer di-1,3-dimethylbenzimidazolin-2-ylidene **DiBzIMe**) was stable until 119°C, which correlates with the observations of Lemal on the stability of **DiBzIMe**.[24] Increasing the temperature above 120°C led to the decomposition of this species. According to these observations, a low temperature of 50°C should trigger the decarboxylation of **BzIMe-CO_2** while the generated species should have a relatively good stability under thermal conditions. Regarding **Bis-BzIMe-CO_2**, a 10% loss in mass representing the first decarboxylation was observed at 50°C, i.e. at the same temperature than the decarboxylation of **BzIMe-CO_2**. However, no other significant loss of weight was observed before a clearer initiation of decomposition at 219°C. The slow decrease of mass between 77°C and 219°C could indicate a progressive and slow loss of the second CO_2 group.

The sulfinate adduct **IMe-^{n}Bu-SO$_2$** decomposed at high temperature (190°C) compared to its carboxylate counterpart (**IMe-^{n}Bu-CO$_2$**, 141°C). The thermal degradation of **IMe-Et-SO$_2$** followed a complex and progressive decomposition process with a significant loss at 160°C.

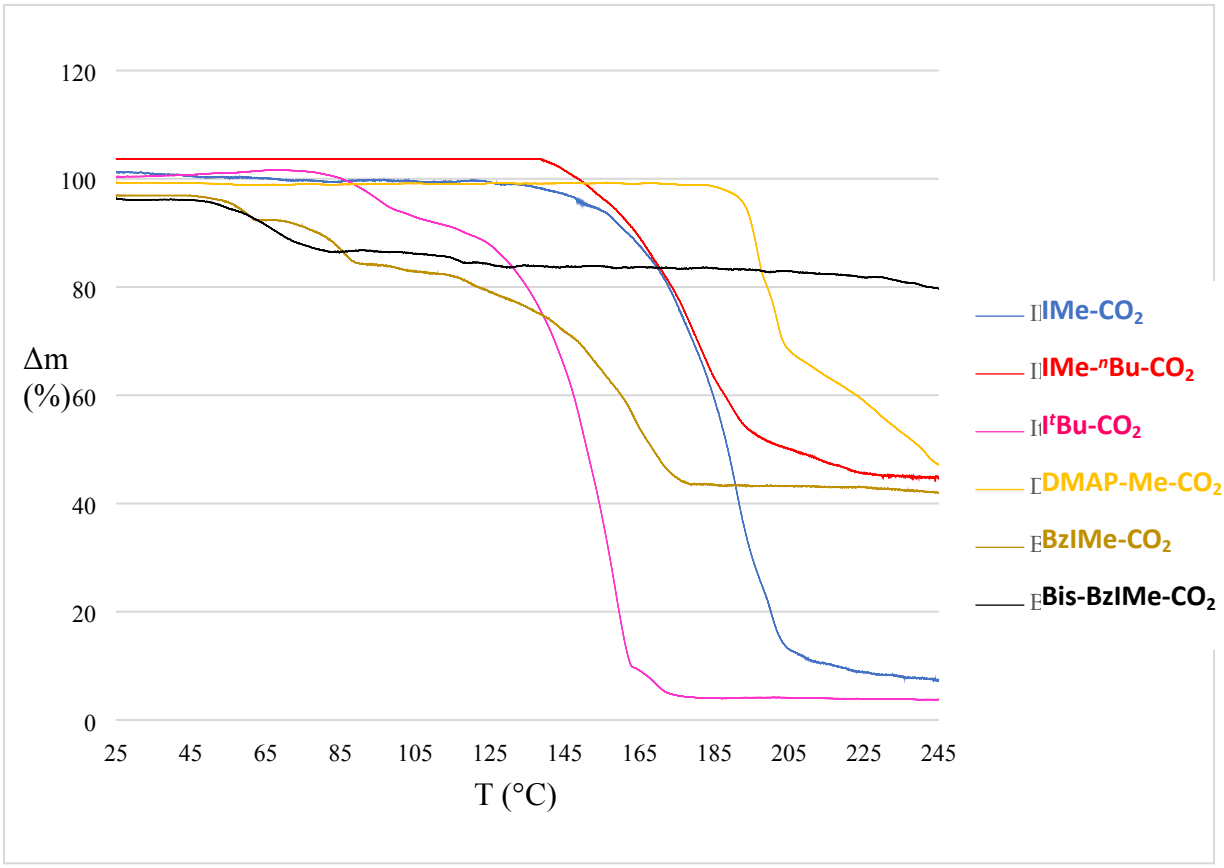

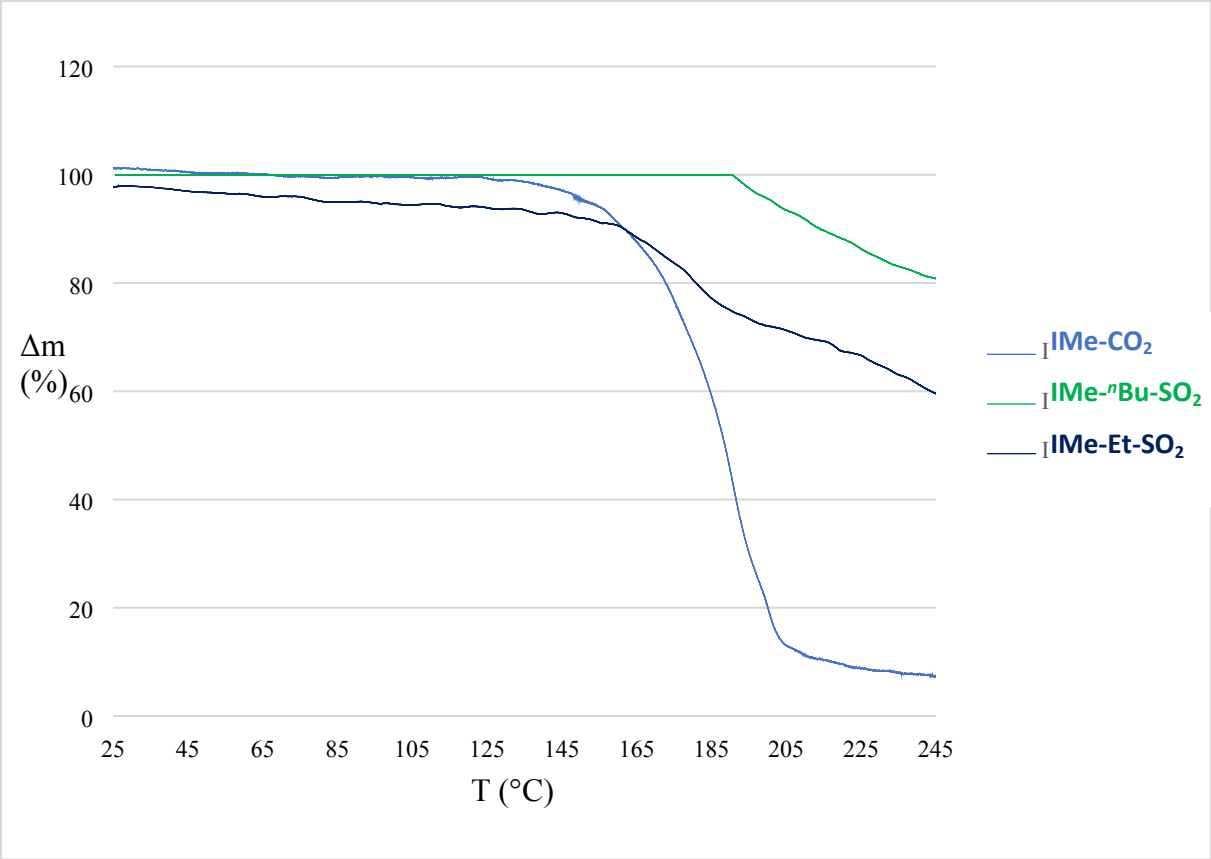

Figure S2. Thermogravimetric analysis of precursors.

B- Infra-Red (IR) frequency analyses of carboxylate adducts - υ_{COasym} [cm $^{-1}$]

IR analyses were carried out on a FTIR spectrometer (Perkin Elmer Spectrum 2), equipped with attenuated total reflectance module (with a diamond internal reflection element) and a standard DTGS detector. Data excerpted from Ref. 14 for **DMAP-Me-CO_2**, **IMe-CO_2** and **I^{t}Bu-CO_2**.

In imidazolium series, J. Louie demonstrated that increasing the steric hindrance around the carboxylate moiety with bulky *N*-substituents led to a diminution of the carbonyl stretching frequency (**IMe-CO_2** 1645 cm^{-1} *vs*. **I^{t}Bu-CO_2** 1609 cm^{-1}).[25] Similarly to TGA, this decrease allows to predict an easier decarboxylation for the **I^{t}Bu-CO_2** precursor. As observed by TGA analyses (Table S1), the carbonyl stretching frequency obtained for **IMe-^{n}Bu-CO_2** (1657 cm^{-1}) (vs. **IMe-CO_2** (1645 cm^{-1})) indicates that the *N*-butyl chain does not bring the expected hindrance on the carboxylate moiety and thus should not ease the decarboxylation of the precursor.

In aminopyridinium (**DMAP-Me-CO_2**, 1624 cm^{-1}) and benzimidazolium series (**BzIMe-CO_2**, 1632 cm^{-1}), the intermediate values of the carbonyl stretching frequencies are in line with an easier decarboxylation of these adducts compared to more thermally stable adducts (**IMe-CO_2** 1645 cm^{-1} and **IMe-^{n}Bu-CO_2** 1657 cm^{-1}). This contrast with the higher frequency value observed for **Bis-BzIMe-CO_2** (1669 cm^{-1}) consistent with the sluggish second decarboxylation observed by TGA.

The difference of carbonyl stretching frequencies between **BzIMe-CO_2** and **IMe-CO_2** that bear the same *N*-methyl groups could be explained by the fact that imidazolinylidenes are more electron rich compared to benzimidazolinylidene carbenes.[26] This higher electron density in **IMe-CO_2** would be partially delocalized towards the CO_2 moiety, in the π * orbital, leading to a strengthened and

shortened C_{NHC}-C_{CO2} bond. The COO^- moiety would thus be closer and more stabilized by the cationic iminium ring, resulting in a higher COO^- asymmetric stretching frequency. Falvey also demonstrated that inductive electron donor substituents on the backbone carbons tend to increase the binding affinity of the CO_2 moiety.[27]

C- UV-absorption spectra

UV-absorption analyses were carried out on an Agilent Technologies Cary 100 UV-visible Spectrophotometer. A solution of 10^{-4} or 10^{-5} mol/L in CH_3CN was prepared for each precursor. The analysis was performed between 200 nm and 800 nm. A scan was realised every 0.1 s and covered 1 nm.

The absorbance of the carboxylate and sulfinate adducts covered a large UV-absorption band, from ca. 224 nm to 330 nm. The maxima of absorbance were observed between 269 nm and 288 nm (Table S1 and Figure S3). Please note that theses UV-absorption wavelengths were out of the range of wavelengths covered by the LED-lamp used for the reduction reactions ($\lambda = 365 \pm 5$ nm).

On the other hand, the di-1,3-dimethylbenzimidazolin-2-ylidene **DiBzIMe** absorbed the light between 264 and 350 nm, close to the wavelength of the LED lamp. This was particularly relevant for our mechanism hypotheses: The water-assisted decarboxylation of the **BzIMe-CO_2** precursor led to the formation of the reducer **DiBzIMe**. Then, UV-irradiations photoexcited the reducer and promoted the electron transfer to the substrate.

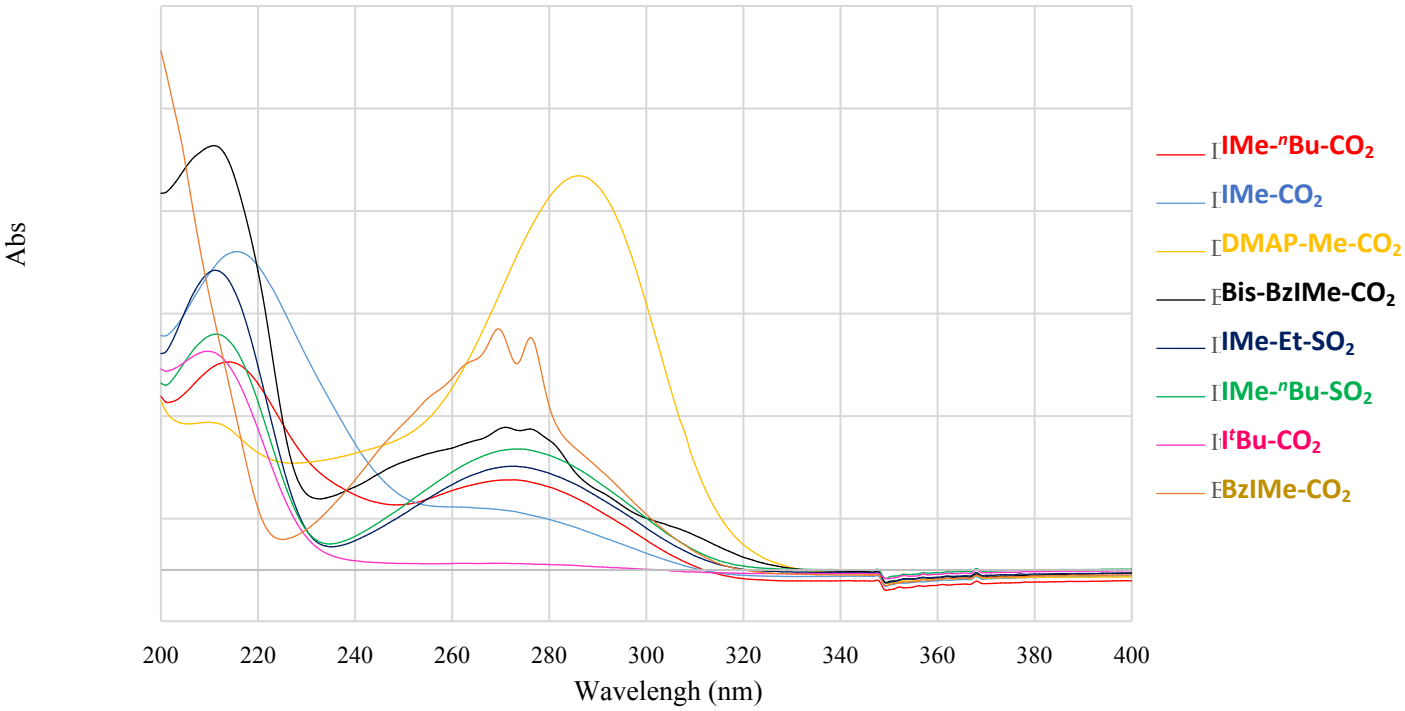

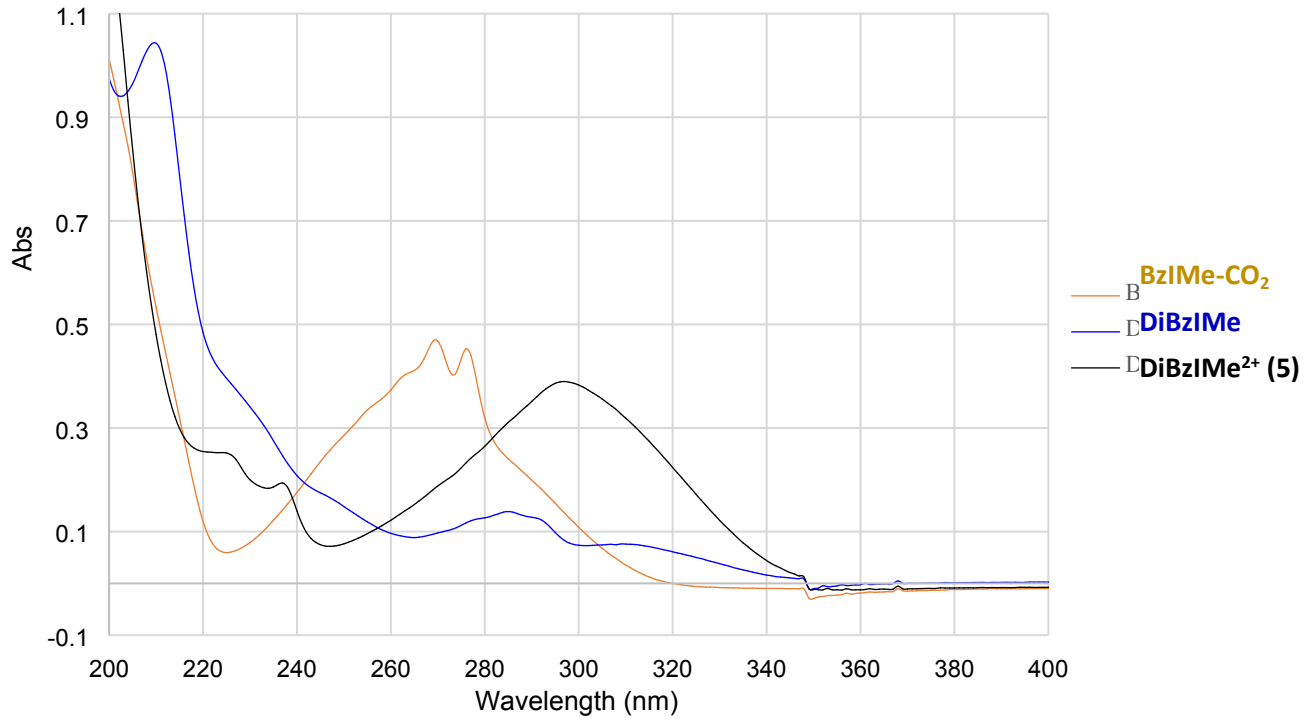

Figure S3. UV-absorbance spectra in CH_3CN of precursors and OED-species.

4. Complementary reactivity and mechanistic data

D- Reactivity under thermal activation of the OED-precursors.

Table S2. Reactivity of the OED precursors under thermal activation. [a]

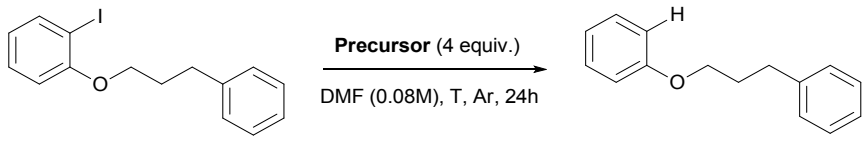

1a **2a**

Entry	Precursor	Temperature (°C)	^{1}H NMR conversion (%)
1	IMe-CO_2	150	>99
2		120	6
3	IMe-^{n}Bu-CO_2	150	49
4	I^{t}Bu-CO_2	150	22
5		70	0
6	DMAP-Me-CO_2	150	>99
7		120	68
8	BzIMe-CO_2	150	88
9	IMe-Et-SO_2	150	>99
10		120	>99
11	IMe-^{n}Bu-SO_2	120	69
12	IMe-^{n}Bu.$HHSO_3$	120	0

[a] Data excerpted from Ref. 14 for **DMAP-Me-CO_2**, **IMe-CO_2** and **I^{t}Bu-CO_2**.

IMe-CO_2 allowed a total reduction of **1a** at 150°C (Entry 1).[14] The temperature was settled following TGA decarboxylation temperature prediction (140°C). A decrease of the temperature led to almost no conversion (Entry 2) as the precursor was not decarboxylated at 120°C.[14] Introduction of a *N*-butyl (Entry 3) or *N*-*tert*-butyl groups (Entries 4-5) on the nitrogen led to a decrease of the conversion rate of the reduction reaction. The steric hindrance was a barrier to the formation of the active diimidazolin-2-ylidene and the corresponding carbene was favoured at this temperature.

Despite a high decomposition temperature predicted by TGA, the aminopyridinium carboxylate **DMAP-Me-CO_2** offered the best reactivity in carboxylate series upon thermal activation at 150°C and 120°C (Entries 6-7).[14] Despite an easy decarboxylation profile, the benzimidazolium **BzIMe-CO_2** afforded 88% of reduction at 150°C (Entry 8). The lower reduction power of the *in situ* generated di-1,3-dimethylbenzimidazolin-2-ylidene **DiBzIMe** probably explained the lower conversion rate observed.

The sulfinate adducts **IMe-Et-SO_2** and **IMe-^{n}Bu-SO_2** allowed a high reduction rate at 120°C (Entries 10-11), demonstrating the easier cleavage of the SO_2 moiety compared to the CO_2 counterpart. Nevertheless, these adducts quickly decomposed at air into the corresponding hydrogen sulfite salt **NHC.$HHSO_3$** (Scheme S1). The latter is not active as precursor (Entry 12). Their poor stability at air storage clearly disqualified sulfinate adducts as convenient OED-precursors.

E- Comparison of the reducer source on the reduction of 1b.

Table S3. Reduction of **1b** using different OED sources.

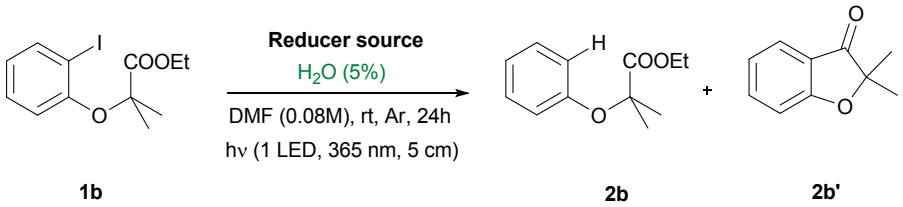

1b **2b** **2b'**

Reducer source	Equiv.	^{1}H NMR conversion % (Yield %)	
		2b	**2b'**
BzIMe-CO_2	4	> 99 (83)	-
DiBzIMe	2	> 99 (80)	-

Under UV-irradiations, water activation of the carboxylate **BzIMe-CO_2** offered the same reactivity than the di-1,3-dimethylbenzimidazolin-2-ylidene **DiBzIMe** ($E_{1/2}$(DMF) = - 0.88 V *vs*. SCE).[28] Generation of the ethyl 2-methyl-2-phenoxypropanoate **2b** and the absence of cyclised compound **2b'** (only obtained through the formation of an aryl anion by DET) argued for a SET mechanism in both cases. Indeed, **DIBzIMe** is known as powerful SET reducer in the reduction of aryl halide derivatives.[29]

F- Stability study of $DiBzIMe^{2+}$ (5)

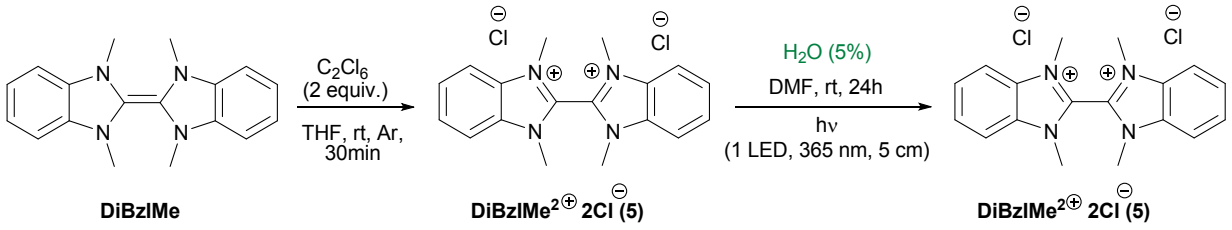

DiBzIMe **$DiBzIMe^{2\oplus}$ 2Cl (5)** **$DiBzIMe^{2\oplus}$ 2Cl (5)**

Scheme S3. Synthesis and stability of the oxidized form **5** under UV-irradiations.

Reaction procedure: In a Schlenk flask, a solution of hexachloroethane C_2Cl_6 (2 equiv.) in tetrahydrofuran (5 mL) was added to a solution of the di-1,3-dimethylbenzimidazolin-2-ylidene **DiBzIMe** (1 equiv.) in dry tetrahydrofuran (0.08 M). The oxidized form **$DiBzIMe^{2+}$** (**5**) immediately precipitated and was isolated as a brown solid (85%) after filtration and washing with Et_2O. **5** was then dissolved in a DMF solution (0.08M) containing 5% of degassed water (35 equiv.). The solution was stirred under UV-irradiations for 24h. After evaporation, the oxidized form **5** was totally retrieved.

Conclusion: At room temperature, DET from the reducer **DiBzIMe** to C_2Cl_6 forms exclusively the oxidized form **5.** Complete recovery of **5** after 24h exposure to UV-irradiations underlined the stability of **5** under the reaction conditions (Scheme S3).

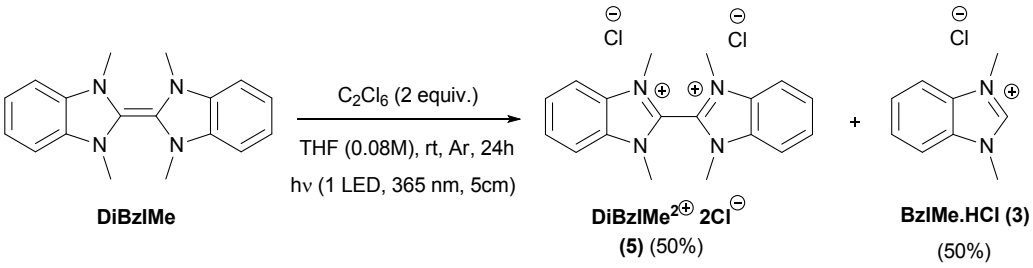

Scheme S4. Formation of the oxidized form **5** under UV-irradiations.

Reaction procedure: In a Schlenk flask, a solution of hexachloroethane C_2Cl_6 (2 equiv.) in tetrahydrofuran (5 mL) was added to a solution of the di-1,3-dimethylbenzimidazolin-2-ylidene **DiBzIMe** (1 equiv.) previously placed under UV-irradiations. After 24h, all the volatiles were removed under vacuum. A mixture of oxidized form **5** and salt **BzIMe.HCl** (**3**) was identified in a 1/1 ratio.

Conclusion: Oxidation of **DiBzIMe** under UV-irradiations led to a mixture of oxidized form **5** and benzimidazolium salt **BzIMe.HCl** (**3**). Knowing that the oxidized form **5** is stable under UV-irradiations (Scheme S3), this result could be explained by the instability of the radical cation **DiBzIMe$^{•+}$** (first ET-oxidation intermediate). Munz[30] showed that **DiBzIMe$^{•+}$** was not persistent and could easily disproportionate, leading to a mixture of the neutral form **DIBzIMe** and the oxidized form **DiBzIMe^{2+}** (**5**). In solution, these two compounds react with each other generating the unstable cation **DiBzIMeH^{+}** which decomposes into benzimidazolium salt **3** and 1,3-dimethylbenzimidazolin-2-ylidene **BzIMe**.[31] Protonation of the carbene also led to salt **3**.

Similarly, hydrogen atom transfer (HAT) to the radical cation **DiBzIMe$^{•+}$** will conduct to the same unstable cation **DiBzIMeH^{+}**, and ultimately to the final salt **3**.

G- Impact of the number of equivalents of the precursor

Table S4. Influence of the number of equivalents of the carboxylate adduct.

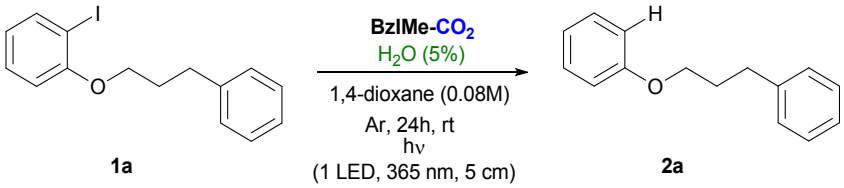

Entry	Equivalent of BzIMe-CO_2	^{1}H NMR conversion (%)
1	0	10
2	1	63
3	2	>99

Change in the number of carboxylate equivalents impacted the reduction of **1a** (Table S4). Under only UV-irradiations, a very small amount of reduced product **2a** was obtained through homolytic cleavage of the Csp^2-I bond (Entry 1, 10%).[32]

One equivalent of carboxylate **BzIMe-CO_2** afforded 63% of reduction (Entry 2) while 2 equivalents led to complete reduction of **1a** (Entry 3). One equivalent of **BzIMe-CO_2** corresponds to the *in situ* formation of 0.5 equivalent of dimer **DiBzIMe**. Theoretically, 50% of reduction should be observed upon SET from **DiBzIMe**, plus 10% of reduction coming from the homolytic cleavage of **1a** under UV-irradiations. Hence, the ca. 63% of reduction can be easily justified.

If the active reducing species at work was the carbene **BzIMe**, *in situ* generation of 1 equivalent of **BzIMe** from 1 equivalent of **BzIMe-CO_2** should have conducted to a full reduction of **1a**. The lower reduction rate (63%) and the known stability of **DiBzIMe** (*vs*. **BzIMe**)[24] are both arguments in favour of the dimer **DiBzIMe** as the active reducer.

H- Formation of DiBzIMe from the carboxylate BzIMe-CO_2

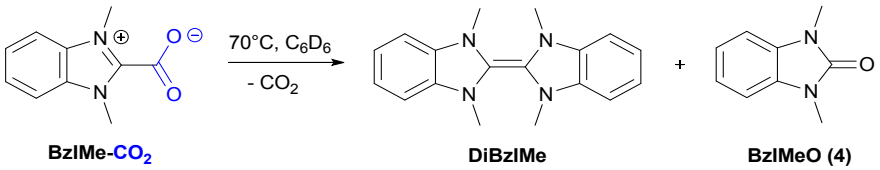

Scheme S5. Formation of **DiBzIMe** from the carboxylate **BzIMe-CO_2**.

Reaction procedure: **BzIMe-CO_2** was added to a J-Young tube containing C_6D_6 solvent under argon. **BzIMe-CO_2** was not soluble in C_6D_6 at room temperature. After few minutes at 70°C, **BzIMe-CO_2** slowly and partially solubilized. The solution became bright yellow, matching with the color of **DiBzIMe** in C_6D_6. The heating temperature of 70°C was chosen according to the indications of the TGA for **BzIMe-CO_2**. Some vacuum cycles were performed to help remove the CO_2 released during the activation of the carboxylate precursor. The decarboxylation reaction was monitored by NMR analysis.

Conclusions: ^{1}H and ^{13}C spectra confirmed the progressive formation of the di-1,3-dimethylbenzimidazolin-2-ylidene **DiBzIMe** upon heating (Figure S4). As expected, no trace of corresponding carbene was detected, even after several days at 70°C. The 1,3-dimethylbenzimidazolin-2-one **BzIMeO** (**4**) was also formed during this thermal activation and was attributed to residual oxygen in the C_6D_6 solvent.

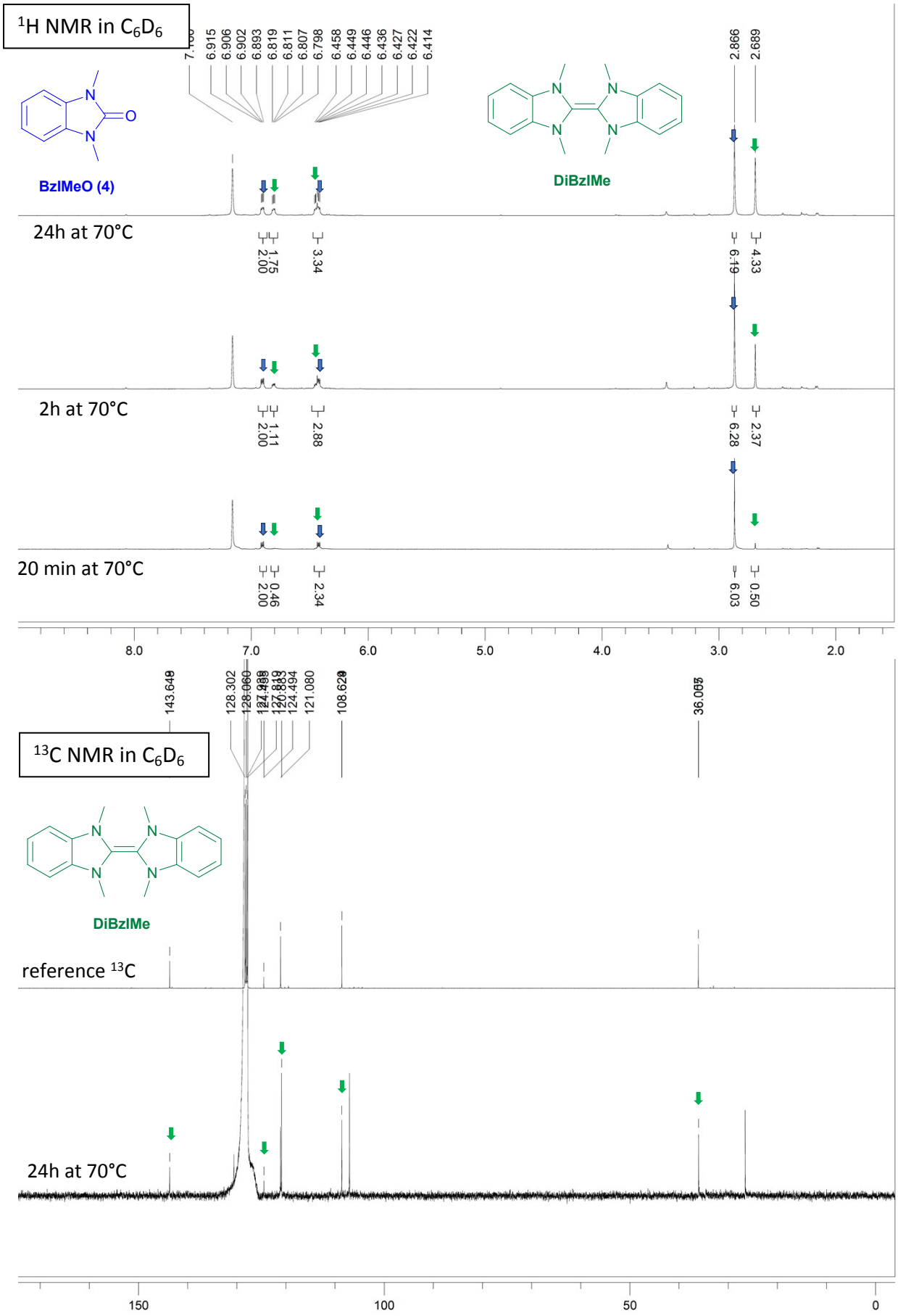

Figure S4. ^{1}H and ^{13}C NMR spectra of the thermal activation of **BzIMe-CO_2** and *in situ* formation of **DiBzIMe**.

5. Procedures for the reduction reactions

Reactions under UV-irradiations were performed with the LED Light Source LIGHTNINGCURE™ LC-L1 V5 of Hamamatsu (Wavelength 365 ± 5 nm, UV light intensity: 14000 mW/cm^2). To evaluate the impact of homolytic cleavage, blank tests using only UV-irradiations were performed with all the substrates. They were all stable or slightly reduced (< 10%) upon 24h exposure under UV-irradiations (1 LED, 5 cm between the reaction and the LED) in the presence of 35 equivalents of water (5%), in different solvents (1,4-dioxane, THF, CH_3CN or DMF). The heat generated by the LED was dissipated by 2 fans placed close to the Schlenk. The reaction media temperature did not exceed 30°C.

General procedure for reduction reactions:

Reaction prepared in the glovebox: **BzIMe-CO_2** (5.91 x 10^{-4} mol, 112 mg, 4 equiv., i.e. 2 equiv of the corresponding **DiBzIMe**) was added to a Schlenk flask containing a solution of the appropriate substrate (1.5 x 10^{-4} mol, 1 equiv.) in dry 1,4-dioxane (1.8 mL, 0.08 M). Out of the glovebox, the reaction flask was connected to a nitrogen line, equipped with a bubbler. 35 equivalents (5.18 x 10^{-3} mol, 0.1 mL) of degassed water were added, and the solution was stirred under UV-irradiations. After 24h, the reaction crude was diluted with water (1.5 mL). The aqueous phase was extracted with Et_2O (3 x 5 mL). The combined organic layers were then washed with brine (2 x 20 mL), dried over sodium sulfate, filtered, and concentrated under vacuum.

Reaction set-up in air: **BzIMe-CO_2** (5.91 x 10^{-4} mol, 112 mg, 4 equiv., i.e. 2 equiv of the corresponding **DiBzIMe**) was added to a Schlenk flask containing a solution of the appropriate substrate (1.5 x 10^{-4} mol, 1 equiv.) in dry 1,4-dioxane (1.8 mL, 0.08 M). The reaction flask was connected to a nitrogen line and degassed under N_2. 35 equivalents (5.18 x 10^{-3} mol, 0.1 mL) of degassed water were added, and the solution was stirred under UV-irradiations. After 24h, the reaction crude was diluted with water (1.5 mL). The aqueous phase was extracted with Et_2O (3 x 5 mL). The combined organic layers were then washed with brine (2 x 20 mL), dried over sodium sulfate, filtered, and concentrated under vacuum.

3-(Phenoxypropyl)benzene, 2a [CAS 64806-63-9]

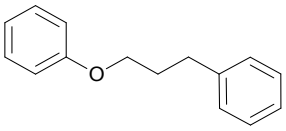

Starting from 1-iodo-2-(3-phenoxypropylbenzene) **1a** (50 mg), 3-(phenoxypropyl) benzene **2a** was obtained after column chromatography (eluent: petroleum ether) as a yellow oil (29 mg, 90%).

Starting from 1-iodo-4-(3-phenoxypropylbenzene) **1h** (50 mg), 3-(phenoxypropyl) benzene **2a** was obtained after column chromatography (eluent: petroleum ether) as a yellow oil (25 mg, 81%).

^{1}H NMR (250 MHz, $CDCl_3$): δ = 2.08-2.15 (m, 2H, CH_2); 2.82 (t, *J* = 7.2 Hz, 2H, *Ph*-CH_2); 3.97 (t, *J* = 6.4 Hz, 2H, O-CH_2); 6.89-6.94 (m, 3H, H^{Ar}); 7.20-7.23 (m, 3H, H^{Ar}); 7.27-7.31 (m, 4H, H^{Ar}).

Ethyl 2-methyl-2-phenoxypropanoate, 2b [CAS 18672-04-3]

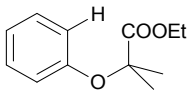

Starting from ethyl 2-(2-iodophenoxy)-2-methylpropanoate **1b** (50 mg), ethyl 2-methyl-2-phenoxypropanoate **2b** was obtained after column chromatography (eluent: petroleum ether) as a colorless oil (25 mg, 83%).

^{1}H NMR (400 MHz, $CDCl_3$): δ = 1.24 (t, *J* = 7.2 Hz, 3H, *C*H_3-CH_2), 1.59 (s, 6H, 2 x CH_3); 4.23 (q, *J* = 7.2 Hz, 2H, CH_3-*C*H_2), 6.82-6.86 (m, 2H, H^{Ar}); 6.97-7.00 (m, 1H, H^{Ar}); 7.21-7.26 (m, 2H, H^{Ar}).

Ethyl 2,2-dimethyl-3-phenylpropanoate, 2c [CAS 94800-92-7]

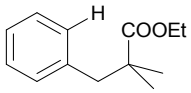

Starting from ethyl 2-(2-iodobenzyl)-2-methylpropanoate **1c** (50 mg), ethyl 2,2-dimethyl-3-phenylpropanoate **2c** was obtained after column chromatography (eluent: petroleum ether) as a yellow oil (30 mg, 99%).

^{1}H NMR (400 MHz, $CDCl_3$): δ = 1.18 (s, 6H, 2 x CH_3); 1.23 (t, *J* = 7.2 Hz, 3H, *C*H_3-CH_2), 2.86 (s, 2H, *Ph*-CH_2), 4.11 (q, *J* = 7.2 Hz, 2H, CH_3-*C*H_2), 7.11-7.13 (m, 2H, H^{Ar}); 7.20-7.27 (m, 3H, H^{Ar}).

Methyl benzoate, 2d [CAS 93-58-3]

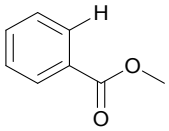

Starting from methyl 2-iodobenzoate **1d** (39 mg), methyl benzoate **2d** was obtained after column chromatography (eluent: petroleum ether/diethyl ether (80/20)) as a yellow oil (19 mg, 95%).

^{1}H NMR (400 MHz, $CDCl_3$): δ = 3.92 (s, 3H, O-CH_3), 7.44 (t, *J* = 7.2 Hz, 2H, H^{Ar}); 7.56 (t, *J* = 7.2 Hz, 1H, H^{Ar}); 8.04 (d, *J* = 7.2 Hz, 2H, H^{Ar}).

Acetophenone, 2e [CAS 98-86-2]

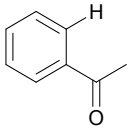

Starting from methyl 2-iodoacetophenone **1e** (36 mg), acetophenone **2e** was obtained after column chromatography (eluent: petroleum ether/diethyl ether (80/20)) as a colorless oil (17 mg, 99%).

^{1}H NMR (400 MHz, $CDCl_3$): δ = 2.61 (s, 3H, CH_3), 7.45-7.83 (m, 2H, H^{Ar}); 7.54-7.58 (m, 1H, H^{Ar}); 7.95-7.98 (m, 2H, H^{Ar}).

3-Methylbenzonitrile, 2f [CAS 620-22-4]

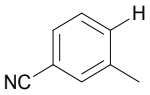

Starting from 4-bromo-3-methylbenzonitrile **1f** (29 mg), 3-methylbenzonitrile **2f** was obtained in an inseparable mixture with **1f** (19 mg) (Conv: 17%, NMR Yield: 12%).

^{1}H NMR (250 MHz, $CDCl_3$): δ = 2.42 (s, 1H, CH_3); 7.51-7.54 (m, 4H, H^{Ar}).

Indole, 2g [CAS 120-72-9]

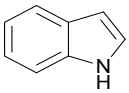

Starting from 1-*p*-toluenesulfonyl-1*H*-indole **1g** (40 mg), indole **2g** was obtained after column chromatography (eluent: hexane/ethyl acetate 5/1) as a colorless oil. (10 mg, 58%).

^{1}H NMR (250 MHz, $CDCl_3$): δ = 6.58 (s, 1H, H^{Ar}); 7.10-7.27 (m, 3H, H^{Ar}); 7.41 (d, *J* = 8.0 Hz, 1H, H^{Ar}); 7.68 (d, *J* = 8.0 Hz, 1H, H^{Ar}); 8.12 (br s, 1H, NH).

Naphtalene, 2i [CAS 91-20-3]

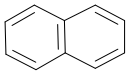

Starting from 1-iodonaphtalene **1i** (38 mg), naphthalene **2i** was obtained as a light orange oil (8 mg, 42%).

^{1}H NMR (250 MHz, $CDCl_3$): δ = 7.49-7.53 (m, 4H, H^{Ar}); 7.86-7.90 (m, 4H, H^{Ar}).

3-methyl-2,3-dihydrobenzofuran, 7 [CAS 13524-73-7] and 3-(iodomethyl)-2,3-dihydrobenzofuran, 8 [CAS 78739-83-0]

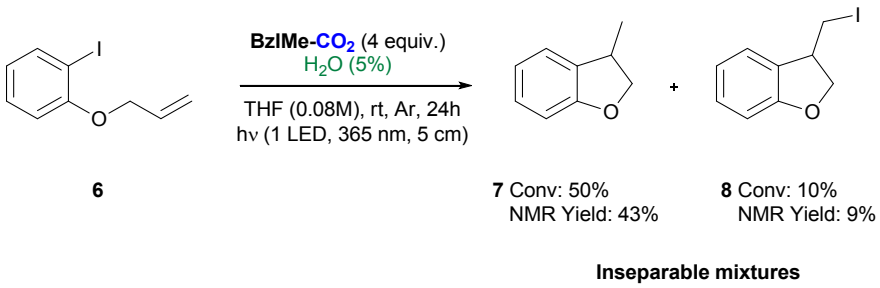

Scheme S6. Reduction of **6**.

Starting from 1-iodo-2-(2-propen-1-yloxy)-benzene **6** (38 mg), partial reduction gave an inseparable mixture (25 mg) of **6**, **7** and **8** after column chromatography (eluent: petroleum ether). Yields were calculated from the ratio determined by ^{1}H NMR.

^{1}H NMR of **7** (400 MHz, $CDCl_3$): δ = 1.33 (d, *J* = 6.8 Hz, 3H, CH_3); 3.54 (m, 1H, *C*H-CH_3), 4.07 (t, *J* = 8.8 Hz, 1H, O-CH_2); 4.68 (t, *J* = 8.8 Hz, 1H, O-CH_2); 6.80 (m, 1H, H^{Ar}), 6.88 (m, 1H, H^{Ar}) 7.12 (m, 2H, H^{Ar}).

^{1}H NMR of **8** (400 MHz, $CDCl_3$): δ = 3.21 (t, *J* = 9.6 Hz, 1H, O-CH_2); 3.46 (dd, *J* = 4 and 9.6 Hz, 1H, CH_2-I); 3.84 (m, 1H, CH); 4.34 (dd, *J* = 4 and 9.6 Hz, 1H, CH_2-I); 4.65 (t, *J* = 9.6 Hz, 1H, O-CH_2); 6.80 (m, 1 H, H^{Ar}); 6.89 (m, 1H, H^{Ar}); 7.22 (m, 2H, H^{Ar}).

Formation of **8** under UV irradiations:

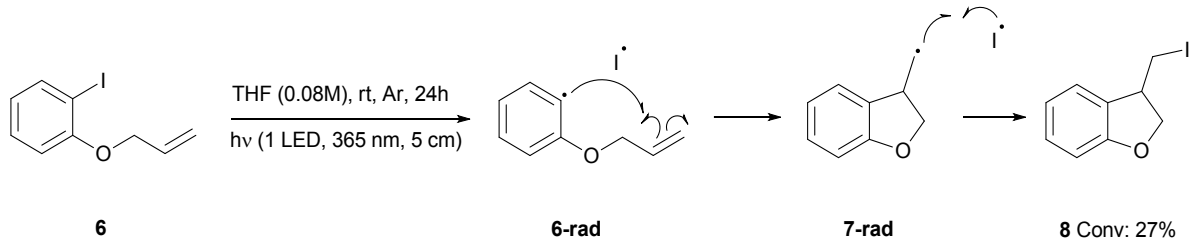

Scheme S7. Mechanism for the formation of **8**.

Homolytic cleavage of the C-I bond under UV-irradiations generated the aryl radical **6-rad** and iodide radical. [29] 5-*exo-trig* cyclisation of **6-rad** gave **7-rad**. Recombination of the radical **7-rad** with iodide radical gave **8** (Starting material **6** accounted for the mass balance).

3-Isopropyl-2,3-dihydrobenzofuran, 10 [CAS 3279-17-2] and 3-(Prop-1-en-2-yl)-2,3-dihydrobenzofuran, 11 [CAS 188474-98-8]

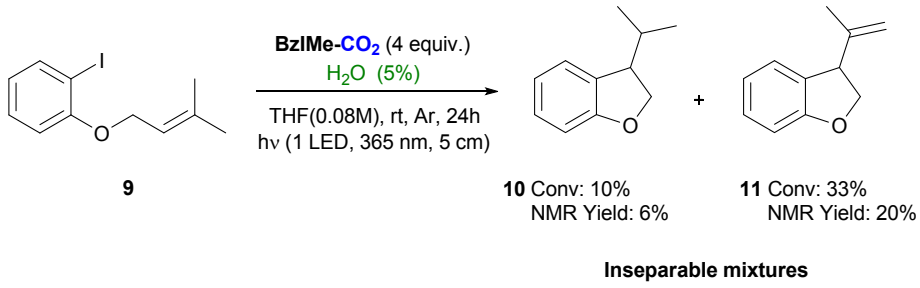

Scheme S8. Reduction of **9**.

Starting from 1-iodo-2-((3-methylbut-2-en-1-yl)oxy)benzene **9** (38 mg), partial reduction gave an inseparable mixture (20 mg) of **9**, **10** and **11** after column chromatography (eluent: petroleum ether). Yields were calculated from the ratio determined by ^{1}H NMR.

^{1}H NMR of **10** (400 MHz, $CDCl_3$): δ = 0.88 (d, *J* = 6.8 Hz, 3H, CH_3), 0.96 (d, *J* = 6.8 Hz, 3H, CH_3), 1.9 (m, 1H, *C*H(CH_3)$_2$), 3.33 (m,1H, *C*H-CH(CH_3)$_2$), 4.37 (m, 1H, O-CH_2), 4.50 (m, 1H, O-CH_2), 6.70 (m, 1H, H^{Ar}), 6.80 (m, 1H, H^{Ar}), 7.04 (m, 1H, H^{Ar}), 7.10 (m, 1H, H^{Ar}).

^{1}H NMR of **11** (400 MHz, $CDCl_3$): δ = 1.44 (s, 3H, CH_3); 4.35 (t, *J* = 10.7 Hz, 1H, O-CH_2); 4.65 (t, *J* = 10.7 Hz, 1H, O-CH_2); 4.86 (m, 1H, H^{Et}); 4.89 (m, 1H, H^{Et}); 5.06 (m, 1H, *C*H-C=CH_2); 6.67-7.28 (m, 4H, H^{Ar}).

(2-(4-Chlorophenyl)ethane-1,1-diyl)dibenzene, 14 [CAS 88382-66-5]

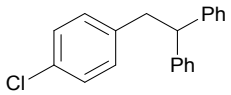

Starting from 1-chloro-4-iodobenzene **12** (35 mg, 1 equiv.) and ethene-1,1-diyldibenzene **13** (36 mg, 3 equiv.), (2-(4-chlorophenyl)ethane-1,1-diyl)dibenzene **14** was formed. After plug filtration on silica gel (eluent: hexane), **14** (NMR Yield: 36%) was obtained in mixtures with the residual alkene **13** (NMR Yield: 6%) as a brown oil (20mg).

^{1}H NMR (400 MHz, $CDCl_3$): δ = 3.32 (d, *J* = 8 Hz, 2H, CH_2); 4.17 (t, *J* = 8 Hz, 1H, *Ph*-CH-*Ph*); 6.91 (d, *J* = 8.4 Hz, 2H, H^{Ar}); 7.13 (d, *J* = 8.4 Hz, 2H, H^{Ar}); 7.16-7.34 (m, 10H, H^{Ar}).

2-(4-Chlorophenyl)-1-methyl-1*H*-pyrrole, 17 [CAS 136146-68-4]

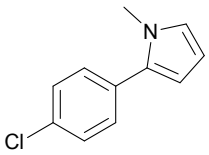

Starting from 1-chloro-4-iodobenzene **12** (35 mg, 1 equiv.) and 1-methyl-1H-pyrrole **16** (36 mg, 3 equiv.), 2-(4-chlorophenyl)-1-methyl-1H-pyrrole **17** was obtained after plug filtration on silica gel (eluent: petroleum ether/ diethyl ether (80/20)) as a brown oil (20mg, 72%).

^{1}H NMR (400 MHz, $CDCl_3$): δ = 3.65 (s, 3H, N-CH_3); 6.19-6.22 (m, 2H, CH^{pyrol}); 6.72 (t, *J* = 2 Hz, 1H, CH^{pyrol}); 7.31-7.38 (m, 4H, H^{Ar}).

1,3-Dimethyl-1*H*-benzo[*d*]imidazol-3-ium hydrogencarbonate, BzIMe.HHCO$_3$ (3) [CAS 31488-67-2]

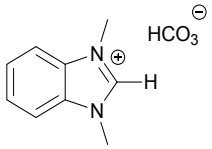

Using **BzIMe-CO$_2$** as precursor, the carbonate salt **3** was recovered in the aqueous phase from the treatment of the reduction reactions.

^{1}H NMR (400 MHz, D_2O) δ = 4.09 (s, 6H, N-CH_3); 7.69-7.71 (m, 2H, H^{Ar}); 7.83-7.86 (m, 2H, H^{Ar}).

^{13}C NMR (100 MHz, D_2O + dioxane) δ = 33.5 (2 x N-CH_3); 113.5 (2 x CH^{Ar}); 127.4 (2 x CH^{Ar}); 132.5 (2 x C^{Ar}); 142.2 triplet (N^+CN); 161.2 (HCO_3).

^{1}H and ^{13}C NMR were consistent with the literature.[33]

NMR spectra

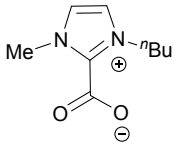

IMe-^{n}Bu-CO_2
(DMSO-d_6)

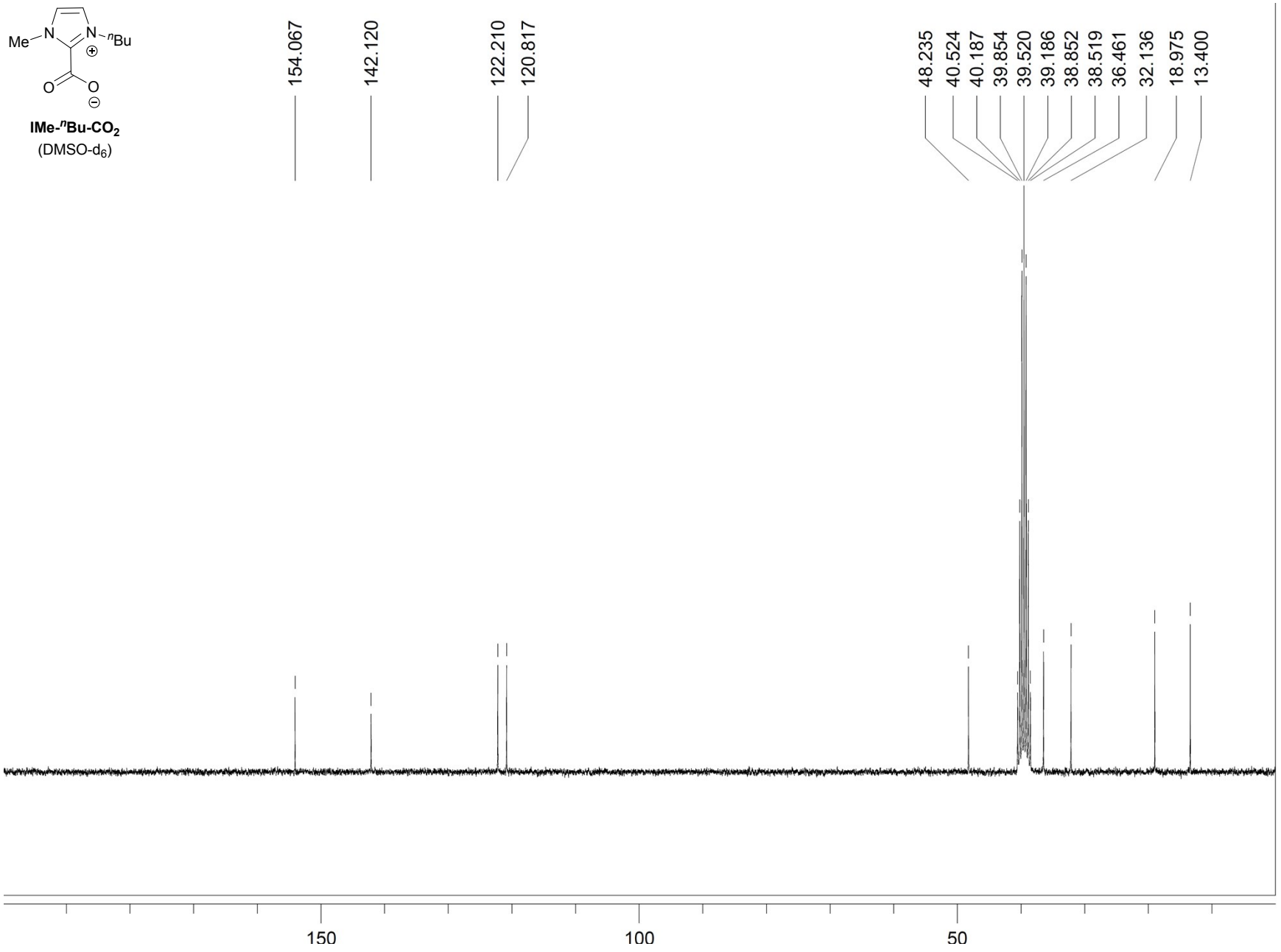
Me
N
N
nBu
O
O
IMe-nBu-CO2
(DMSO-d6)
154.067
142.120
122.210
120.817
48.235
40.524
40.187
39.854
39.520
39.186
38.852
38.519
36.461
32.136
18.975
13.400
150
100
50

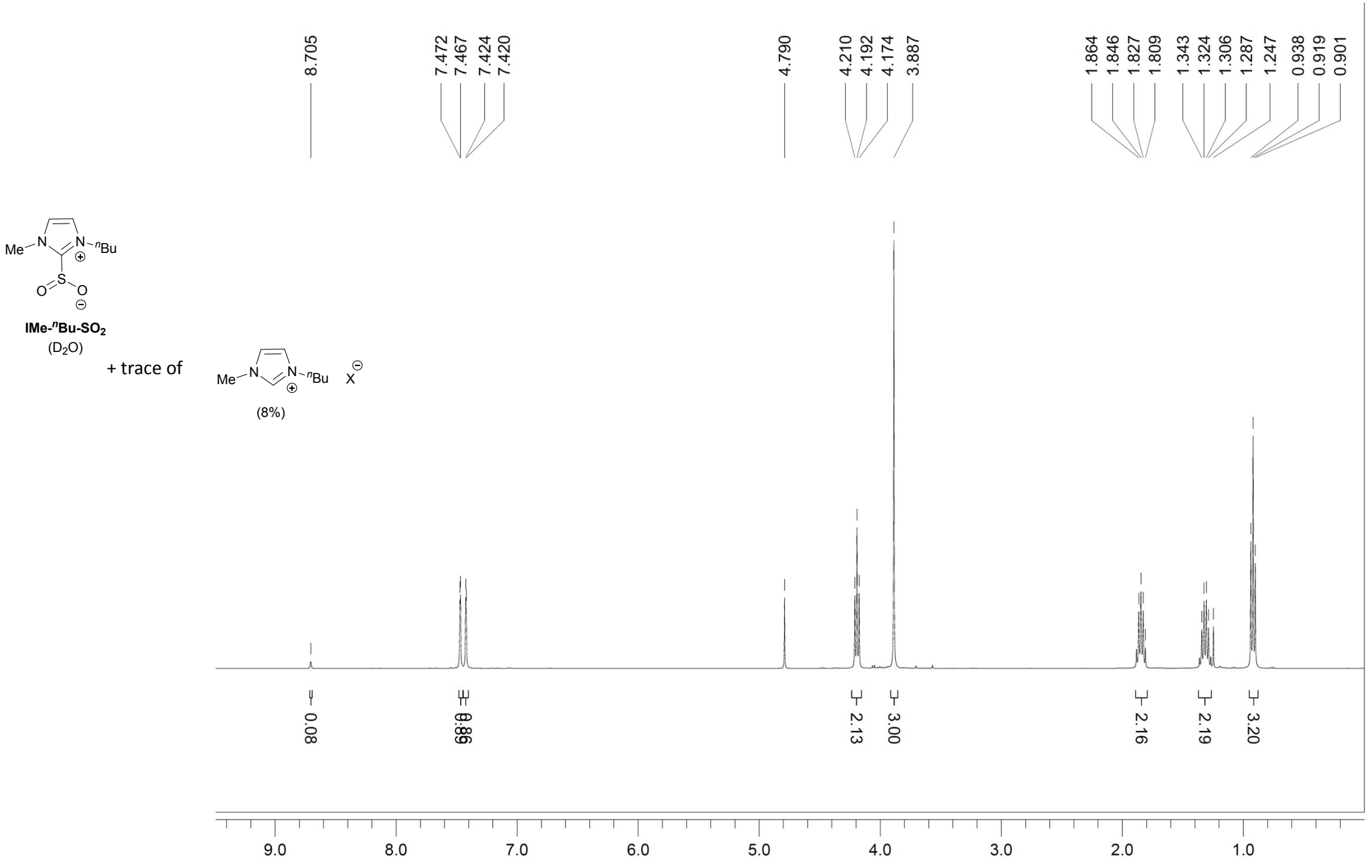
8.705
7.472
7.467
7.424
7.420
4.790
4.210
4.192
4.174
3.887
1.864
1.846
1.827
1.809
1.343
1.324
1.306
1.287
1.247
0.938
0.919
0.901
Me
N
N
nBu
S
O
O
IMe-nBu-SO2
(D2O)
+ trace of
Me
N
N
nBu
X
(8%)
0.08
0.86
0.89
2.13
3.00
2.16
2.19
3.20
9.0
8.0
7.0
6.0
5.0
4.0
3.0
2.0
1.0

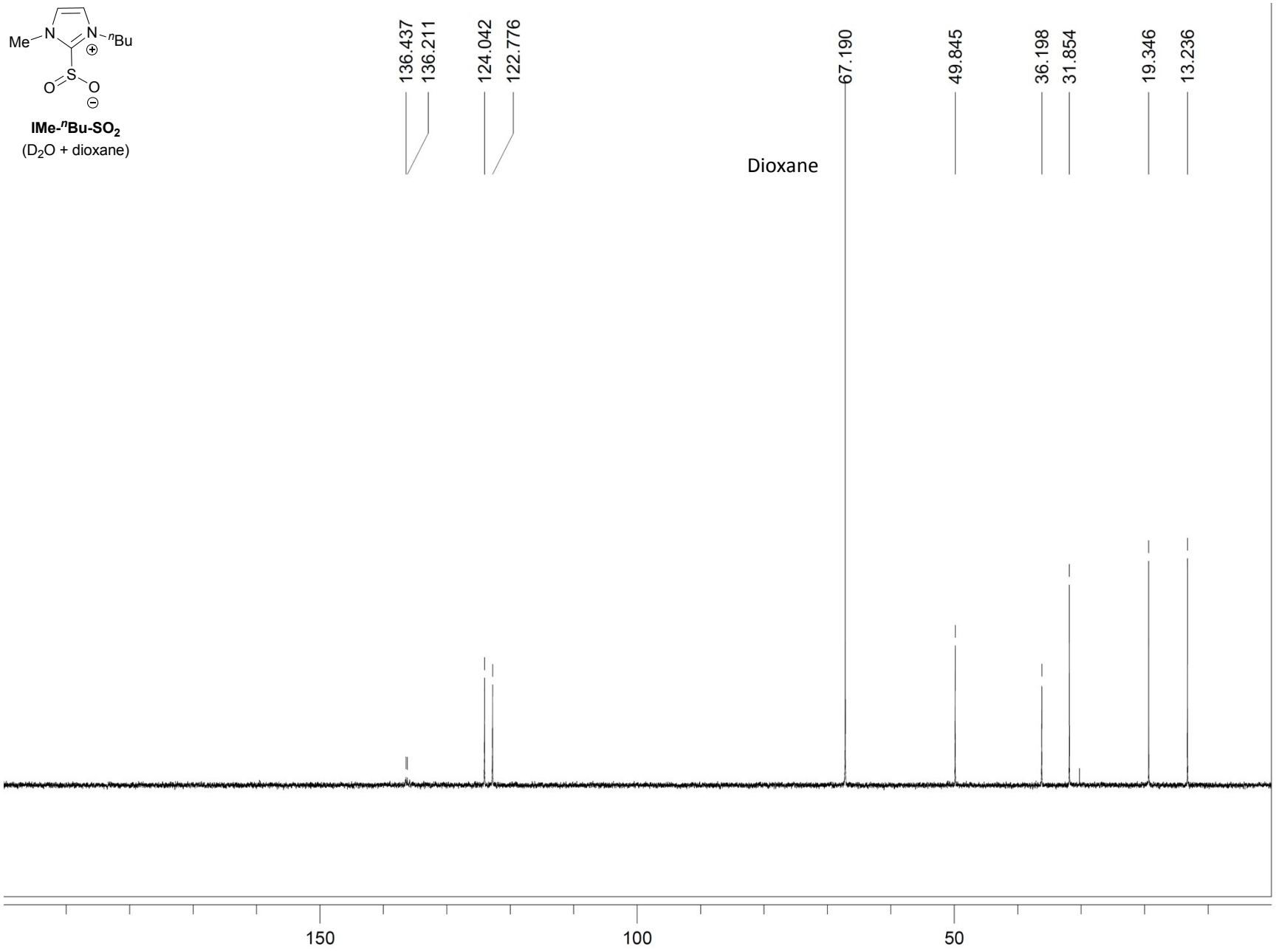
Me
N
N
nBu
S
O
O
IMe-nBu-SO2
(D2O + dioxane)
136.437
136.211
124.042
122.776
67.190
49.845
36.198
31.854
19.346
13.236
Dioxane
150
100
50

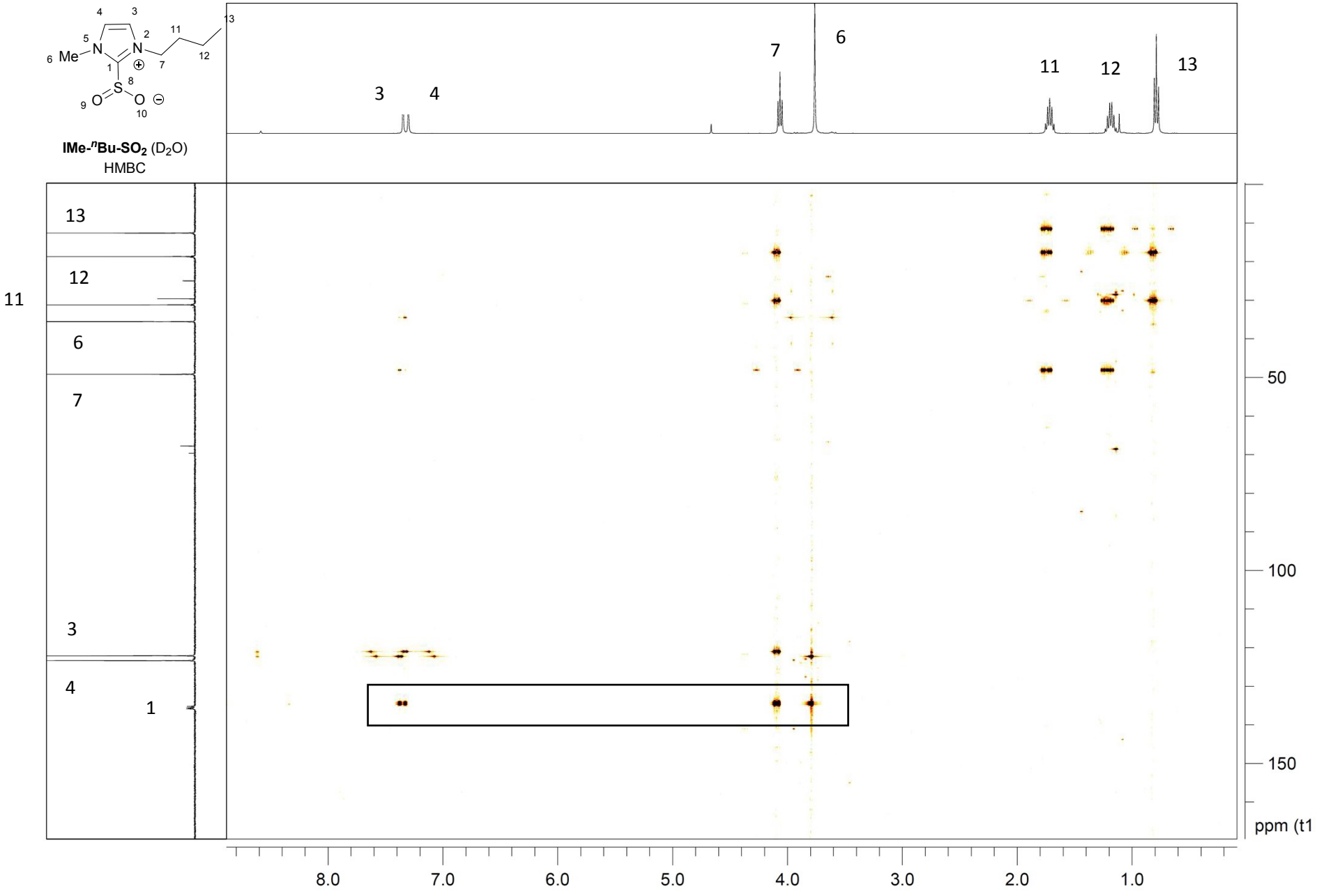
IMe-nBu-SO2 (D2O)
HMBC
3
4
7
6
11
12
13
1
ppm (t1
8.0
7.0
6.0
5.0
4.0
3.0
2.0
1.0
50
100
150

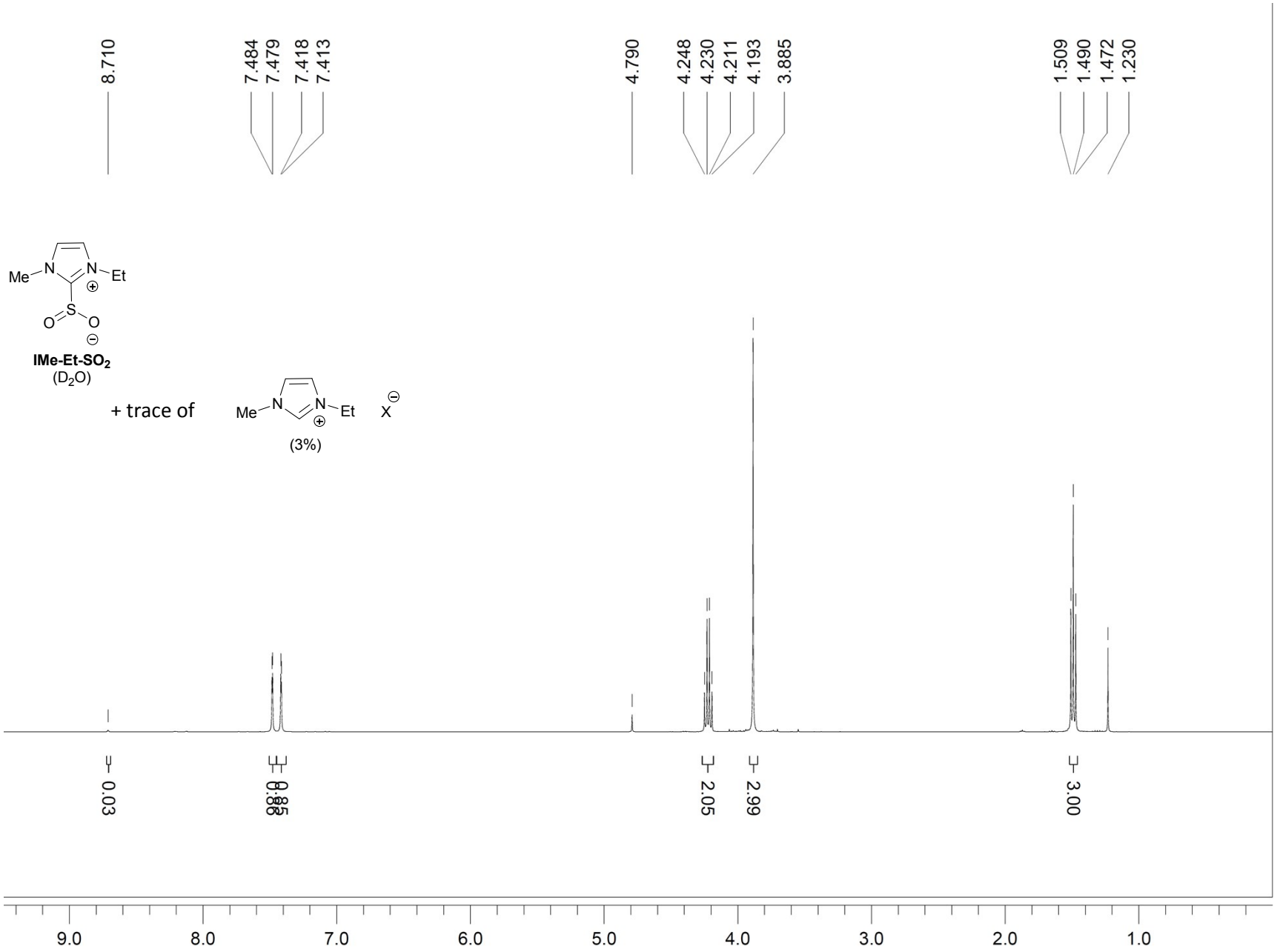
8.710
7.484
7.479
7.418
7.413
4.790
4.248
4.230
4.211
4.193
3.885
1.509
1.490
1.472
1.230
Me
N
N
Et
S
O
O
IMe-Et-SO2
(D2O)
+ trace of
Me
N
N
Et
X
(3%)
0.03
0.85
0.85
2.05
2.99
3.00
9.0
8.0
7.0
6.0
5.0
4.0
3.0
2.0
1.0

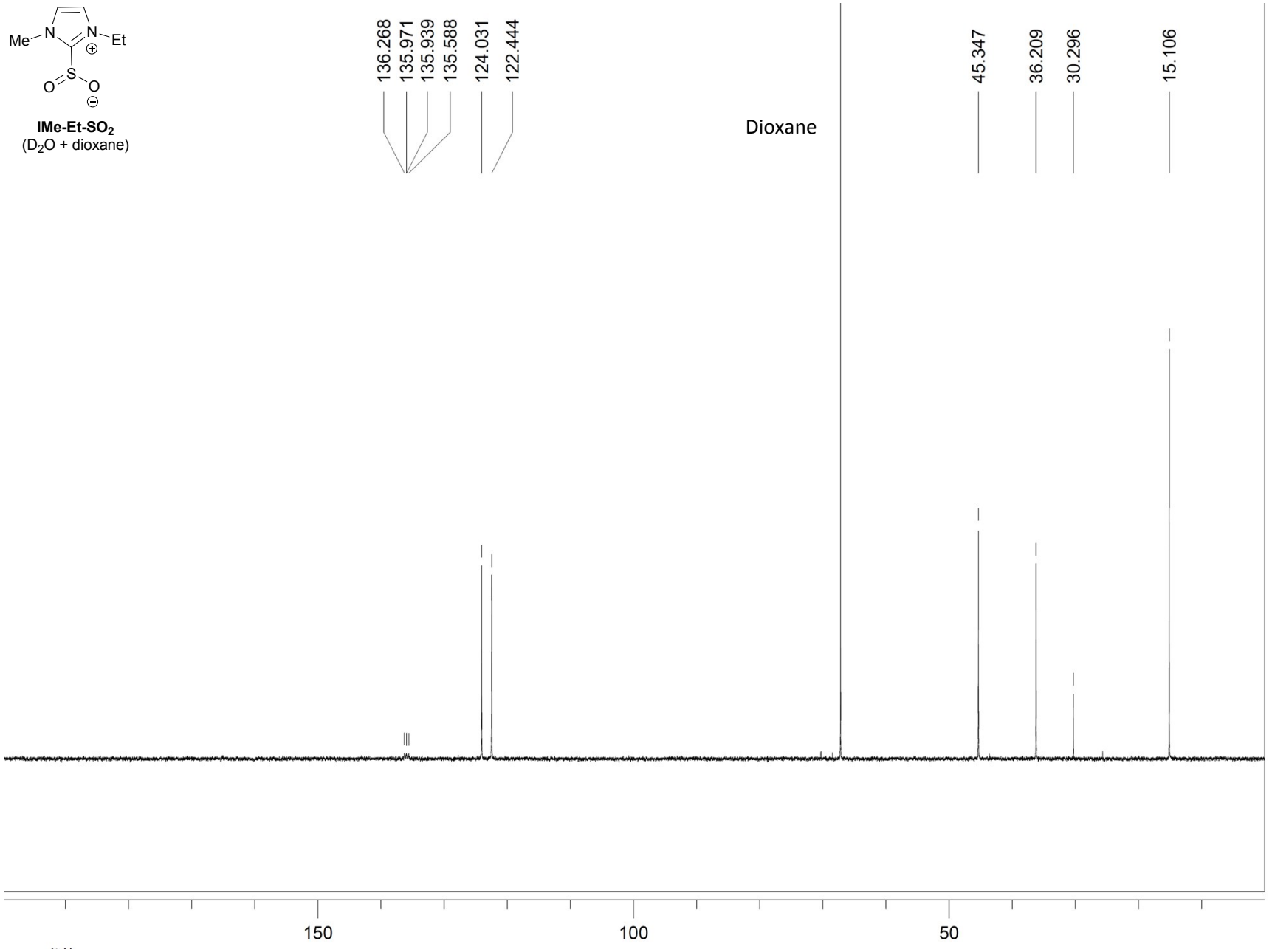
Me
N
N
Et
O
S
O
IMe-Et-SO2
(D2O + dioxane)
136.268
135.971
135.939
135.588
124.031
122.444
Dioxane
45.347
36.209
30.296
15.106
150
100
50

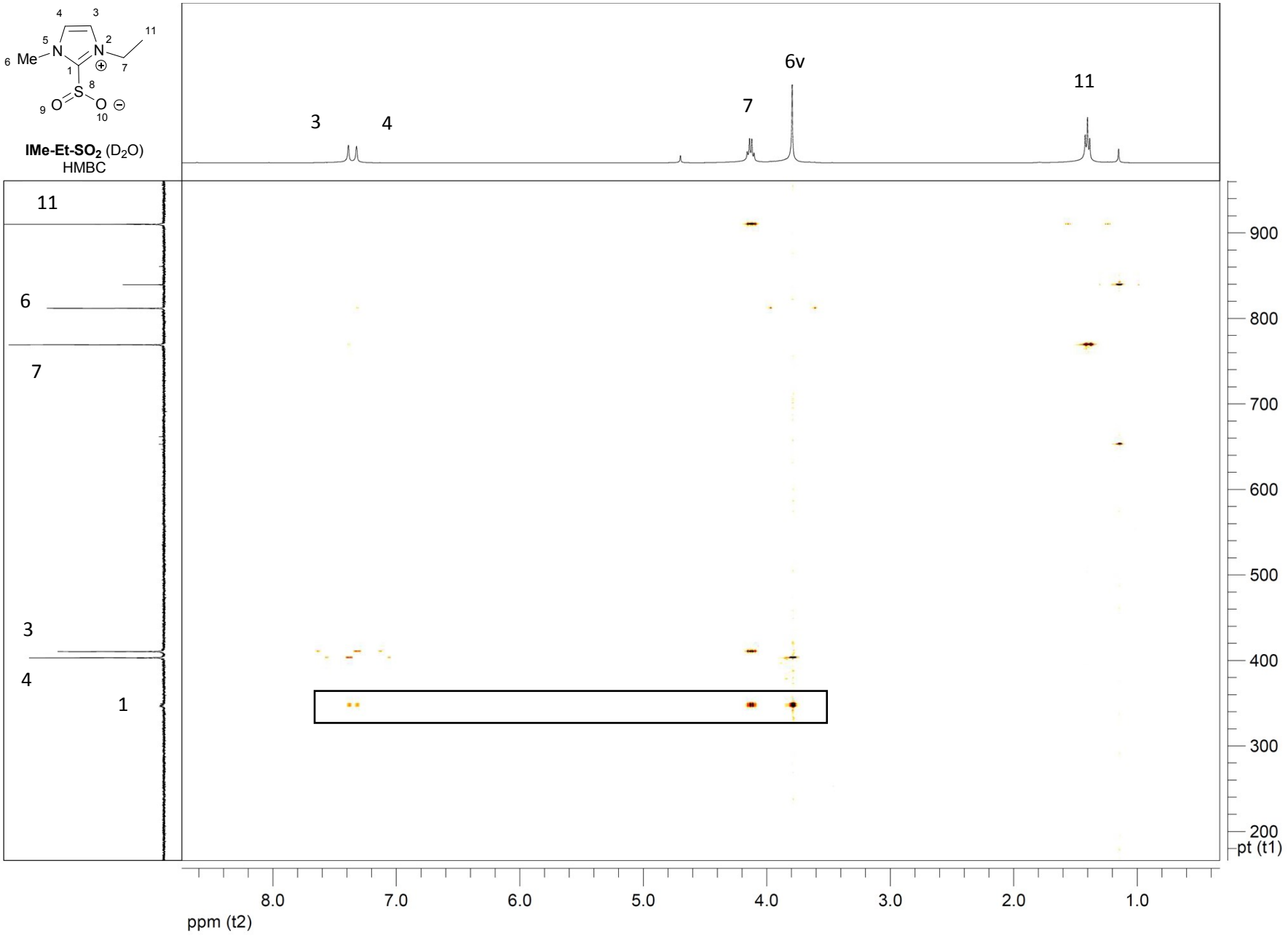
IMe-Et-SO2 (D2O)
HMBC
3
4
7
6v
11
11
6
7
3
4
1
900
800
700
600
500
400
300
200
pt (t1)
8.0
7.0
6.0
5.0
4.0
3.0
2.0
1.0
ppm (t2)

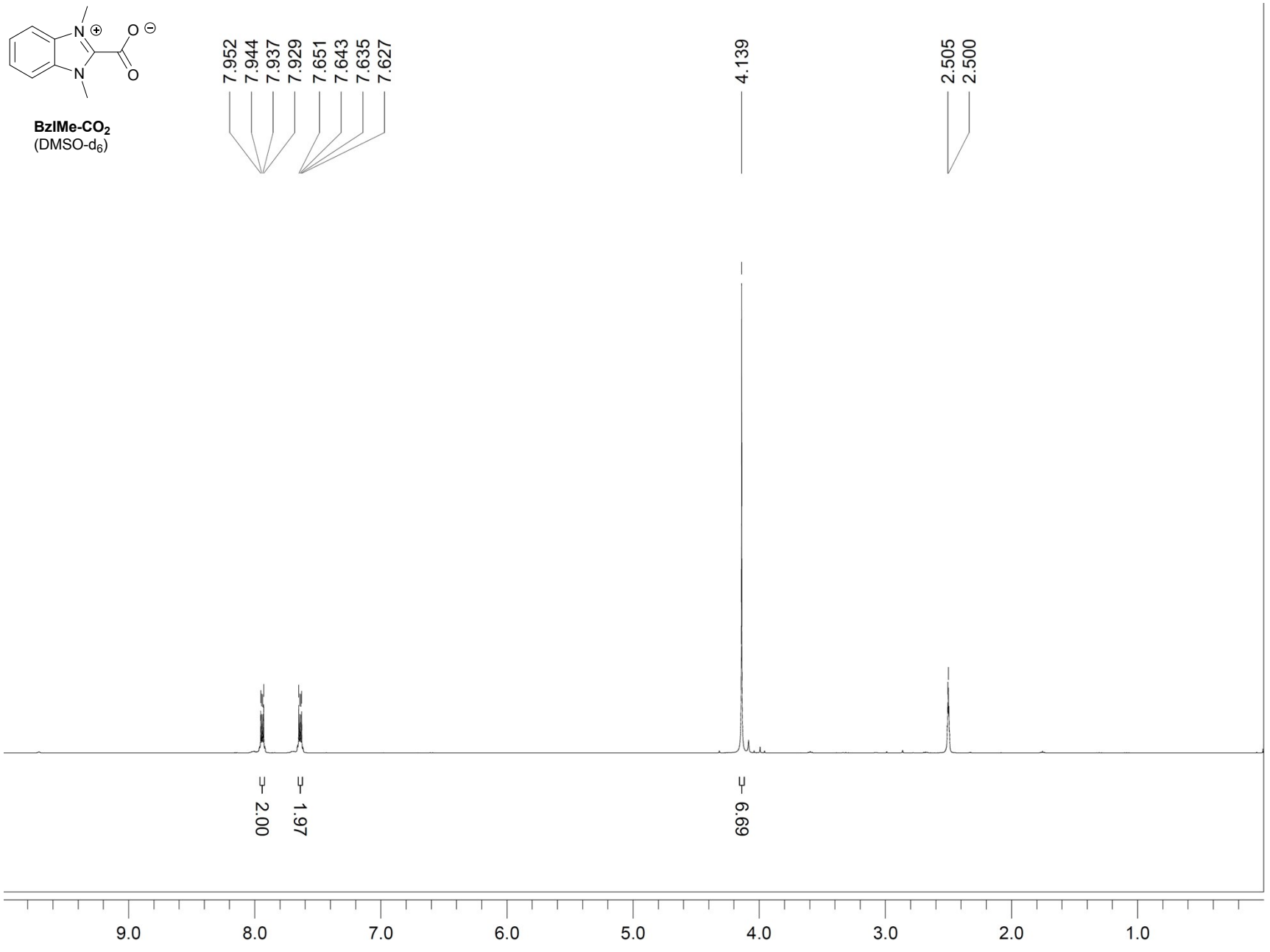

BzlMe-CO_2
(DMSO-d_6)

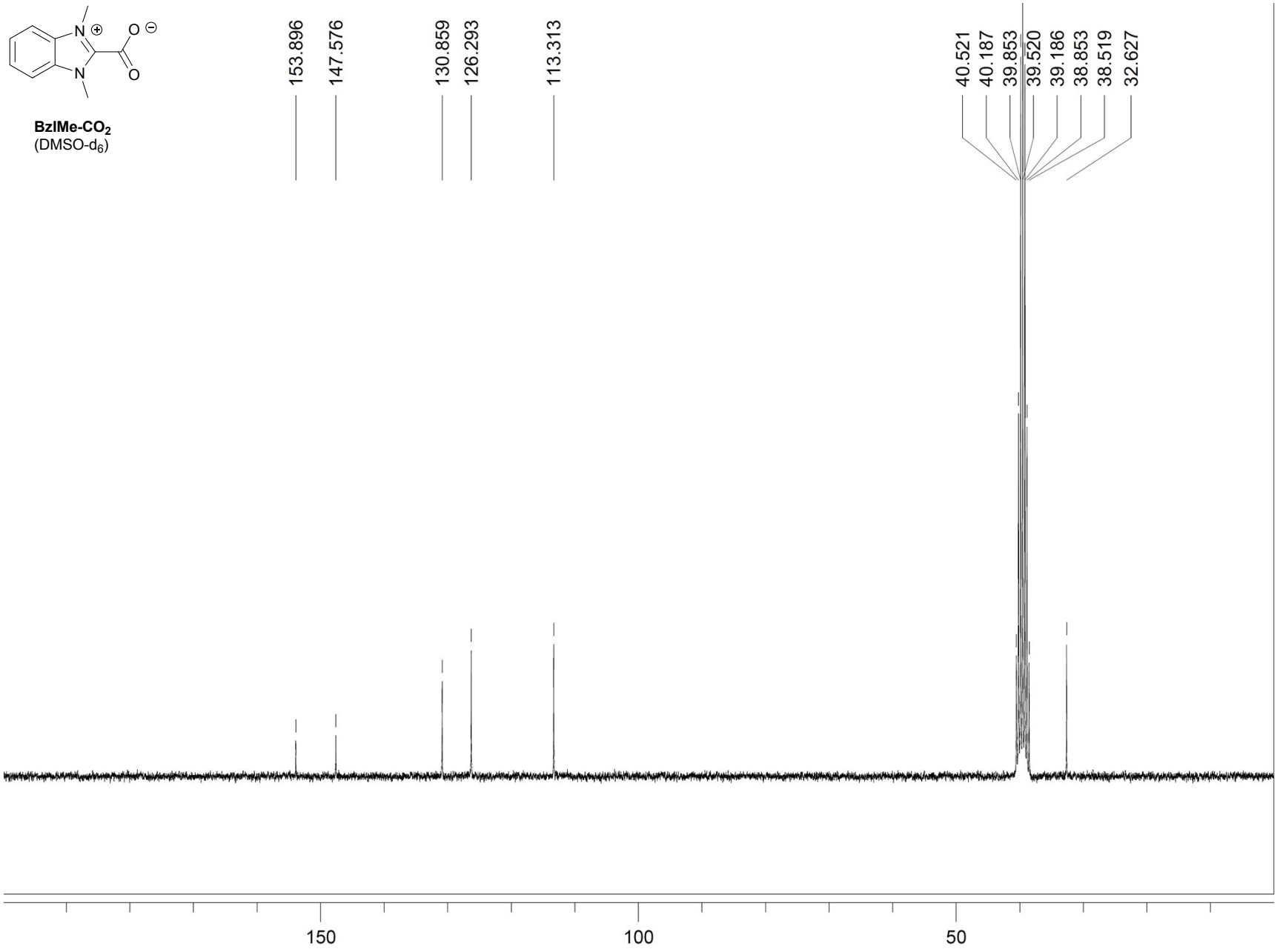

BzlMe-CO_2
(DMSO-d_6)

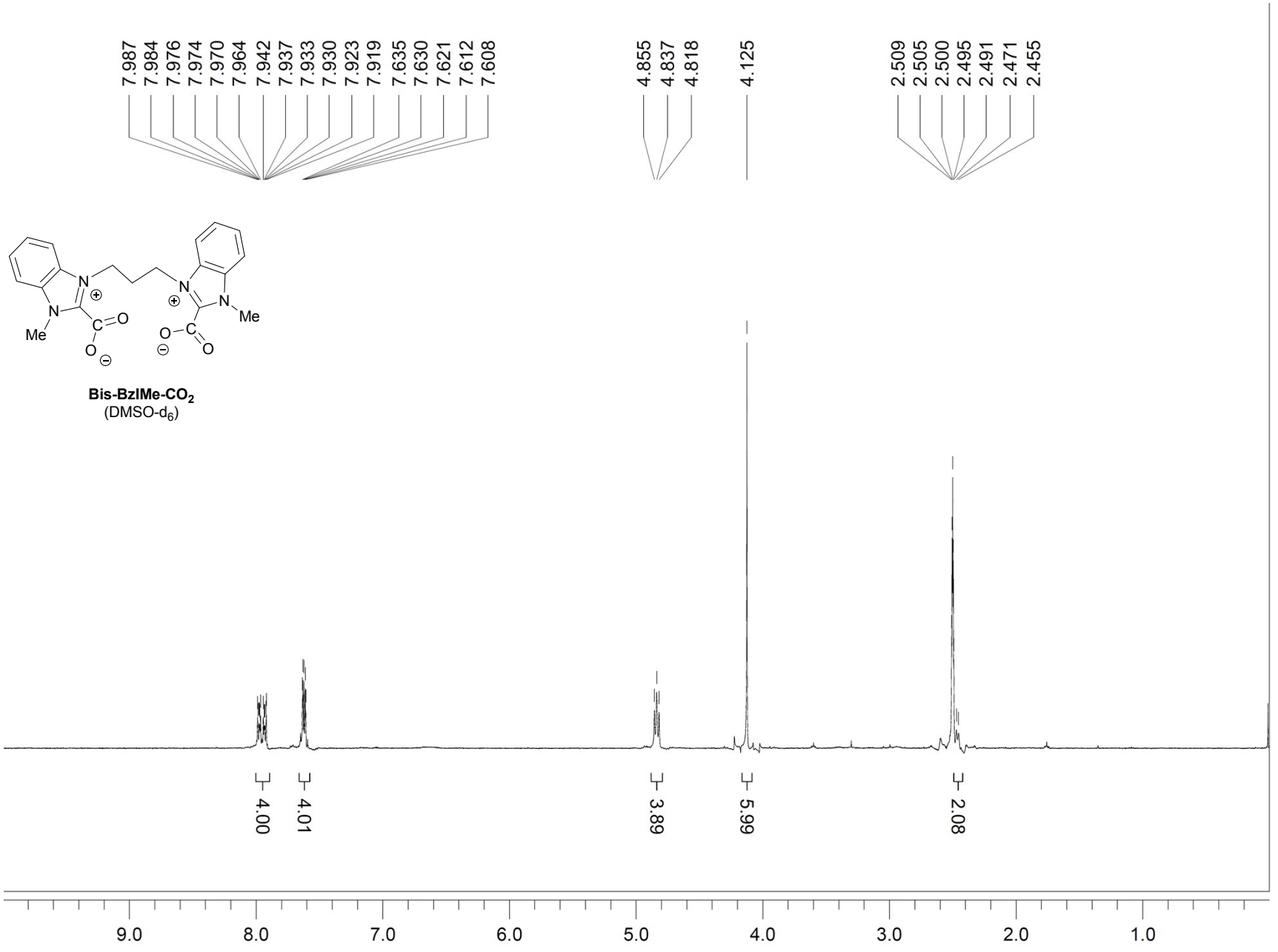

Bis-BzlMe-CO_2
(DMSO-d_6)

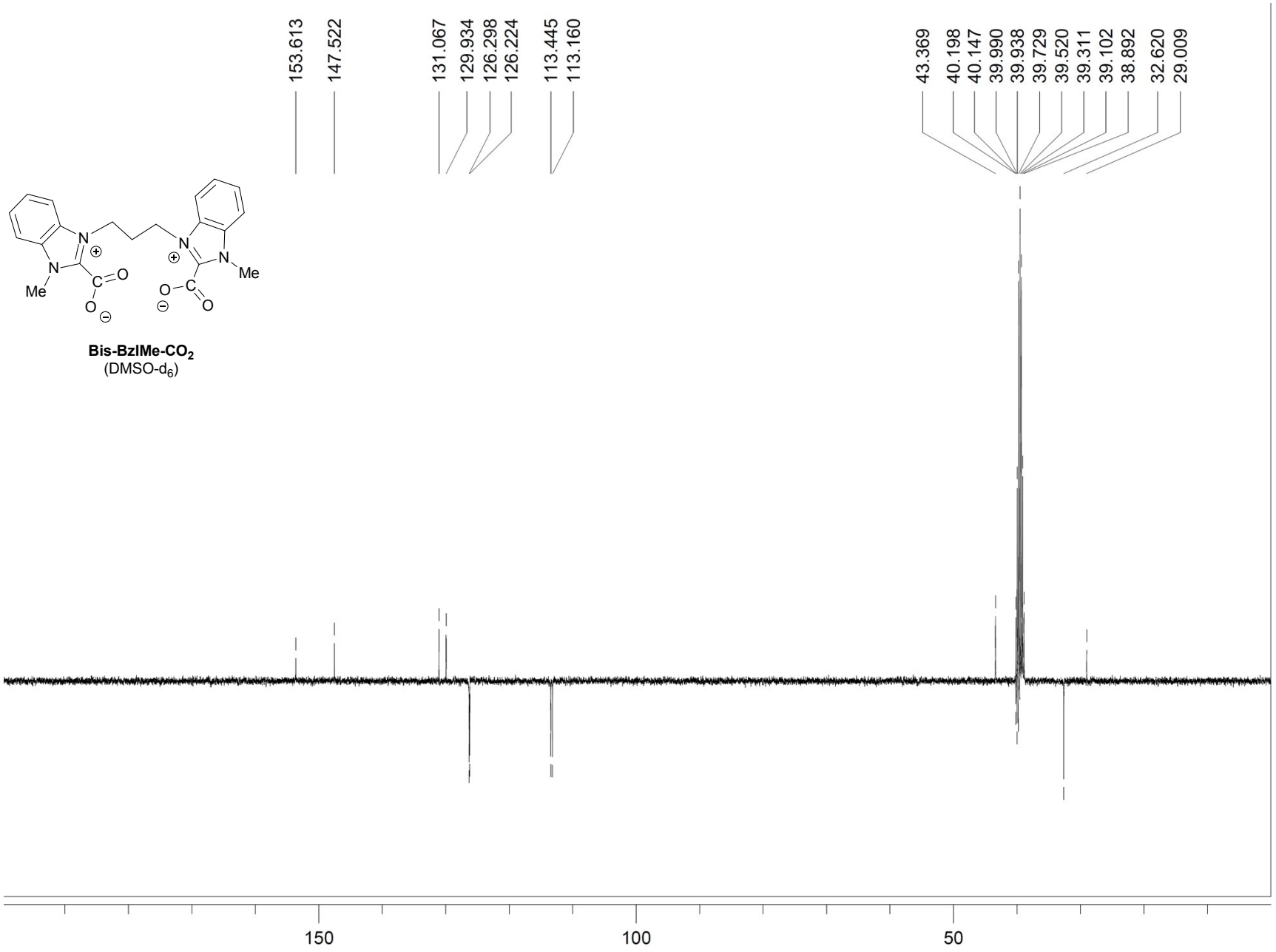

Bis-BzlMe-CO_2
(DMSO-d_6)

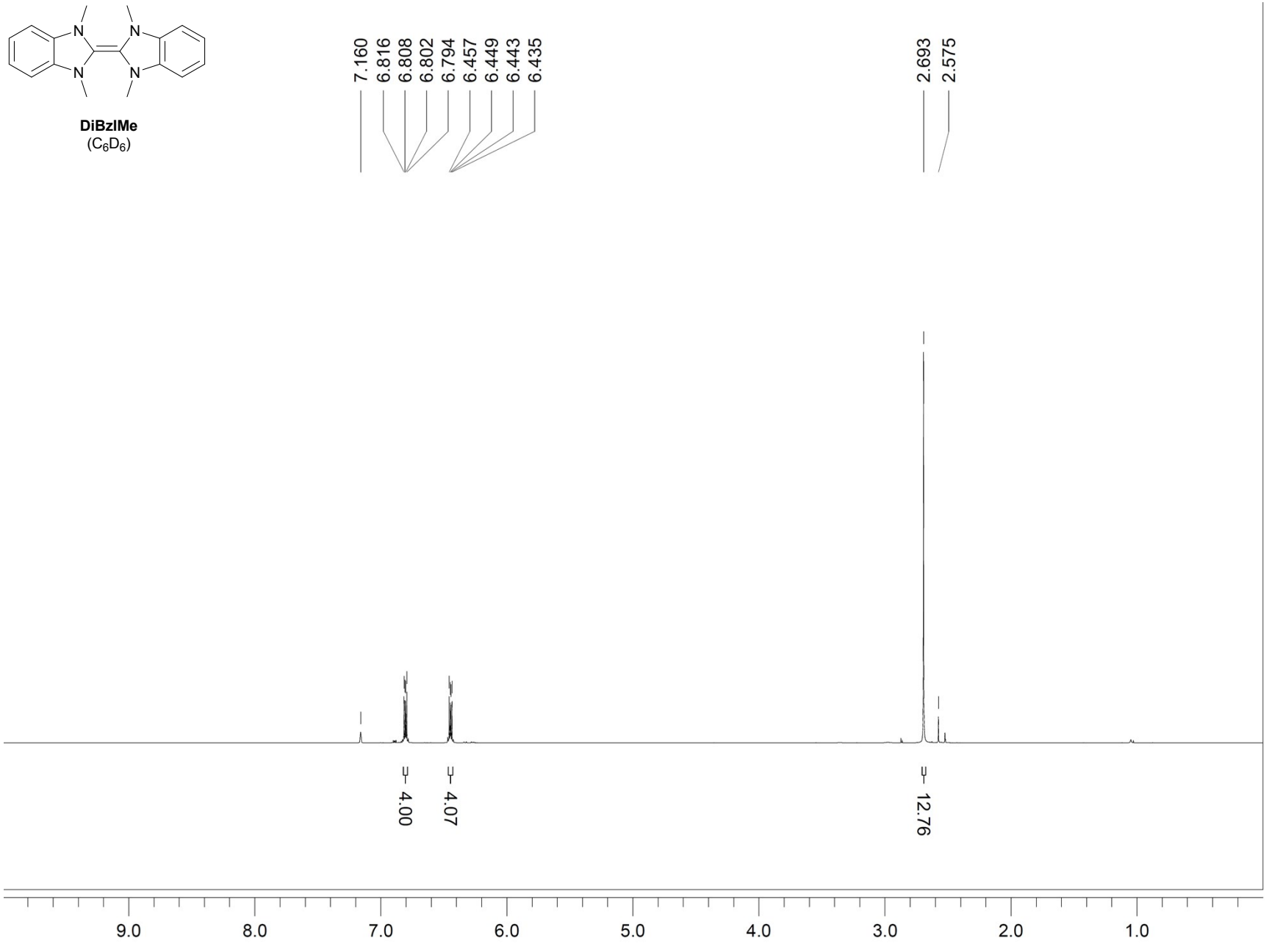
DiBzlMe
(C6D6)
7.160
6.816
6.808
6.802
6.794
6.457
6.449
6.443
6.435
2.693
2.575
4.00
4.07
12.76
9.0
8.0
7.0
6.0
5.0
4.0
3.0
2.0
1.0

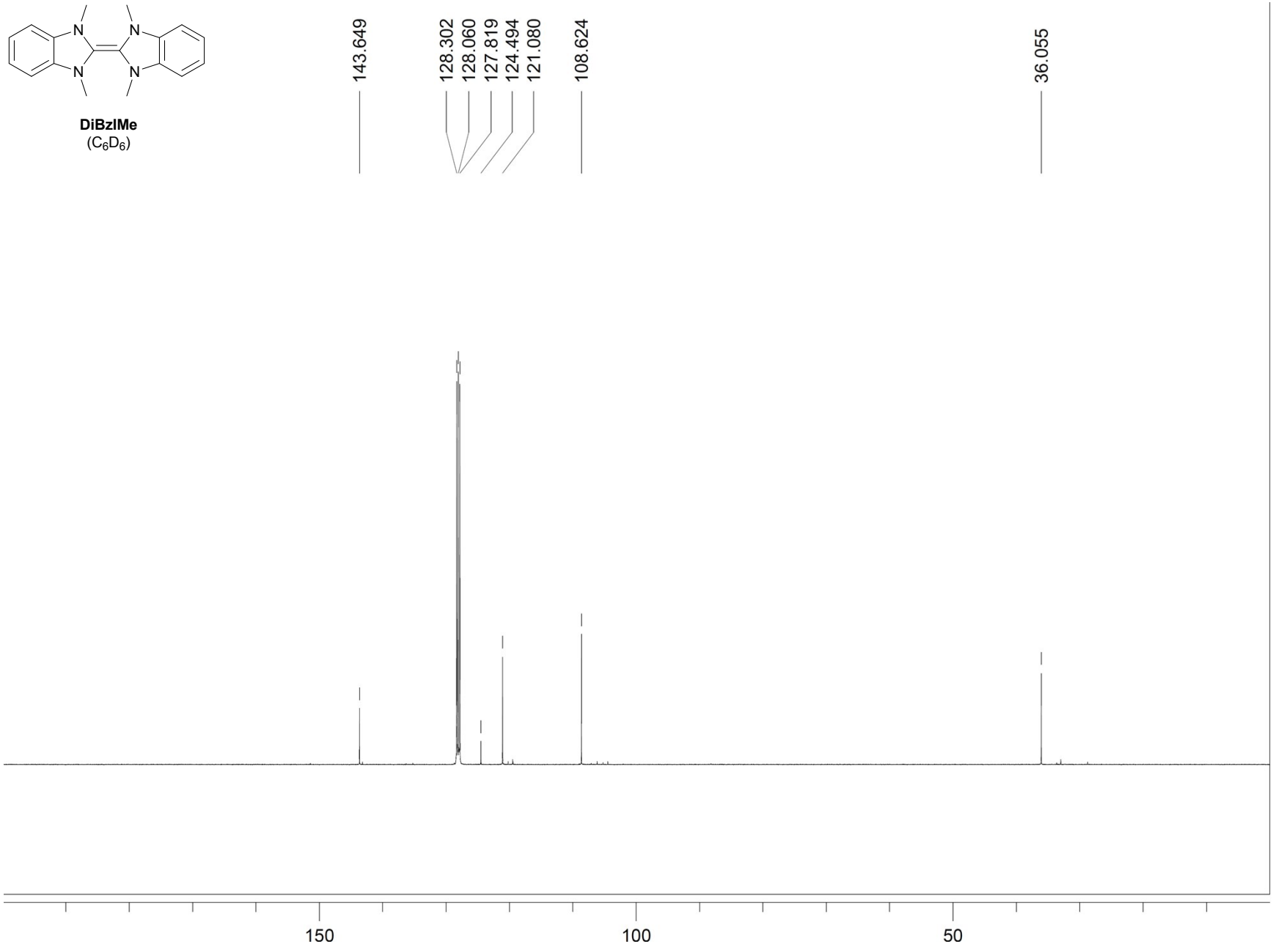
DiBzlMe
(C6D6)
143.649
128.302
128.060
127.819
124.494
121.080
108.624
36.055
150
100
50

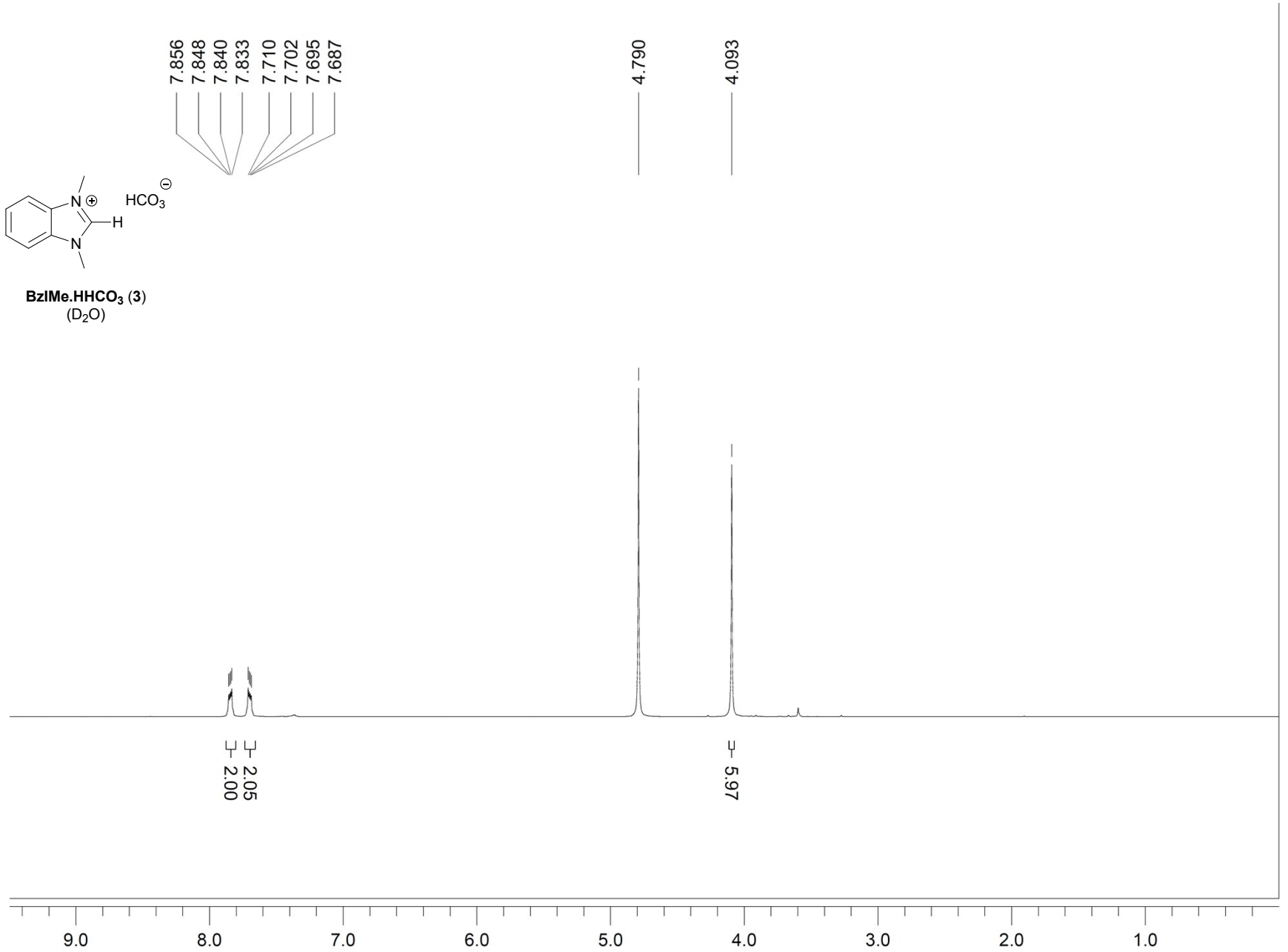

BzlMe.HHCO$_3$ (**3**)
(D_2O)

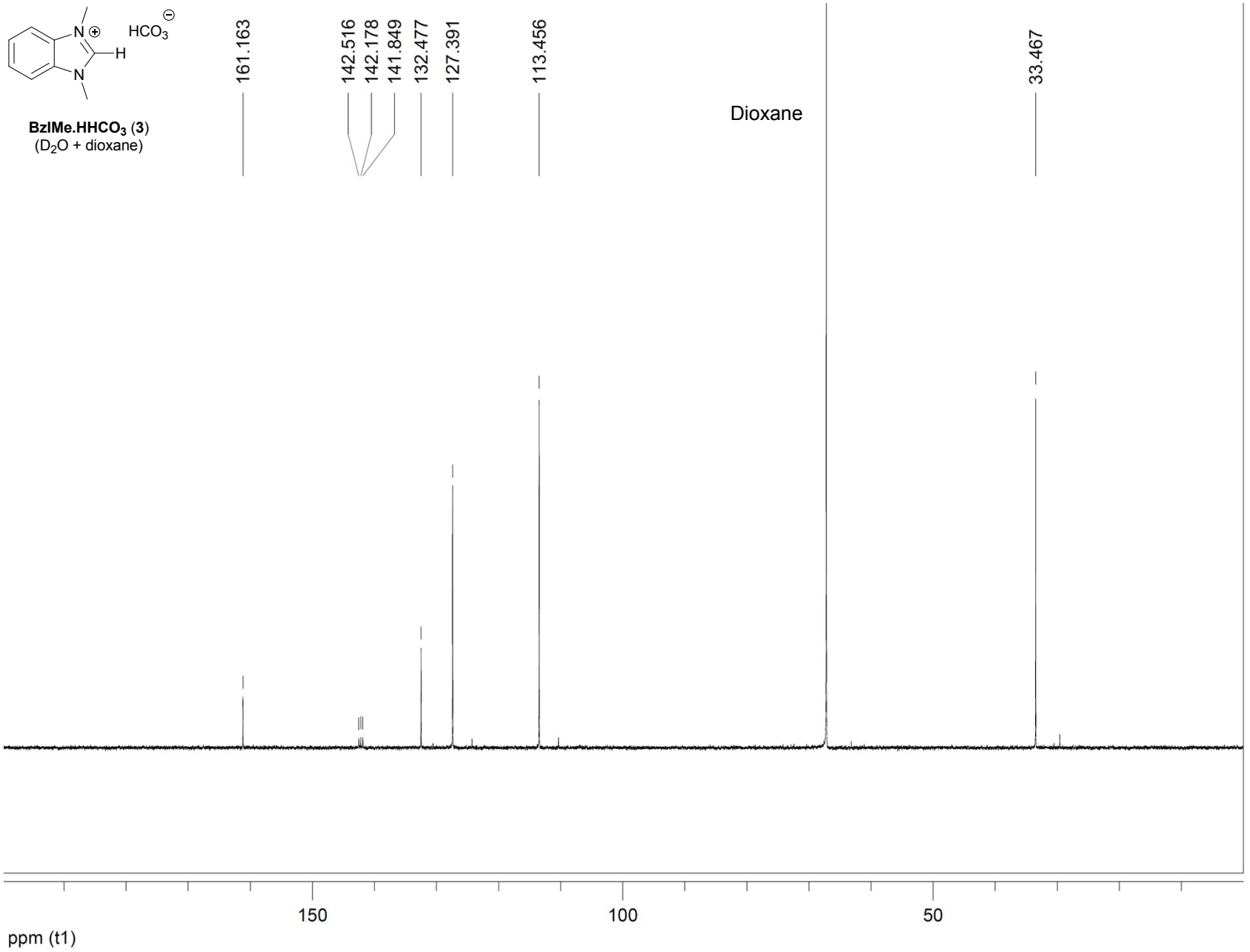
HCO3
H
BzlMe.HHCO3 (3)
(D2O + dioxane)
161.163
142.516
142.178
141.849
132.477
127.391
113.456
Dioxane
33.467
150
100
50
ppm (t1)

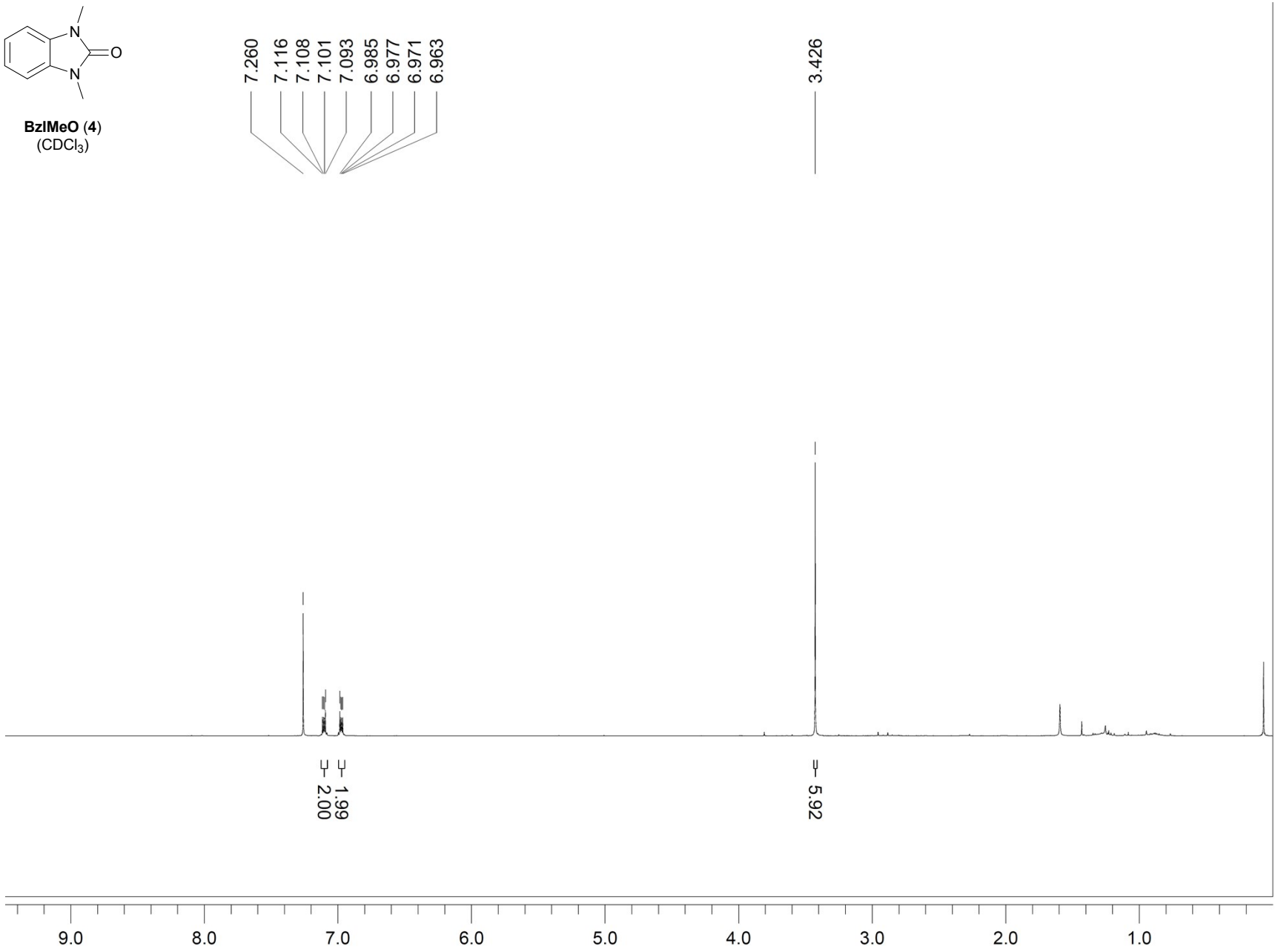

BzIMeO (**4**)
($CDCl_3$)

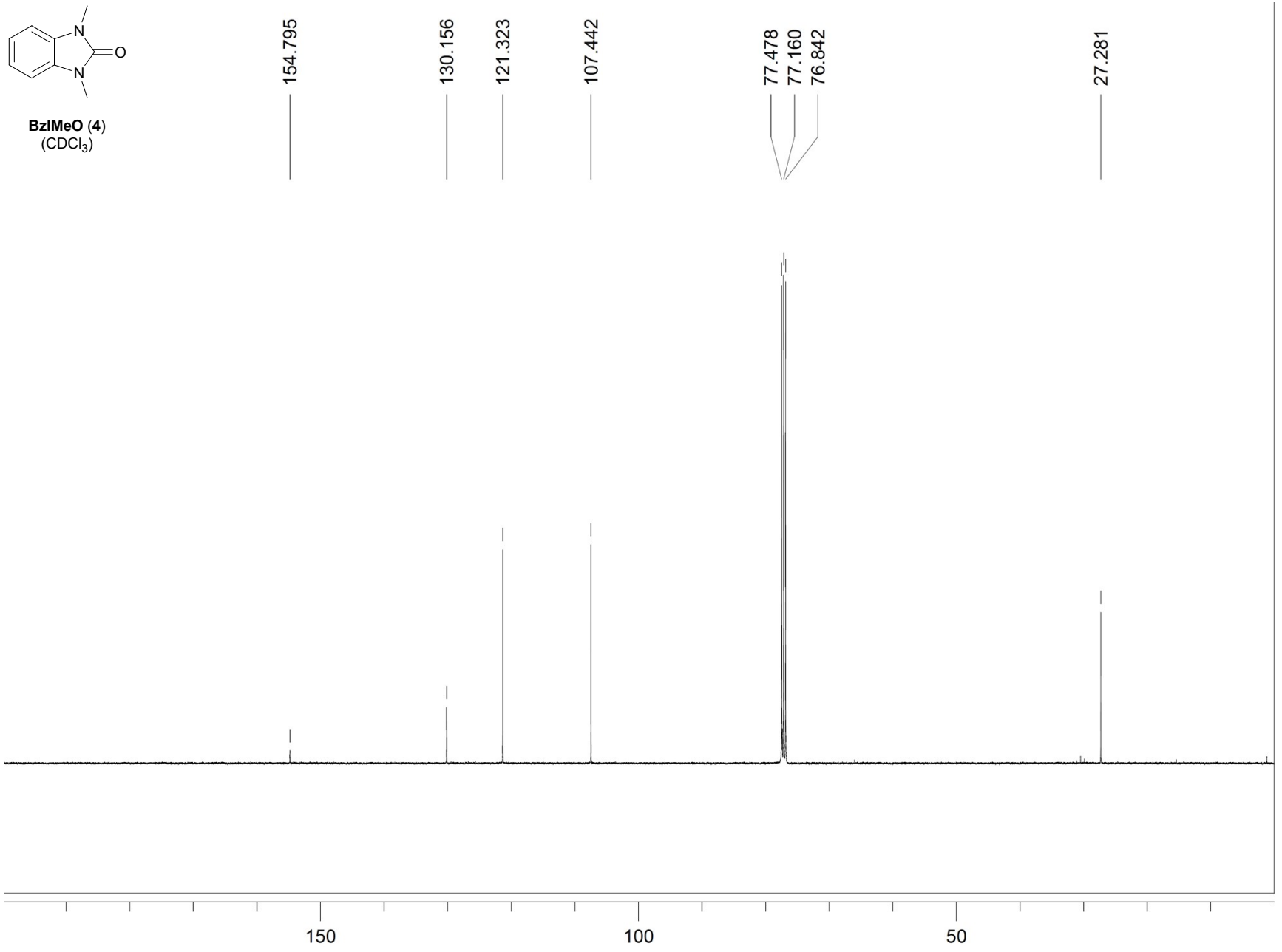

BzIMeO (**4**)
($CDCl_3$)

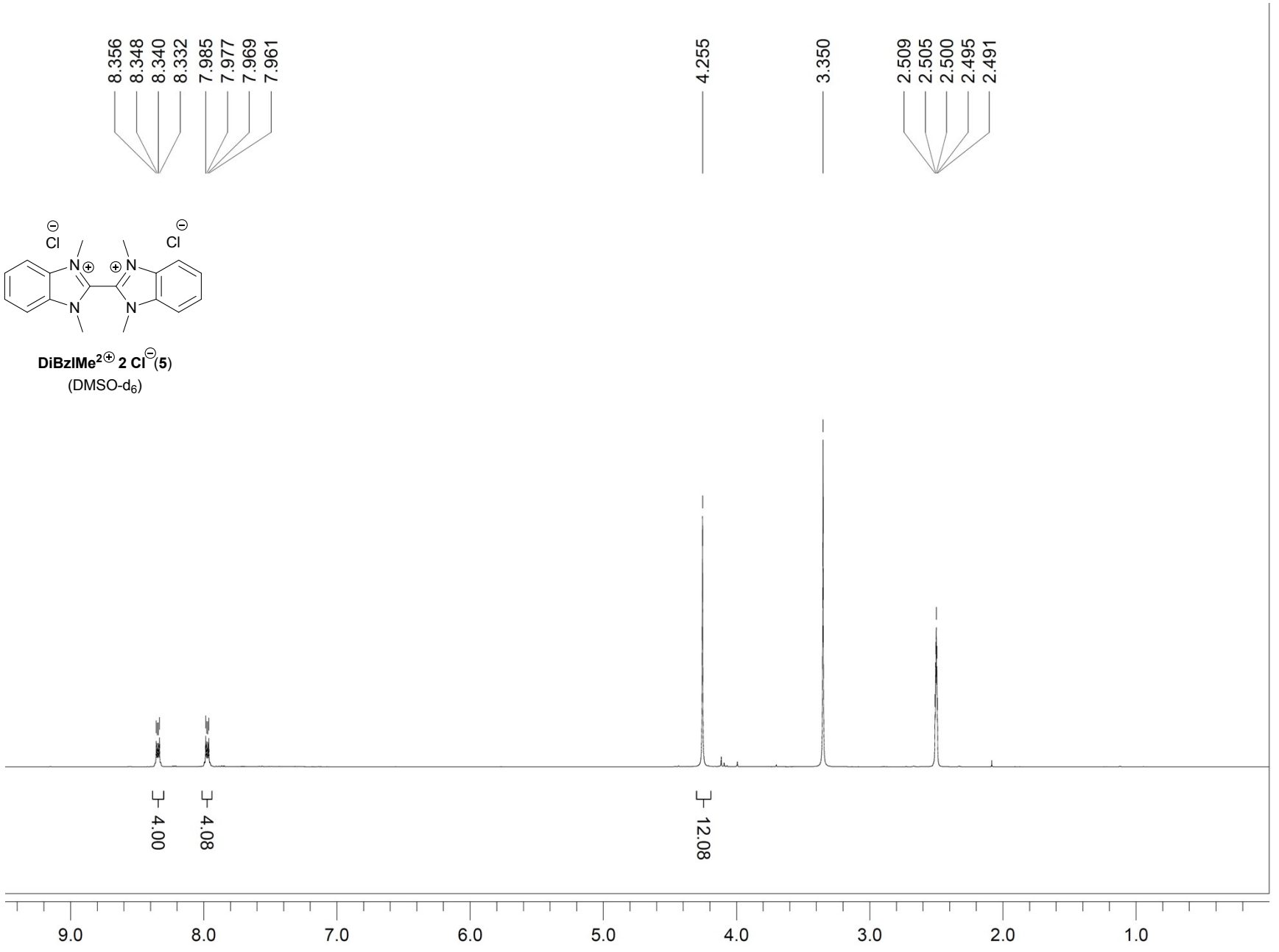
8.356
8.348
8.340
8.332
7.985
7.977
7.969
7.961
4.255
3.350
2.509
2.505
2.500
2.495
2.491
Cl
Cl
DiBzlMe2⊕ 2 Cl⊖ (5)
(DMSO-d6)
4.00
4.08
12.08
9.0
8.0
7.0
6.0
5.0
4.0
3.0
2.0
1.0

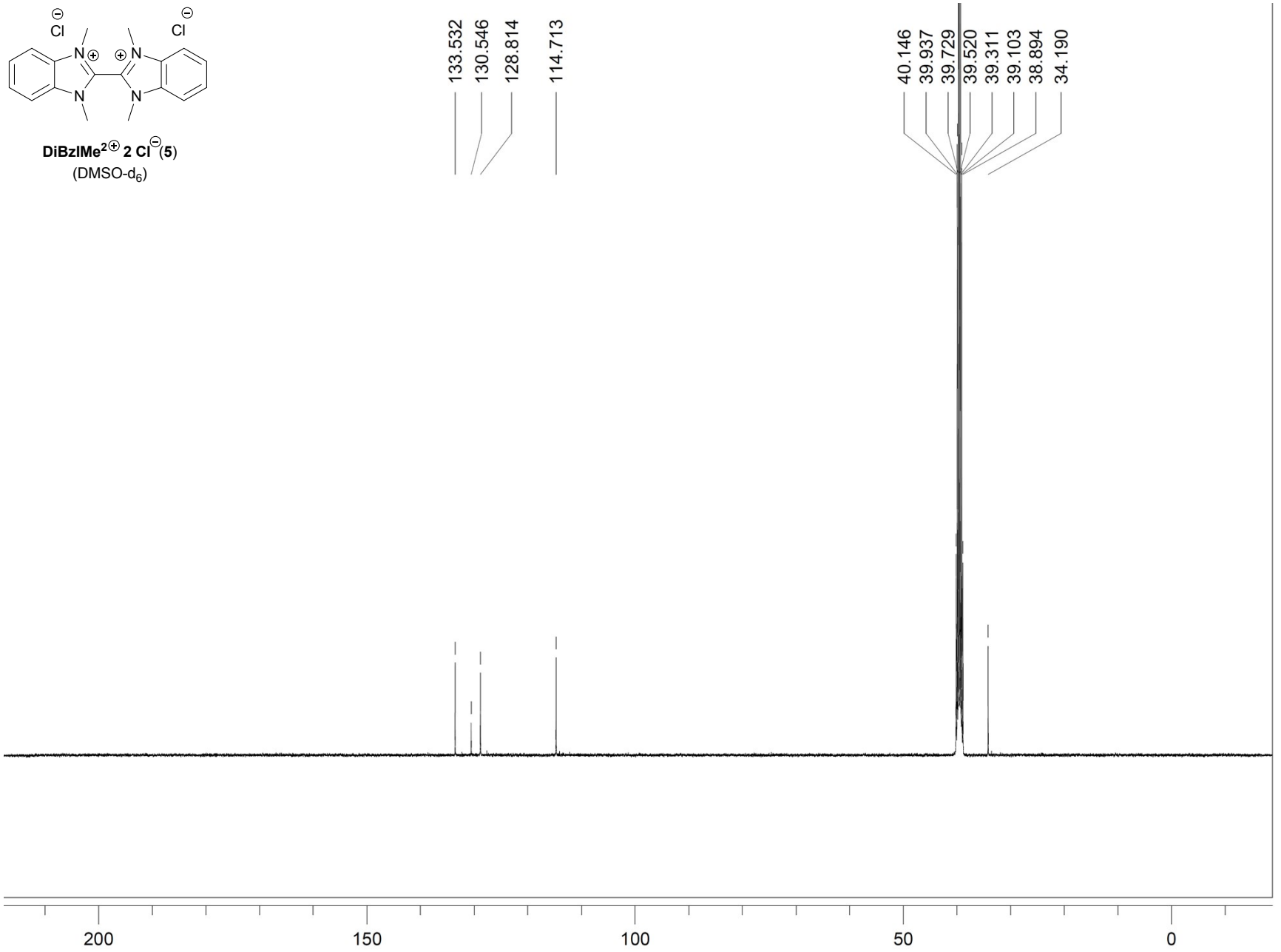
Cl
Cl
N
N
N
N
DiBzlMe2⊕ 2 Cl⊖(5)
(DMSO-d6)
133.532
130.546
128.814
114.713
40.146
39.937
39.729
39.520
39.311
39.103
38.894
34.190
200
150
100
50
0

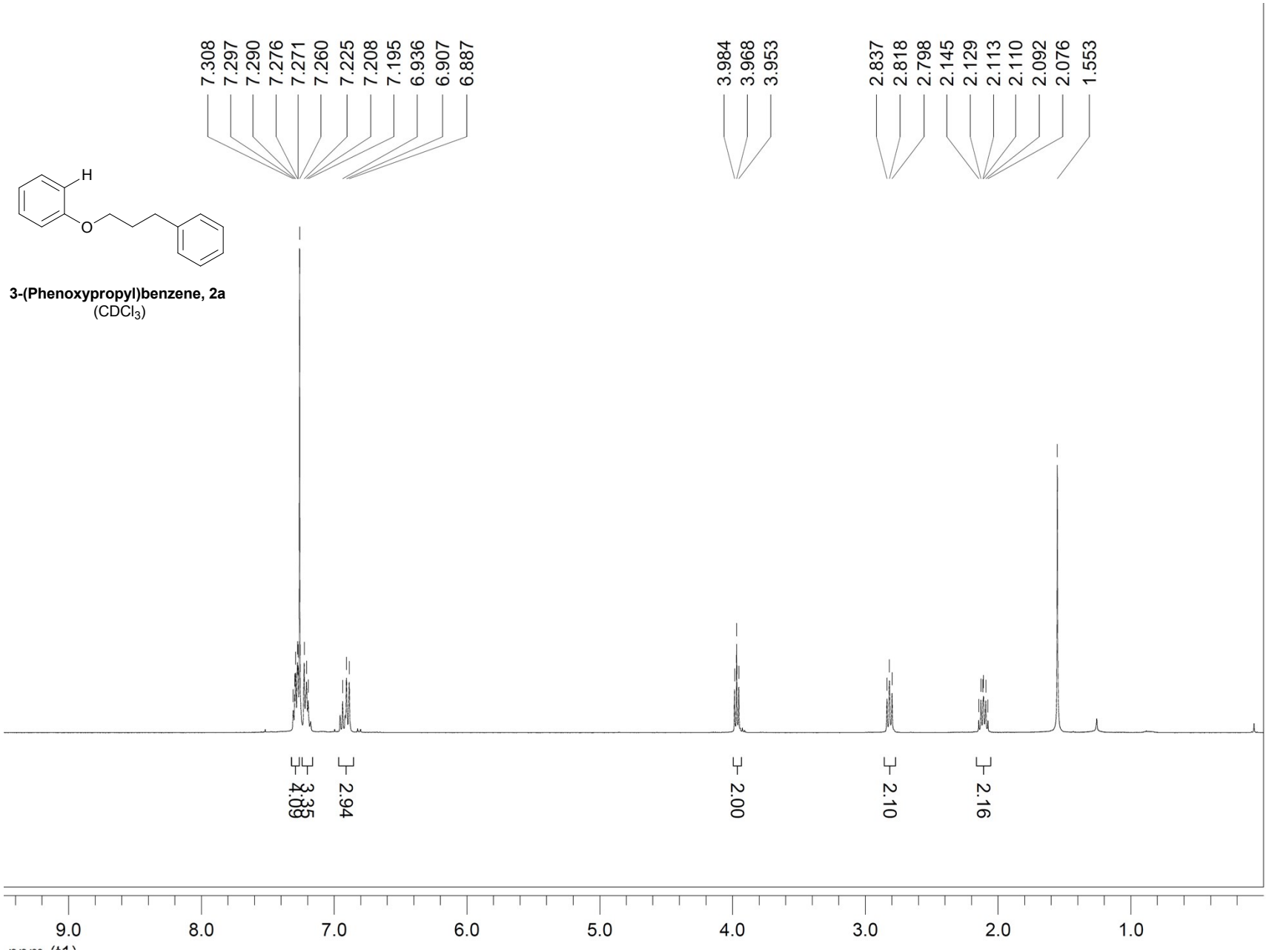
7.308
7.297
7.290
7.276
7.271
7.260
7.225
7.208
7.195
6.936
6.907
6.887
3.984
3.968
3.953
2.837
2.818
2.798
2.145
2.129
2.113
2.110
2.092
2.076
1.553
H
O
3-(Phenoxypropyl)benzene, 2a
(CDCl3)
4.09
3.35
2.94
2.00
2.10
2.16
9.0
8.0
7.0
6.0
5.0
4.0
3.0
2.0
1.0

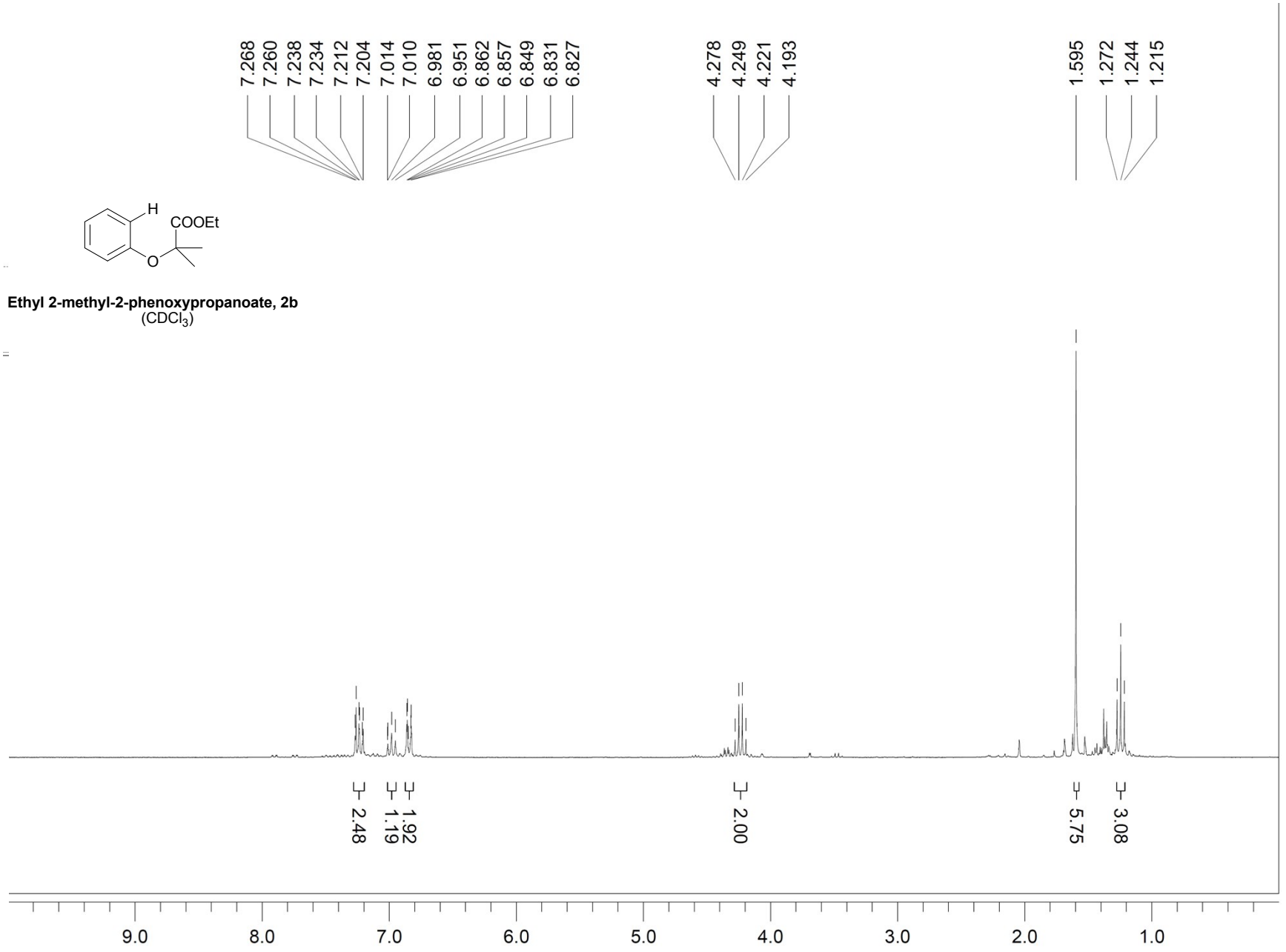

Ethyl 2-methyl-2-phenoxypropanoate, 2b
($CDCl_3$)

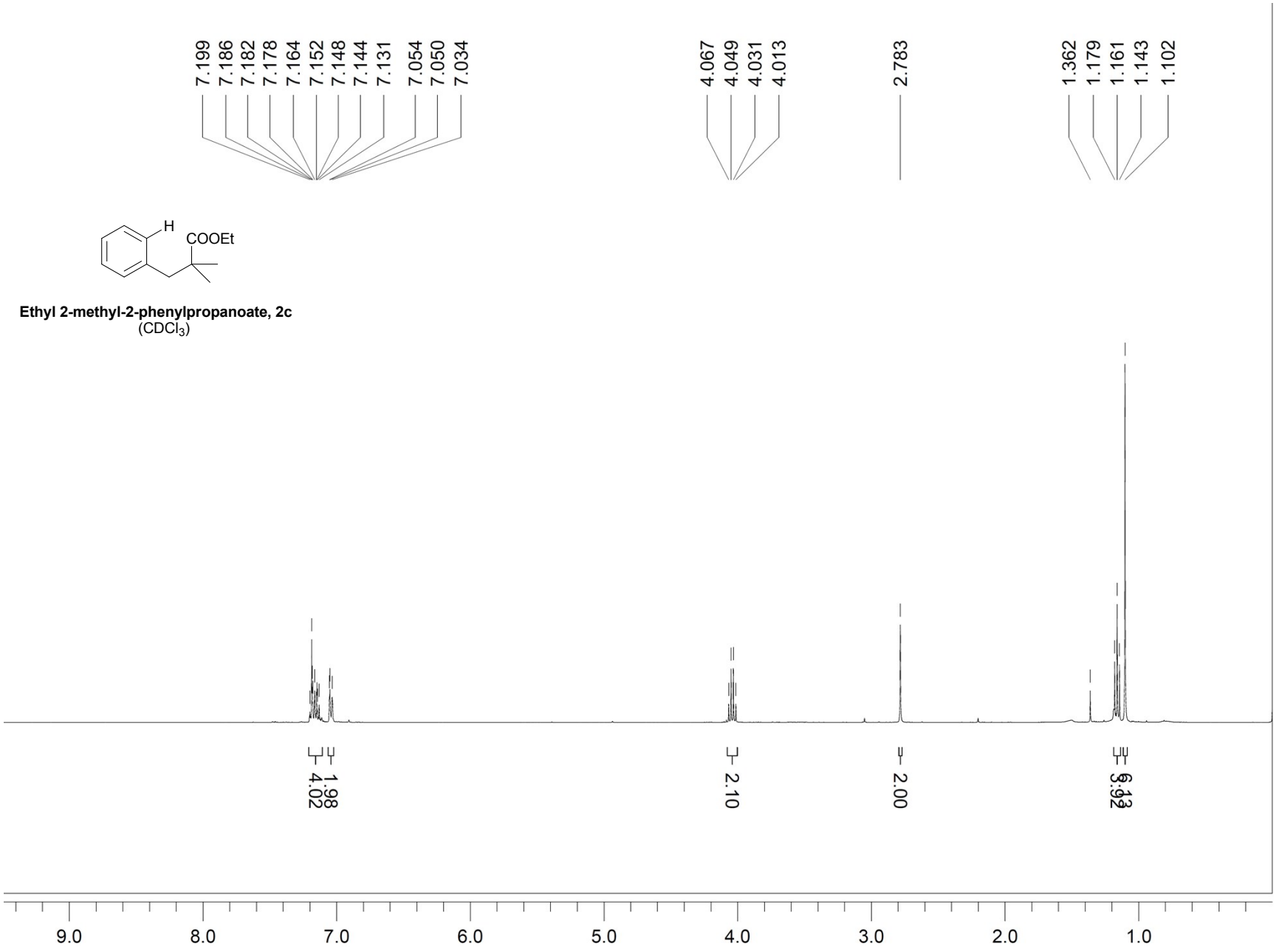

Ethyl 2-methyl-2-phenylpropanoate, 2c
($CDCl_3$)

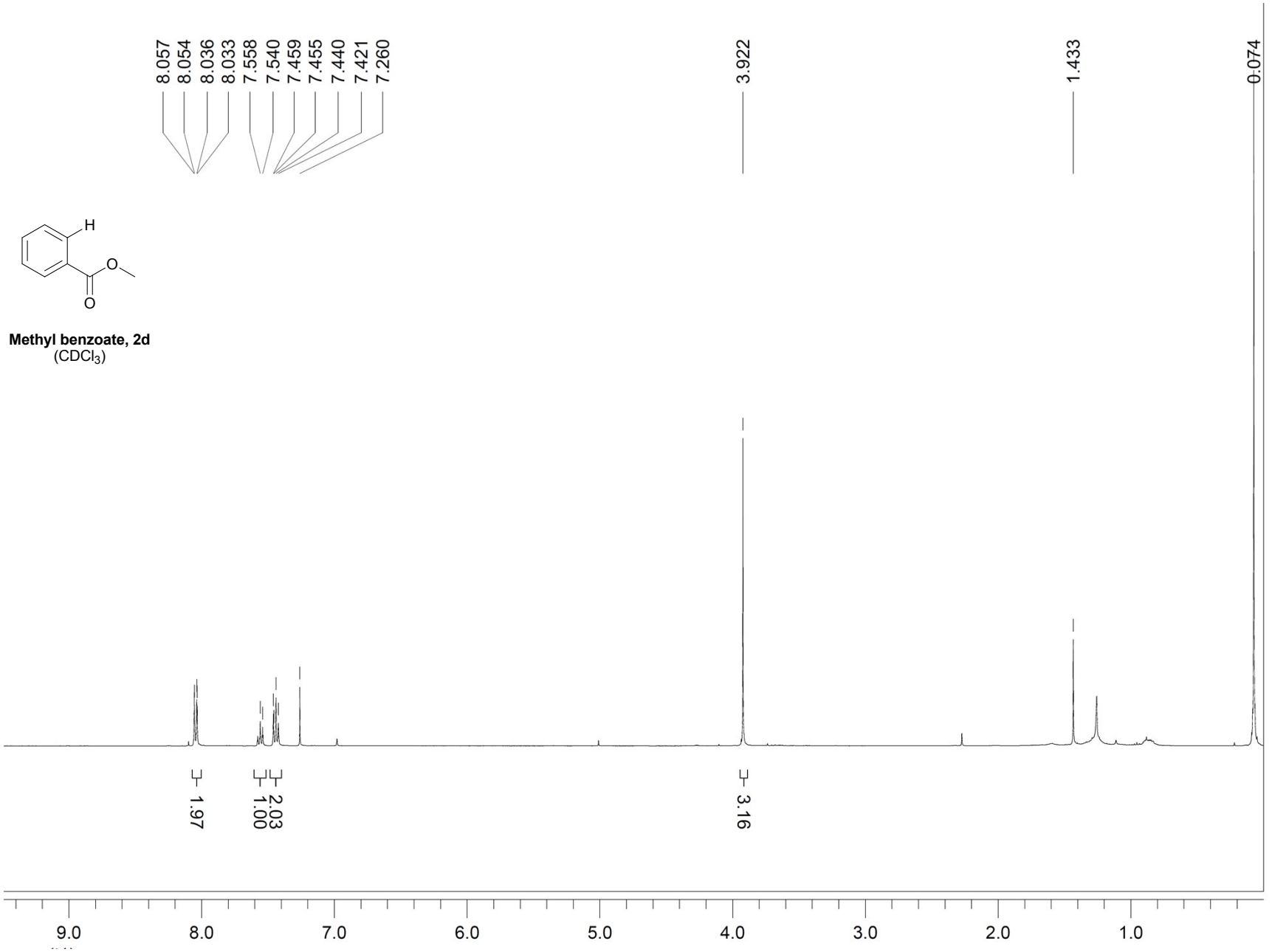

Methyl benzoate, 2d
($CDCl_3$)

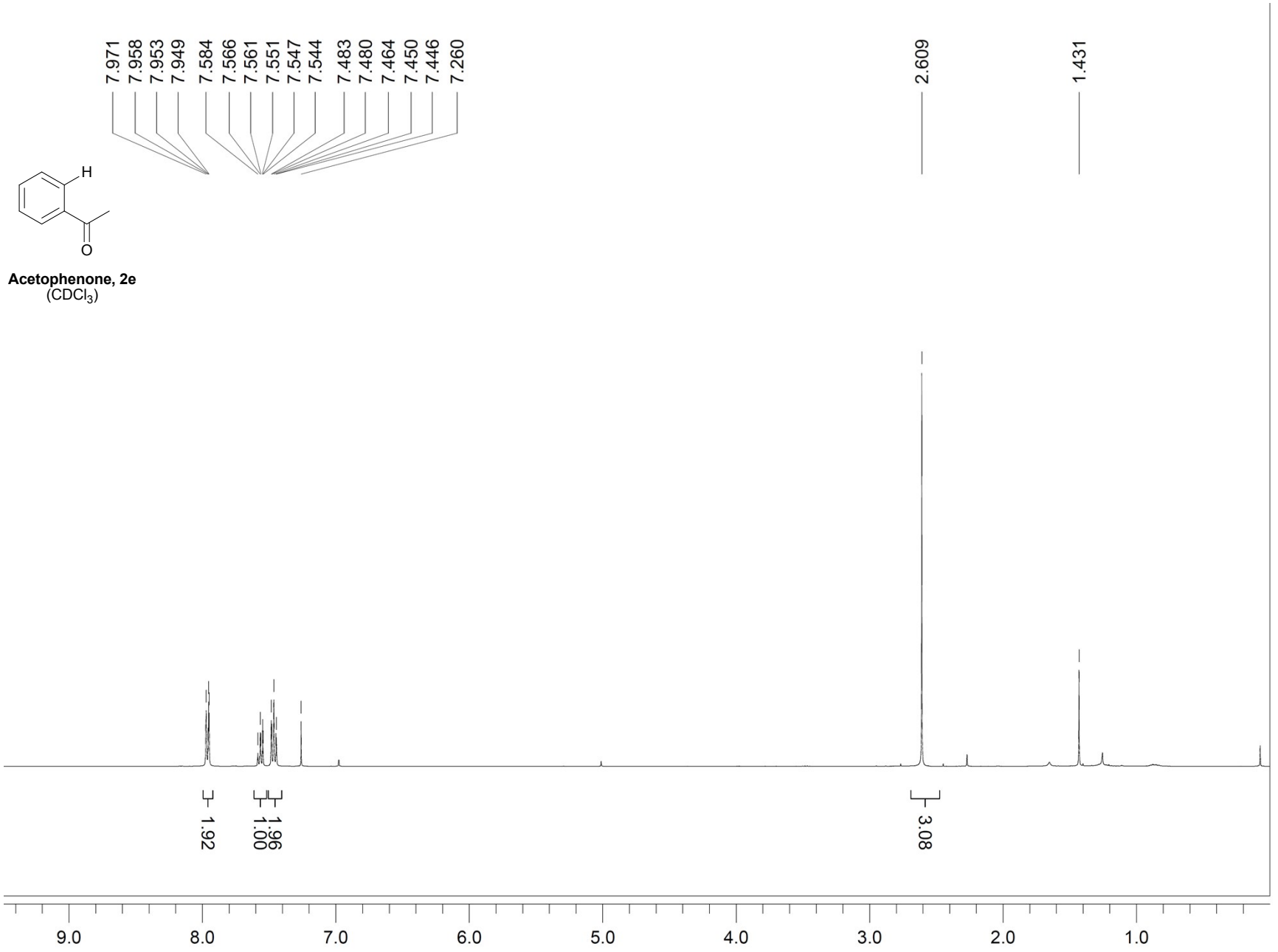
7.971
7.958
7.953
7.949
7.584
7.566
7.561
7.551
7.547
7.544
7.483
7.480
7.464
7.450
7.446
7.260
2.609
1.431
H
O
Acetophenone, 2e
(CDCl3)
1.92
1.00
1.96
3.08
9.0
8.0
7.0
6.0
5.0
4.0
3.0
2.0
1.0

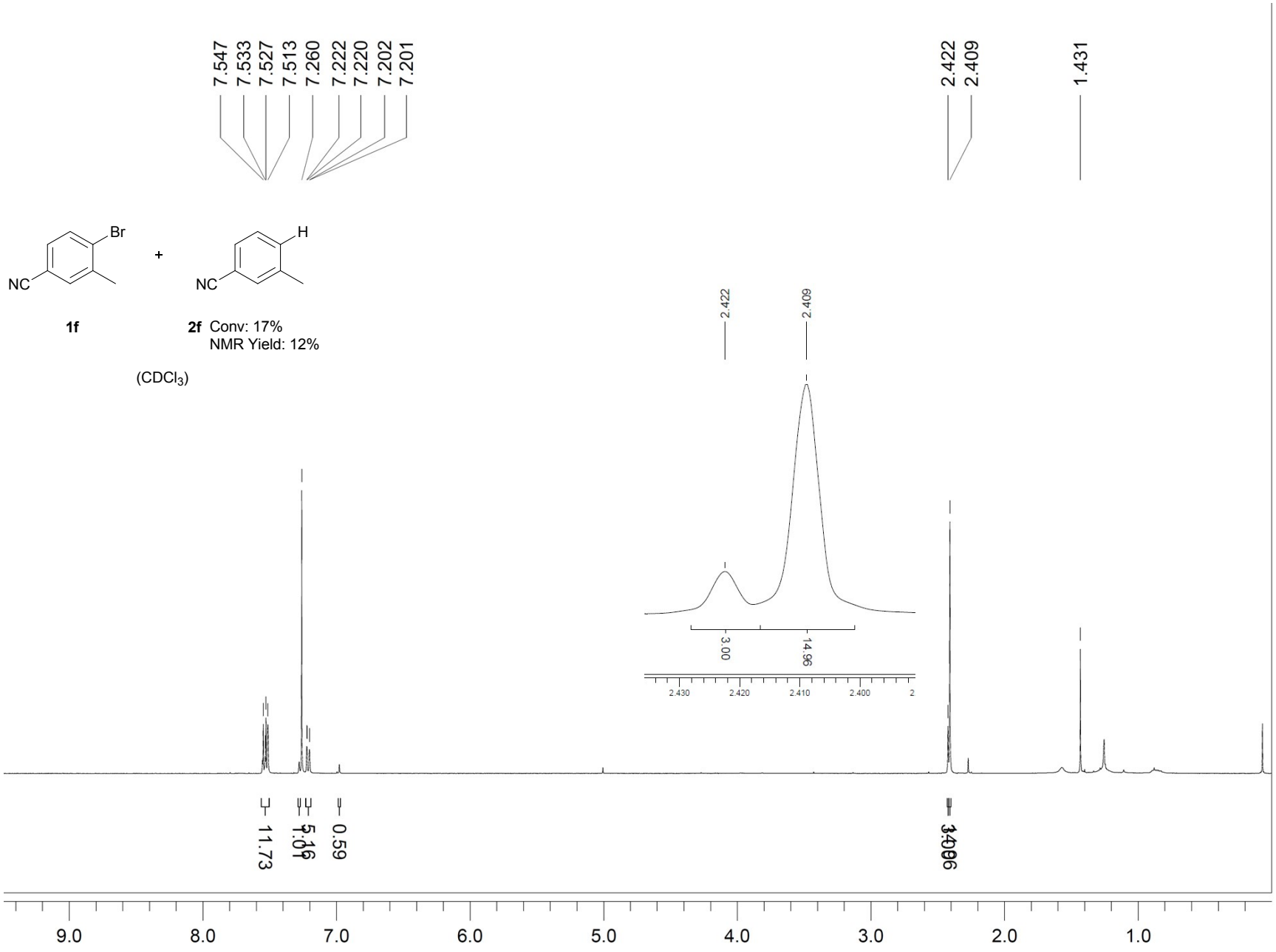
7.547
7.533
7.527
7.513
7.260
7.222
7.220
7.202
7.201
2.422
2.409
1.431
Br
NC
+
H
NC
1f
2f Conv: 17%
NMR Yield: 12%
(CDCl3)
2.422
2.409
3.00
14.96
2.430
2.420
2.410
2.400
11.73
5.16
5.01
0.59
14.96
9.0
8.0
7.0
6.0
5.0
4.0
3.0
2.0
1.0

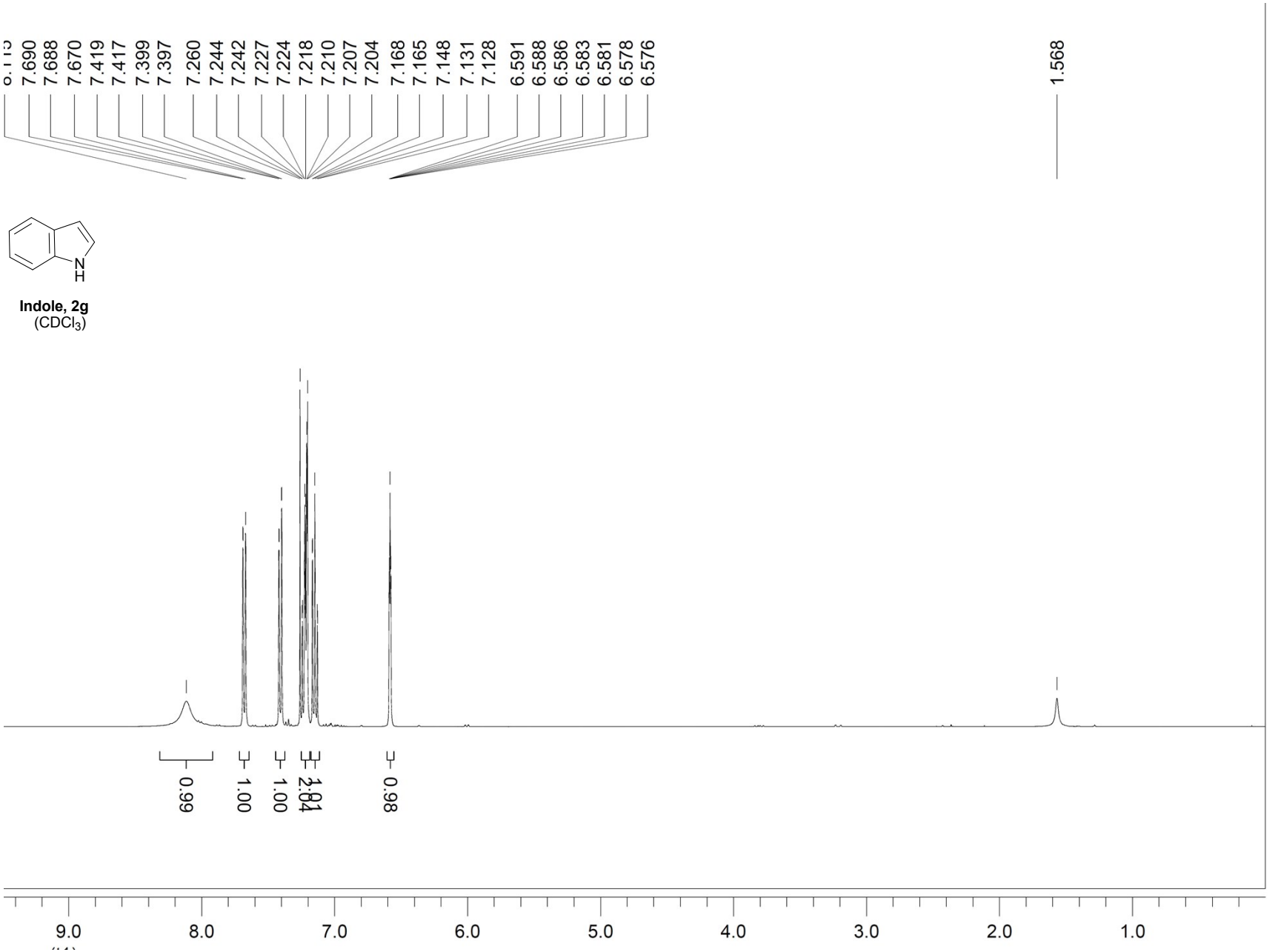

Indole, 2g
($CDCl_3$)

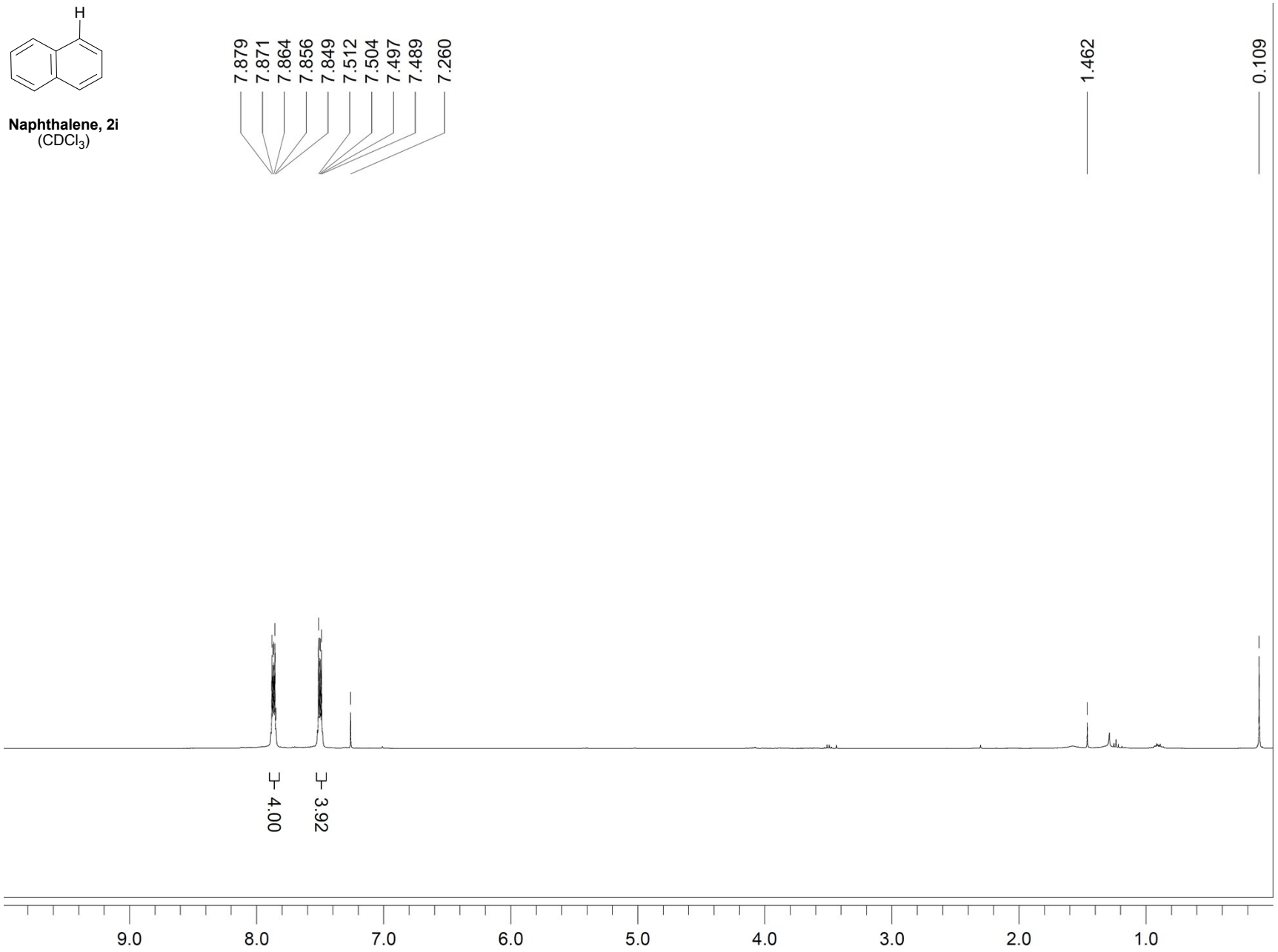
H
Naphthalene, 2i
(CDCl3)
7.879
7.871
7.864
7.856
7.849
7.512
7.504
7.497
7.489
7.260
1.462
0.109
4.00
3.92
9.0
8.0
7.0
6.0
5.0
4.0
3.0
2.0
1.0

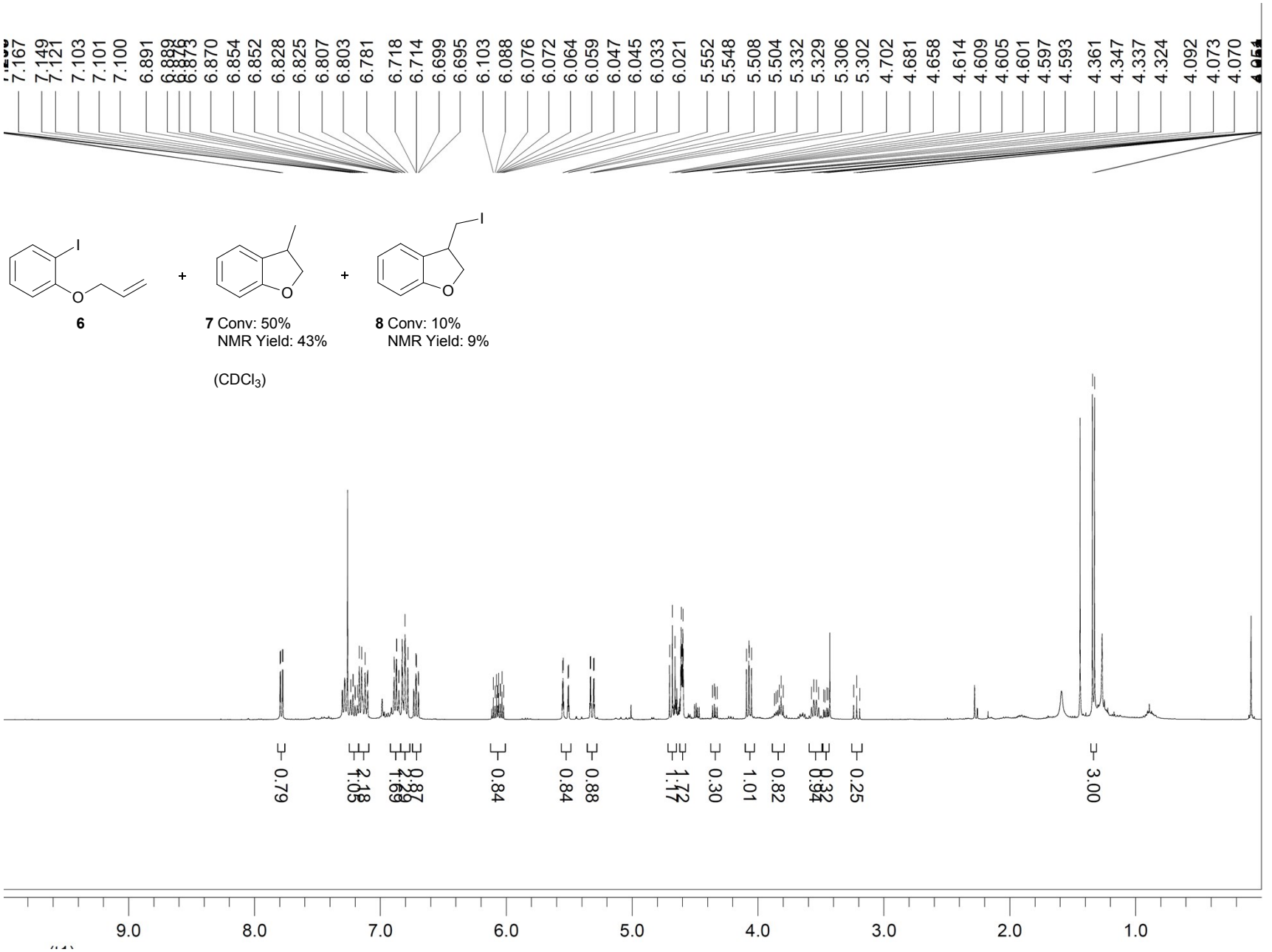
7.167
7.149
7.121
7.103
7.101
7.100
6.891
6.870
6.854
6.852
6.828
6.825
6.807
6.803
6.781
6.718
6.714
6.699
6.695
6.103
6.088
6.076
6.072
6.064
6.059
6.047
6.045
6.033
6.021
5.552
5.548
5.508
5.504
5.332
5.329
5.306
5.302
4.702
4.681
4.658
4.614
4.609
4.605
4.601
4.597
4.593
4.361
4.347
4.337
4.324
4.092
4.073
4.070
I
O
+
+
I
O
O
6
7 Conv: 50%
NMR Yield: 43%
8 Conv: 10%
NMR Yield: 9%
(CDCl3)
0.79
2.18
2.05
0.87
4.69
0.84
0.84
0.88
1.17
0.30
1.01
0.82
0.94
0.32
0.25
3.00
9.0
8.0
7.0
6.0
5.0
4.0
3.0
2.0
1.0

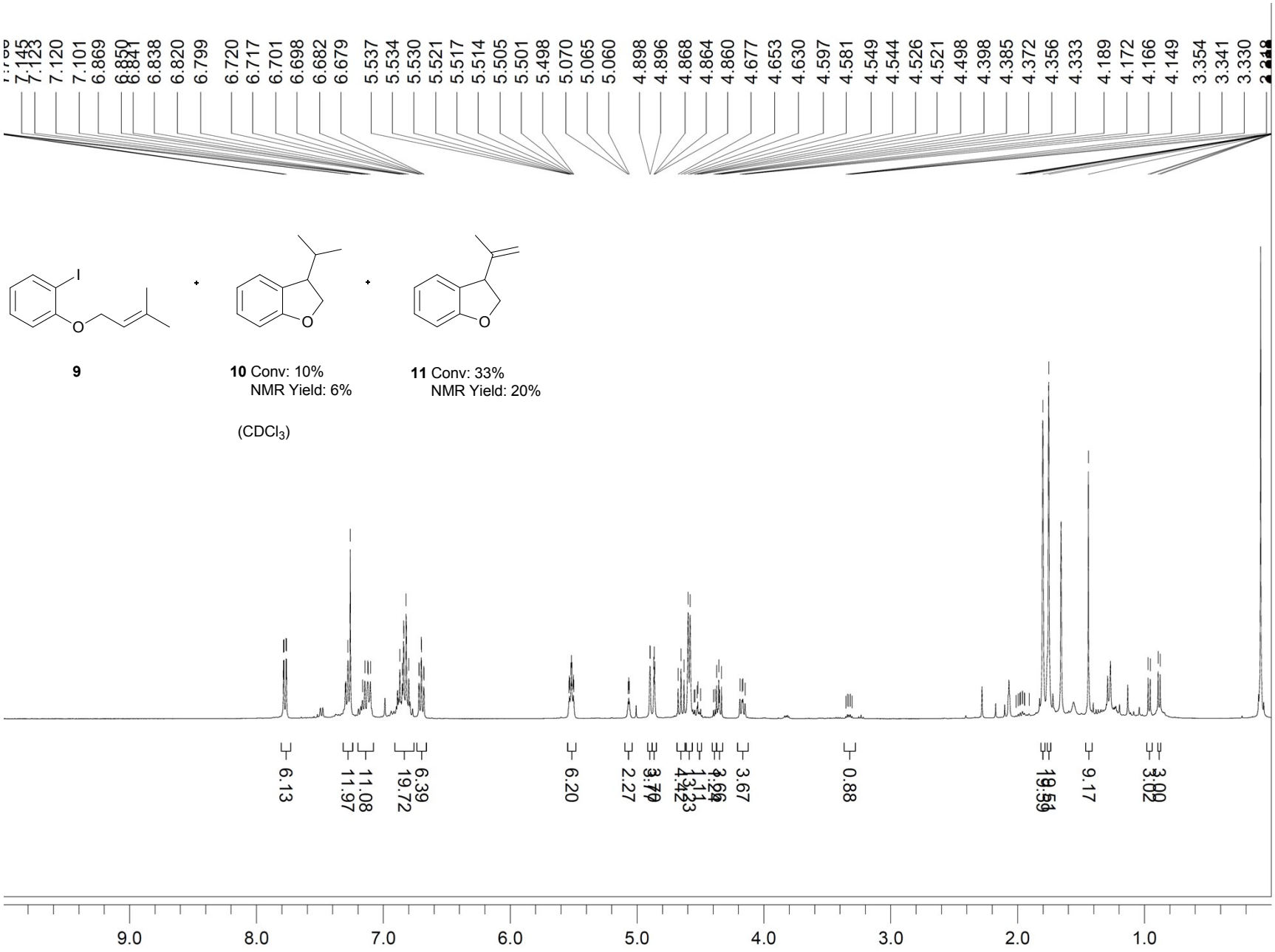
7.145
7.123
7.120
7.101
6.869
6.850
6.841
6.838
6.820
6.799
6.720
6.717
6.701
6.698
6.682
6.679
5.537
5.534
5.530
5.521
5.517
5.514
5.505
5.501
5.498
5.070
5.065
5.060
4.898
4.896
4.868
4.864
4.860
4.677
4.653
4.630
4.597
4.581
4.549
4.544
4.526
4.521
4.498
4.398
4.385
4.372
4.356
4.333
4.189
4.172
4.166
4.149
3.354
3.341
3.330
I
O
O
O
9
10 Conv: 10%
NMR Yield: 6%
11 Conv: 33%
NMR Yield: 20%
(CDCl3)
6.13
11.08
11.97
6.39
19.72
6.20
2.27
3.67
0.88
9.17
9.0
8.0
7.0
6.0
5.0
4.0
3.0
2.0
1.0

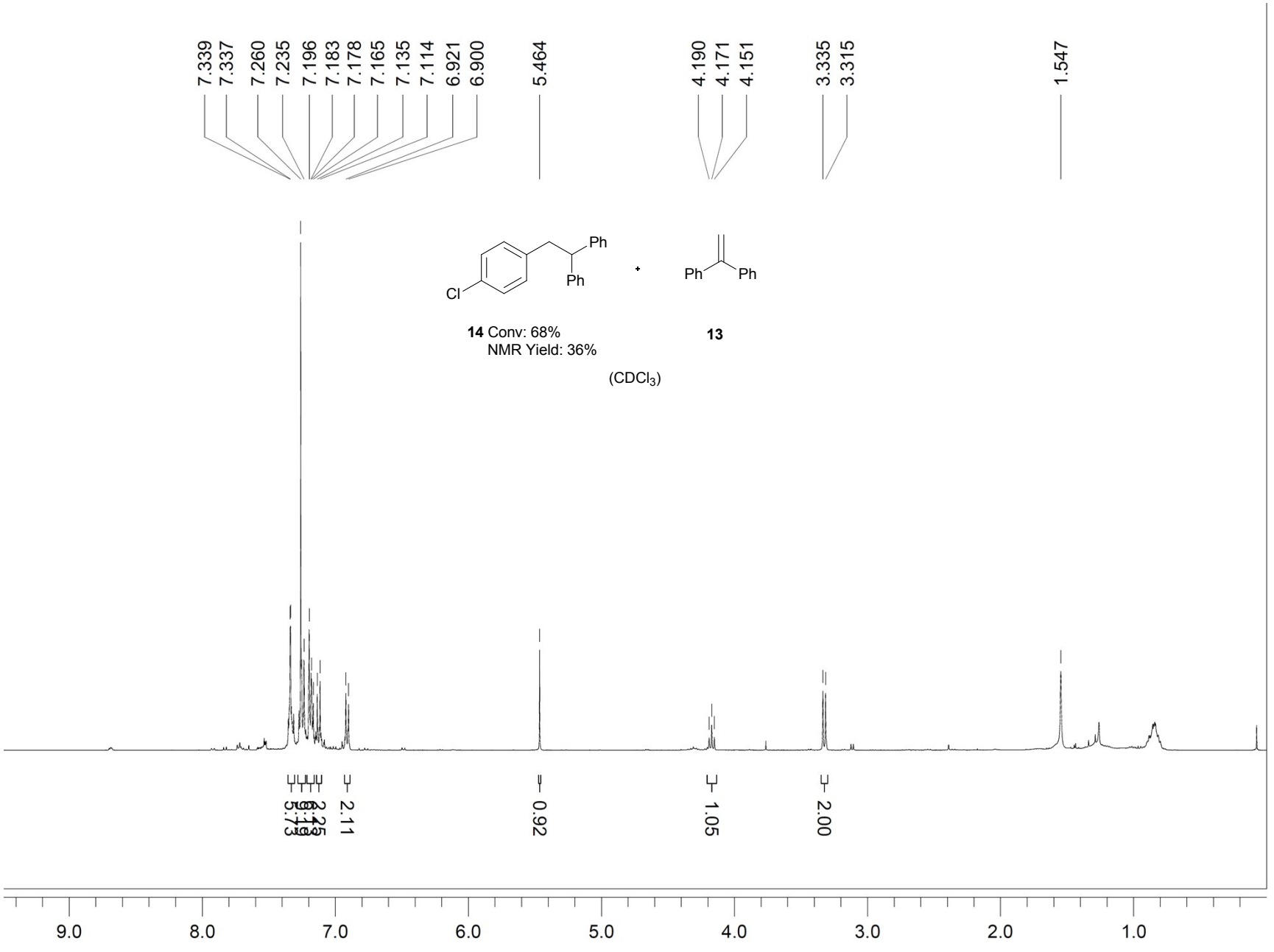
7.339
7.337
7.260
7.235
7.196
7.183
7.178
7.165
7.135
7.114
6.921
6.900
5.464
4.190
4.171
4.151
3.335
3.315
1.547
Ph
Ph
Cl
Ph
Ph
14 Conv: 68%
NMR Yield: 36%
13
(CDCl3)
2.11
0.92
1.05
2.00
9.0
8.0
7.0
6.0
5.0
4.0
3.0
2.0
1.0

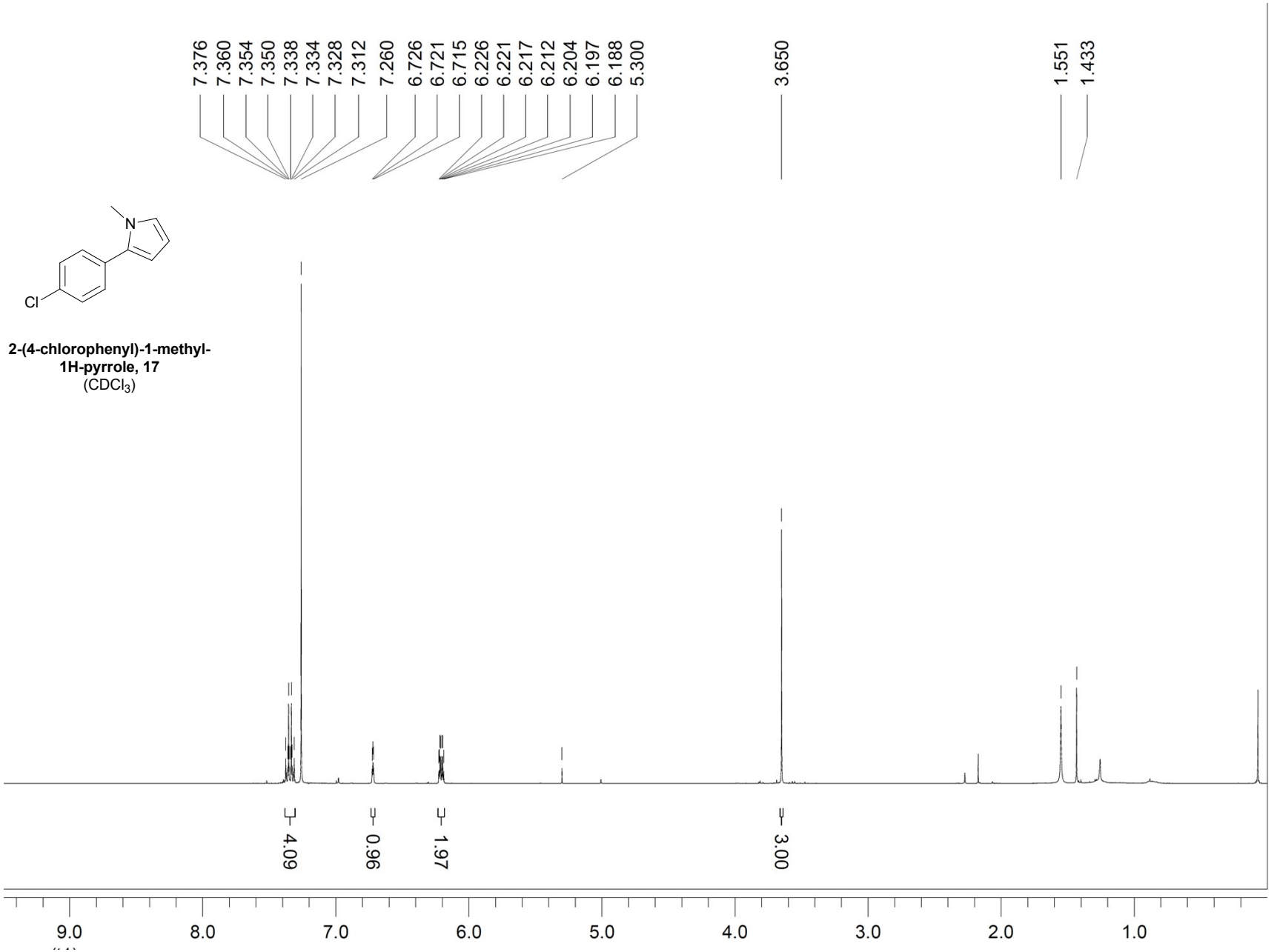

2-(4-chlorophenyl)-1-methyl-1H-pyrrole, 17
($CDCl_3$)

7. References

1 A. V. Astakhov, O. V. Khazipov, E. S. Degtyareva, V. N. Khrustalev, V. M. Chernyshev and V. P. Ananikov, Facile Hydrolysis of Nickel(II) Complexes with *N*-Heterocyclic Carbene Ligands, *Organometallics*, 2015, **34**, 5759.

2 A. Al Ghatta, J. D. E. T. Wilton-Ely and J. P. Hallett, Strategies for the Separation of the Furanic Compounds HMF, DFF, FFCA, and FDCA from Ionic Liquids, *ACS Sustain. Chem. Eng.*, 2019, **7**, 16483.

3 L. Yu, L. Guo, W. Hu, Z. Zhang, Y. Bai, J. Ye, Y. Wang and L. Li, One-pot conversion of ketones to amides via Beckmann rearrangement catalyzed by metal chloride-ionic liquids under solvent-free condition, *Catal. Commun.,* 2019, **123**, 119.

4 W. A. Herrmann, V. P. W. Böhm, C. W. K. Gstöttmayr, M. Grosche, C-P. Reisinger and T. Weskamp, Synthesis, structure and catalytic application of palladium(II) complexes bearing *N*-heterocyclic carbenes and phosphines, *J. Organomet. Chem.*, 2001, 616.

5 C. Thomas, A. Milet, F. Peruch and B. Bibal, Activation of carbonyl bonds by quaternary ammoniums and a (Na^+:crown-ether) complex: investigation of the ring-opening polymerization of cyclic esters, *Polym. Chem.*, 2013, **4**, 3491.

6 G. M. Roberts, P. J. Pierce and L. Keith Woo, Palladium Complexes with *N*-Heterocyclic Carbene Ligands As Catalysts for the Alkoxycarbonylation of Olefins, *Organometallics*, 2013, **32**, 2033.

7 K. Nozawa-Kumada, S. Ito, K. Noguchi, M. Shigeno and Y. Kondo, Super electron donor-mediated reductive desulfurization reactions, *Chem. Commun.*, 2019, **55**, 12968.

8 J. A. Murphy, J. Garnier, S. R. Park, F. Schoenebeck, S. Zhou and A. T. Turner, Super-Electron Donors: Bis-pyridinylidene Formation by Base Treatment of Pyridinium Salts, *Org. Lett.*, 2008, **10**, 1227.

9 J. A. Murphy, S. Zhou, D. W. Thomson, F. Schoenebeck, M. Mahesh, S. R. Park, T. Tuttle and L. E. A. Berlouis, The Generation of Aryl Anions by Double Electron Transfer to Aryl Iodides from a Neutral Ground-State Organic Super-Electron Donor, *Angew. Chem. Int. Ed.*, 2007, **46**, 5178.

10 P. I. Jolly, S. Zhou, D. W. Thomson, J. Garnier, J. A. Parkinson, T. Tuttle and J. A. Murphy, Imidazole-derived carbenes and their elusive tetraazafulvalene dimers, *Chem. Sci.*, 2012, **3**, 1675.

11 C. W. Williams, R. Shenje and S. France, Catalytic, Interrupted Formal Homo-Nazarov Cyclization with (Hetero)arenes: Access to α-(Hetero)aryl Cyclohexanones, *J. Org. Chem.*, 2016, **81**, 8253.

12 D. B. Huple and R. Liu, Gold-catalyzed diastereoselective [2+2+2]-cycloaddition of 1,7-enynes with carbonyl compounds, *Chem. Commun.*, 2012, **48**, 10975.

13 M. Ohashi, N. Ishida, K. Ando, Y. Hashimoto, A. Shigaki, K. Kikushima and S. Ogoshi, CuI-Catalyzed Pentafluoroethylation of Aryl Iodides in the Presence of Tetrafluoroethylene and Cesium Fluoride: Determining the Route to the Key Pentafluoroethyl Cu^I Intermediate, *Chem. Eur. J.*, 2018, **24**, 9794.

14 G. Tintori, P. Nabokoff, R. Buhaibeh, D. Bergé-Lefranc, R. Redon, J. Broggi and P. Vanelle, Base-Free Generation of Organic Electron Donors from Air-Stable Precursors, *Angew. Chem. Int. Ed.*, 2018, **57**, 3148.

15 A. M. Voutchkova, L. H. Appelhans, A. R. Chianese and R. H. Crabtree, Disubstituted Imidazolium-2-Carboxylates as Efficient Precursors to *N*-Heterocyclic Carbene Complexes of Rh, Ru, Ir, and Pd, *J. Am. Chem. Soc.*, 2005, **127**, 17624.

16 Y. Kayaki, M. Yamamoto and T. Ikariya, *N*-Heterocyclic Carbenes as Efficient Organocatalysts for CO_2 Fixation Reactions, *Angew. Chem. Int. Ed.*, 2009, **48**, 4194.

17 I. Tommasi and F. Sorrentino, Synthesis of 1,3-dialkylimidazolium-2-carboxylates by direct carboxylation of 1,3-dialkylimidazolium chlorides with CO_2, *Tetrahedron Lett.*, 2006, **47**, 6453.

18 W. Li, S. Dai, D. Li, Q. Zhang, H. Zhang and Z. Zhang, Redox Reaction: A New Route for the Synthesis of Water-Miscible Imidazolium Ionic Liquids*, Synthesis*, 2017, **49**, 1065.

19 L. H. Finger, J. Guschlbauer, K. Harms and J. Sundermeyer, *N*-Heterocyclic Olefin-Carbon Dioxide and -Sulfur Dioxide Adducts: Structures and Interesting Reactivity Patterns, *Chem. Eur. J.*, 2016, **22**, 16292.

20 R. Lindner, M. L. Lejkowski, S. Lavy, P. Deglmann, K. T. Wiss, S. Zarbakhsh, L. Meyer and M. Limbach, Ring-Opening Polymerization and Copolymerization of Propylene Oxide Catalyzed by *N*-Heterocyclic Carbenes, *ChemCatChem.*, 2014, **6**, 618.

21 E. Zetinkaya, P. B. Hitchcock, H. Küçükbay, M. F. Lappert and S. Al-Juaid, Preparation and characterization of two enetetramine-derived carbenerhodium(I) chloride complexes $RhCl(L^R)_3$ and $[RhCl(COD)L^R]$ (L^R = dCN(Me)Cu$(CH)_4$CNMe-*o*) and the preparation and X-ray structures of the enetetramine $L^R{}_2$ and its salt $[L^R{}_2][BF_4]_2$, *J. Organomet. Chem.*, 1994, **481**, 89.

22 R. Das, M. Banerjee, R. K. Rai, R. Karri and G. Roy, Metal-free C(sp^2)-H functionalization of azoles: K_2CO_3/I_2-mediated oxidation, imination, and amination, *Org. Biomol. Chem.*, 2018, **16**, 4243.

23 B. R. Van Ausdall, J. L. Glass, K. M. Wiggins, A. M. Aarif and J. Louie, A Systematic Investigation of Factors Influencing the Decarboxylation of Imidazolium Carboxylates, *J. Org. Chem.*, 2009, **74**, 7935.

24 (*a*) V. P. W. Böhm and W. A. Herrmann*,* The "Wanzlick Equilibrium", *Angew. Chem. Int. Ed.*, 2000, **39**, 4036; (*b*) Y. Liu, P. E. Lindner and D. M. Lemal, Thermodynamics of a Diaminocarbene-Tetraaminoethylene Equilibrium, *J. Am. Chem. Soc.*, 1999, **121***,* 10626.

25 B. R. Van Ausdall, J. L. Glass, K. M. Wiggins, A. M. Aarif and J. Louie, A Systematic Investigation of Factors Influencing the Decarboxylation of Imidazolium Carboxylates, *J. Org. Chem.*, 2009, **74**, 7935.

26 D. J. Nelson and S. P. Nolan, Quantifying and Understanding the Electronic Properties of N-Heterocyclic Carbenes, *Chem. Soc. Rev.* 2013, **42**, 6723.

27 D. M. Denning and D. E. Falvey, Substituent and Solvent Effects on the Stability of *N*-Heterocyclic Carbene Complexes with CO_2, *J. Org. Chem.*, 2017, **82**, 1552.

28 S. Hüning, H. Schlad, G. Kieblich and S. Scheutzow, Zweistufige, reversible redoxsysteme mit stabilem radikalkation, *Tetrahedron Lett.*, 1969, **27**, 2271.

29 J. A. Murphy, T. A. Khan, S. Zhou, D. W. Thomson and M. Mahesh, Highly Efficient Reduction of Unactivated Aryl and Alkyl Iodides by Ground-State Neutral Organic Electron Donor, *Angew. Chem. Int. Ed.*, 2005, **44**, 1356.

30 J. Messelberger, A. Grünwald, S. J. Goodner, F. Zeilinger, P. Pinter, M. E. Miehlich, F.W. Heinemann, M. M. Hansmann and D. Munz. Aromaticity and sterics control whether a cationic olefin radical is resistant to disproportionation, *Chem. Sci.*, 2020, **11**, 4138.

31 T. P. Vaid and M. S. Sanford, An organic super-electron-donor as a high energy density negative electrolyte for nonaqueous flow batteries, *Chem. Commun.*, 2019, **55**, 11037.

32 (*a*) J. Grimshaw and A. P. de Silva, Photochemistry and Photocyclization of Aryl Halides, *Chem. Soc. Rev.*, 1981, **10**, 181; (*b*) L. Li, W. Liu, H. Zeng, X. Mu, G. Cosa, Z. Mi and C. Li, Photo-induced Metal-Catalyst-Free Aromatic Finkelstein Reaction, *J. Am. Chem. Soc.*, 2015, **137**, 8328; (*c*) X. Yang, W. Liu, L. Li, W. Wei and C. Li, Photo-induced Carboiodination: A Simple Way to Synthesize Functionalized Dihydrobenzofurans and Indolines, *Chem. Eur. J.*, 2016, **22**, 15252.

33 G. De Robillard, C. H. Devillers, D. Kunz, H. Cattey, E. Digard and J. Andrieu, Electrosynthesis of Imidazolium Carboxylates, *Org. Lett.*, 2013, **15**, 4410.